UNIVERSITY OF CALABRIA
Department of Civil Engineering

PhD Thesis in
Materials and Structures Engineering

With the support of
Secretaría de Educación Superior, Ciencia y Tecnología (SENESCYT)

XXVII CYCLE

THESIS TITLE
SUSTAINABLE FABRIC-REINFORCED CEMENTITIOUS COMPOSITES FOR THE STRENGTHENING OF MASONRY ELEMENTS

Scientific Field:
ICAR/08 - STRUCTURAL MECHANICS

Coordinator: Prof. Renato S. Olivito

Adviser/Tutor: Prof. Renato S. Olivito

PhD student: Eng. Oscar Alfredo Cevallos Velásquez

CONTENTS

ABSTRACT VII
SOMMARIO XI
RESUMEN XV

INTRODUCTION 1
1.1 Thesis Scope and Objectives 5
1.2 Thesis synopsis 6
1.3 References 8

LITERATURE REVIEW 11
2.1 Composite materials: Basic concepts 11
2.1.1 Constituent materials 15
2.1.1.1 Reinforcing phase 15
2.1.1.2 Matrix phase 25
2.1.2 Types of composite materials 26
2.1.3 Properties and mechanical behaviour of FRCM composites 29
2.2 Natural fibre-reinforced cementitious composites 32
2.2.1 Production techniques 32
2.2.2 Durability of natural fibres in cementitious composites 34
2.3 FRCM composites in construction applications 36
2.4 Technical guides for the strengthening with FRCM composites 38
2.5 References 39

FLAX AND SISAL-FRCM COMPOSITES 45
3.1 Introduction 45
3.2 Experimental programme 47
3.2.1 Materials 48
3.2.2 Fibre characterisation 50
3.2.3 Compression and Flexion test on cementitious matrices 53
3.2.4 Fibre impregnation and durability 54
3.2.5 Tensile properties of composite materials 54
3.3 Results and discussion 55
3.3.1 Materials Characterisation 55

3.3.2 Ageing effects 62
3.3.3 Tensile tests on flax and sisal FRCM composites 66
3.4 References 71

TENSILE BEHAVIOUR OF SUSTAINABLE FRCM SYSTEMS 75
4.1 Introduction 75
4.2 Experimental programme 77
4.2.1 Materials 77
4.2.2 Sample preparation 79
4.2.3 Tensile test 81
4.3 Results and discussion 81
4.3.1 Composite performance 82
4.3.2 Effects of geometry and physical properties of the fabrics 87
4.3.3 Effects of mechanical properties of the fabrics 92
4.3.4 Effects of volume fraction of fibres: 94
4.4 References 99

REPAIR AND STRENGTHENING OF MASONRY ELEMENTS 103
5.1 Introduction 103
5.2 Materials and Methods 106
5.2.1 Materials and masonry elements 106
5.2.1.1 Masonry elements for tensile tests 111
5.2.1.2 Masonry elements for concentric and eccentric load tests 112
5.2.2 Strengthening of URM subjected to eccentric loading 113
5.2.3 Tensile load tests 114
5.2.4 Concentric and eccentric load tests 115
5.2.5 Repair of masonry samples 118
5.3 Results 119
5.3.1 Tensile behaviour of masonry elements 119
5.3.2 Concentric and eccentric load tests on masonry elements 122
5.3.2.1 URM specimens under concentric loads 122
5.3.2.2 URM specimens under eccentric loads 124
5.3.2.3 Strengthened specimens under eccentric loads 129
5.4 Discussion 134
5.5 References 139

PREDICTING THE STRESS-STRAIN RESPONSE OF SUSTAINABLE FRCM SYSTEMS 145
6.1 Introduction 145
6.2 Theoretical background 147
6.2.1 ACK theory 148
6.2.2 Stochastic model 151
6.2.3 Modification of the stochastic model 155
6.3 Experimental programme 156
6.4 FRCM modelling 158
6.4.1 ACK theory 158
6.4.2 Stochastic model 161
6.5 References 164

CONCLUSIONS 168

ABSTRACT

In Europe and America, a great number of old masonry structures are still in service. This fact reveals the importance and popularity that this constructive system had; even today, masonry structures remain one of the most used. Many of these structures are important cultural heritages, which provide evidence of the history of our ancient civilisations. In addition to these structures, large residential buildings that were built in the last century that used only unreinforced masonry (URM) in their load-bearing elements can also be considered as old masonry structures in the context of this thesis. Unfortunately, these structures have not been properly projected due to lack of technology and limited knowledge at that time regarding the mechanics of these structures and the behaviour of its resistant elements. With the passage of time, these structures have resisted unfavourable loading conditions, such as earthquakes, overloads, settlements of their foundations, and even accelerated erosion and deterioration at the time of their constituent materials, which have caused serious structural problems. This situation demands urgent intervention for strengthening and restoration. Among the strengthening techniques, the use of fibre-reinforced polymer (FRP) composites has been one of the most popular in the last decades. Despite presenting good effectiveness to improve the mechanical behaviour of

structures, there are several limitations that restrict the use of FRP composites when the structures are subjected to particular conditions of humidity and temperature. In addition, there is poor compatibility between the substrate material and the polymer matrix in the case of masonry structures. Motivated by these problems, researchers have directed their attention toward the study of composites produced using alternative constituent materials. Fabric-reinforced cementitious matrix (FRCM) composites are currently used successfully to strengthen concrete and masonry structures. The use of a cementitious matrix instead of resins or polymeric materials improves compatibility with the substrate material and the matrix in masonry structures. Currently, conventional fabric reinforcement, such as glass, carbon, aramid and basalt, are used successfully in FRCM systems.

From an environmental point of view, the requirements and regulations are becoming more stringent every day. Currently, an increasing number of investigations are being performed regarding the replacement of traditional materials with new materials that are sustainable and can be produced with low energy consumption. In this regard, natural fibres are one of the most studied materials. Although the use of natural fabrics in FRCM composites is a challenge to researchers, the use of these materials to solve problems of sustainability in the construction industry is revealed as a promising research area. Note that these composite systems could be successfully used in masonry structures and mainly in old masonry structures due to the load ranges and load conditions to which these systems are subject. The stiffness and strength of these structures is lower than that of structural elements made of reinforced concrete in which both FRP and FRCM composite systems reinforced with mineral or synthetic fibres can significantly improve their mechanical behaviour.

The present PhD thesis addresses the development of a sustainable composite system made from natural fabrics and a cementitious matrix for strengthening masonry structures. Woven fabrics of flax and sisal fibres and a lime-based cementitious matrix were used to prepare FRCM composites. An extensive physical and mechanical characterisation of the constituent materials and the resulting composites was conducted at the Laboratory of Testing Materials and Structures of the Department of Civil Engineering at

the University of Calabria. The durability of the fibres was considered as the main parameter to evaluate the feasibility of using the cementitious matrices for incorporation into composites reinforced with natural fibres. Composite samples were prepared using one, two or three layers of flax and sisal fabric strips and the cementitious matrix that did not affect the mechanical performance of the fibres aged in the matrix. The composites were subjected to tensile tests to study their behaviour both numerically and experimentally. To further examine the properties of the fibres, glass fibres were also used to study the tensile behaviour of glass fabric-reinforced composites and contrast the results with those obtained for the natural fabric-reinforced composites. Finally, to assess the efficacy for strengthening URM elements and study the interaction between the FRCM systems developed and the substrate material, various types of masonry elements were strengthened and then subjected to tensile loading and compressive eccentric loading. For this purpose, bi-directional flax fabrics were used to produce cementitious composites that were applied to masonry elements subjected to tensile and eccentric compressive loads to provide strengthening. The mechanical behaviour of the masonry elements subjected to eccentric loads was then compared with specimens strengthened with cementitious composites produced using polyparaphenylene benzobisoxazole (PBO) fabrics. Analysis of the load–displacement and moment–curvature response were used to determine the effectiveness of the flax- and PBO-based strengthening systems to improve the strength and deformability of masonry elements.

Keywords: natural fibres, fabric, cement-based composite, structural strengthening, masonry structure.

SOMMARIO

In Europa e in America, la maggior parte di strutture antiche in muratura appartengono al costruito esistente. Questo evidenzia la popolarità che ha avuto questo sistema costruttivo, data la facilità di reperire materiale e soprattutto i costi ridotti. Molte di queste strutture appartengono al patrimonio culturale costituendo anche parte della storia delle nostre antiche civiltà. Oltre a queste strutture antiche, anche i grandi edifici residenziali, costruiti nel secolo scorso, utilizzando muratura non rinforzata (URM) nei loro elementi portanti, possono essere considerati come strutture murarie analizzate nel contesto di questa tesi. Purtroppo, queste strutture, attualmente, non risultano adeguatamente progettate, a causa delle scarse tecnologie dell'epoca e della limitata conoscenza della meccanica strutturale e del comportamento degli elementi resistenti. Con il passare del tempo, queste strutture hanno subito diverse condizioni di carico, soprattutto sfavorevoli, come ad esempio i terremoti, i sovraccarichi, i cedimenti nelle fondazioni o anche il deterioramento dei loro materiali costituenti, i quali hanno causato gravi problemi strutturali. Questa situazione ha reso necessari interventi di rinforzo e di riabilitazione. Tra le tecniche di rinforzo più diffuse negli ultimi decenni, l'uso dei materiali compositi a base di matrice polimerica (FRP) rappresenta il più popolare. Nonostante l'efficacia nel

migliorare il comportamento meccanico delle strutture, esistono diverse limitazioni nell'uso di materiali compositi FRP, nel caso di strutture soggette a particolari condizioni di umidità e temperatura. Inoltre, la compatibilità tra il substrato di muratura e matrice polimerica risulta evidentemente scarsa. Inseguito a questi problemi, molti ricercatori hanno rivolto la loro attenzione verso lo studio di compositi prodotti con materiali alternativi. Materiali compositi a base di matrice cementizia (FRCM) sono attualmente utilizzati, con buoni risultati, per rinforzare strutture esistenti sia in calcestruzzo che in muratura. L'uso di una matrice cementizia, al contrario delle resine o dei materiali polimerici, migliora la compatibilità tra la matrice e il substrato in muratura. Tessuti di rinforzo come il vetro, carbonio, aramide e basalto sono tra i più utilizzati per la produzione di sistemi FRCM.

Da un punto di vista della sostenibilità, i requisiti da soddisfare, ma anche le normative, al giorno d'oggi, sono sempre più restrittive. Per questo motivo, il numero di studi sviluppati per sostituire i materiali tradizionali con quelli sostenibili, prodotti a basso consumo energetico, è sempre più frequente, tanto che le fibre naturali costituiscono uno dei principali argomenti di studio. L'uso di tessuti di fibre naturali nei compositi FRCM è una sfida per i ricercatori, e l'uso di questi materiali per risolvere i problemi di sostenibilità nel settore delle costruzioni si rivela come un'area di ricerca promettente. Risulta importante menzionare, che questi sistemi compositi potrebbero essere applicati, con successo, sulle strutture in muratura e soprattutto su quelle antiche, dato il loro basso livello strutturale e le sfavorevoli condizioni di carico a cui esse sono soggette. La rigidezza e la resistenza delle strutture murarie risultano inferiori rispetto a quelle solitamente garantite nelle costruzioni in calcestruzzo armato. Infatti per queste ultime sono necessari materiali compositi rinforzati con fibre ad alte prestazioni, tali da assicurare un miglioramento significativo nel loro comportamento meccanico.

Nella presente tesi di dottorato, è stato sviluppato un sistema composito sostenibile a base di fibre naturali e una matrice cementizia per il rinforzo di strutture in muratura. Sono stati usati per la preparazione dei materiali compositi FRCM, tessuti di lino e sisal e una matrice di calce idraulica. È stata condotta presso il Laboratorio Ufficiale di Prove sui Materiali e Strutture del Dipartimento di Ingegneria Civile dell'Università della Calabria

una vasta indagine relativa alle proprietà fisiche e meccaniche dei materiali costitutivi e dei compositi prodotti. La durabilità delle fibre è stata considerata come parametro principale per valutare la possibilità di utilizzare le matrici cementizie in compositi rinforzati con fibre naturali. Campioni di compositi sono stati preparati usando uno, due o tre strisce di tessuto di lino e sisal e la matrice cementizia che non ha influenzato le prestazioni meccaniche delle fibre. I materiali compositi sono stati sottoposti a prove di trazione per studiare sia sperimentalmente che numericamente il loro comportamento meccanico. Per esaminare ulteriormente le proprietà delle fibre, il comportamento a trazione di compositi cementizi rinforzati con tessuti di vetro è stato studiato per confrontare i risultati con quelli dei materiali compositi rinforzati con fibre naturali. In fine, per valutare l'efficacia del sistema, sono stati rinforzati varie tipologie di elementi murari e successivamente analizzati considerando carichi di trazione e di compressione eccentrica. A tal fine, tessuti di lino bidirezionali sono stati usati per produrre composti cementizi e rinforzare gli elementi murari. Il comportamento meccanico di elementi murari soggetti a carichi eccentrici è stato confrontato con quello di elementi rinforzati con compositi prodotti usando tessuto di polyparaphenylene benzobisoxazole (PBO). Un'analisi della risposta carico-spostamento e momento-curvatura è stata eseguita per valutare l'efficacia dei sistemi di rinforzo per migliorare la resistenza e la deformabilità degli elementi murari.

Parole chiave: fibre naturali, tessuti, compositi a base di cemento, rinforzo strutturale, struttura in muratura.

RESUMEN

En Europa y América, existe gran cantidad de estructuras de mampostería antigua que se encuentran todavía en servicio. Esto revela la importancia y popularidad que tuvo este sistema constructivo; incluso actualmente sigue siendo uno de los sistemas mas usados. Muchas de estas estructuras constituyen importantes patrimonios culturales, las cuales son una evidencia de la historia de nuestras civilizaciones antiguas. Además de estas estructuras, grandes edificaciones residenciales que fueron construidas en el siglo pasado usando solo mampostería no reforzada (URM de sus siglas en ingles) en sus elementos portantes también pueden ser consideradas como estructuras de mampostería antigua en el contexto de esta tesis. Desafortunadamente, estas estructuras no han sido correctamente proyectadas debido a la falta de tecnología y a los limitados conocimientos en aquella época acerca de la mecánica de estas estructuras y del comportamiento de sus elementos resistentes. Con el pasar del tiempo, estas estructuras han resistido condiciones de carga desfavorables tales como sismos, sobrecargas, asentamientos de sus cimentaciones e incluso erosión acelerada y deterioro de sus materiales constituyentes, los cuales han causado serios problemas estructurales. Esto ha obligado a realizar urgentes intervenciones de reforzamiento y restauración. Entre las técnicas de

reforzamiento usadas, el uso de materiales compuestos de fibras de refuerzo con polímeros (FRP) ha sido una de las mas populares en las ultimas décadas. A pesar de demostrar buena eficacia para mejorar el comportamiento mecánico de las estructuras, hay varios limitantes que restringen el uso de los materiales compuestos FRP cuando las estructuras están sometidas a condiciones particulares de humedad y temperatura. Adicionalmente, existe poca compatibilidad entre el material de sustrato y la matriz polimérica en el caso de las estructuras de mampostería. Motivados por estos problemas, los investigadores han direccionado su atención hacia el estudio de materiales compuestos producidos con materiales constituyentes alternativos. Los materiales compuestos de tejidos y una matriz cementicia (FRCM) son actualmente usados con éxito para el reforzamiento de estructuras de concreto y mampostería. El uso de una matriz cementicia en lugar de resinas o materiales poliméricos mejora la compatibilidad con el material de substrato y la matriz en las estructuras de mampostería. Actualmente, tejidos de reforzamiento convencionales tales como vidrio, carbono, aramida y basalto son usados con éxito en los sistemas FRCM.

Desde un punto de vista del medioambiente, los requisitos y las regulaciones son cada vez mas estrictas cada día. Hoy en día, hay un creciente número de investigaciones que se llevan a cabo para reemplazar a los materiales tradicionales por nuevos materiales que sean sustentables y puedan ser producidos con bajo consumo energético. En este sentido, las fibras naturales son uno de los materiales mas estudiados. El uso de tejidos de fibras naturales en los materiales compuestos FRCM es un reto para los investigadores, y el uso de estos materiales para solucionar problemas de sustentabilidad en la industria de la construcción se revela como una prometedora área de investigación. Es importante destacar que estos sistemas podrían ser usados exitosamente en estructuras de mampostería y principalmente en estructuras de mampostería antigua debido a los particulares niveles y condiciones de cargas a las que estas están sometidas. La rigidez y resistencia de este tipo de estructuras es mucho menor a aquella de elementos estructurales de concreto reforzado, en los cuales los materiales compuestos deben ser reforzados con fibras de altas prestaciones para mejorar significativamente su comportamiento mecánico.

La presente tesis de PhD trata del desarrollo de un sistema compuesto sustentable elaborado con tejidos de fibras naturales y una matriz cementicia para el reforzamiento de estructuras de mampostería. Tejidos de lino y sisal y una matriz cementicia a base de cal fueron usados para elaborar los materiales compuestos. Una extensa caracterización física y mecánica de los materiales constituyentes, así como de los materiales compuestos resultantes fue conducida en el Laboratorio de Pruebas de Materiales y Estructuras del Departamento de Ingeniería Civil de la Universidad de la Calabria. La durabilidad de las fibras fue considerado como el principal parámetro para evaluar la viabilidad de usar las matrices cementicias para preparar materiales compuestos reforzados con fibras naturales. Muestras de materiales compuestos se prepararon usando uno, dos o tres capas de telas de refuerzo de lino y sisal y la matriz cementicia que no afectó al rendimiento mecánico de las fibras envejecidas. Los materiales compuestos fueron sometidos a pruebas de tracción para estudiar tanto numérica y experimentalmente su comportamiento. Para examinar adicionalmente las propiedades de las fibras, también se utilizaron fibras de vidrio para estudiar el comportamiento a tracción de compuestos cementicios reforzados con tejidos de vidrio y contrastar los resultados con los obtenidos por los materiales compuestos reforzados con fibras naturales. Finalmente, para evaluar la eficacia para reforzar elementos de mampostería no reforzada y estudiar la interacción entre los sistemas FRCM desarrollados y el material de sustrato, varios tipos de elementos mampostería fueron reforzados y luego sometidos a cargas de tracción y a cargas de compresión excéntrica. Para este fin, se utilizaron telas de lino bidireccionales para producir compuestos cementicios que se aplicaron a los elementos de mampostería sometidos a cargas de tracción y compresión excéntricas para su reforzamiento. El comportamiento mecánico de los elementos de mampostería sometidos a cargas excéntricas fue comparado con muestras reforzadas con compuestos de cemento reforzados con telas de benzobisoxazol poliparafenileno (PBO). Mediante un análisis de la respuesta carga-desplazamiento y momento-curvatura de las muestras se determinó la eficacia de los sistemas de reforzamiento de lino y de PBO para mejorar la resistencia y deformabilidad de los elementos de mampostería.

Palabras clave: Fibras naturales, tejido, compuesto a base de cemento, reforzamiento estructural, estructura de mampostería.

Chapter 1

INTRODUCTION

The key to forming composites involves combining two or more materials that have very different properties in such a way that better utilises their advantages while minimising the effects of their weaknesses. The term 'composite' implies a wide range of individual combinations that can be included in this class of materials. For example, metallic, ceramic and polymeric composites are among the most common and largest group of engineering materials [1].

Although it is difficult to say with certainty when composites began to be used by man, nature provides us with numerous examples. Indeed, as is the case of many scientific inventions, nature teaches us how to use the synergistic effects of two or more materials to increase the strength and stiffness of the resultant material, with wood and bone being the best examples [2]. The oldest existing reference regarding one of the first man-made fibrous composites is recorded in the book of Exodus in the Old Testament, which describes the straw-reinforced clay bricks used by the Israelites, and in this case, fibrous reinforcements were probably used to

prevent the appearance of cracks in the clay during drying instead of a structural application [3]. Since the 20th century, with the industrialised use of steel, invention of polymers and fibres such as fiberglass, carbon and many others, fibre-reinforced composites emerge as an ideal material for a wide range of applications. The total worldwide annual usage of polymer composites is over 8 million tonnes, and the market is growing at an annual rate of 5-10% [4]. Given the very high usage and the fact that polymers and traditional fibres are not ecologically sustainable materials, concern about environmental issues has promoted research on new biodegradable composites based on natural fibres as reinforcement, and currently, the use of natural fibres in composite materials is emphasised in many industrial sectors. Natural fibres, being sustainable and environmentally friendly, lightweight, durable and low cost, have started to replace glass fibres and mineral fillers in many engineering applications in automobiles, furniture, packaging and construction [5-14]. The factors driving this research are the available information related to the mechanical behaviour of natural materials, such as lignocellulose fibres, and the new technology and capability to characterise their properties and morphologies. Natural fibres such as flax and sisal have already shown that they can be used successfully as reinforcement fibres in composite materials for structural applications, thereby reducing weight and costs and achieving a suitable performance [15-17]. However, bio-composites still face many challenges, mainly related to a poor durability and the complexity in developing theoretical models to predict their mechanical behaviour.

In the construction industry, composite materials produced using natural fibres and a cementitious matrix rather than a polymer resin increase, without a doubt, the condition of sustainable material. Moreover, from the perspective of economic development, cement-based composites reinforced with natural fibres provide an opportunity to develop an economy based on agriculture in arid lands generating materials for housing construction. Economic growth in developing countries could be enormous if farms industrialise natural fibres with low capital investment and low energy consumption to produce final products.

Fibre-reinforced cement (FRC) composites have been studied for the past 20 years, and a significant amount of research is found in the literature on

FRC systems reinforced with glass and carbon fibres [18,19]. The requirements in these materials involve better performance for placement and compaction without segregation, long-term mechanical properties, early age strength, toughness, stability and durability in severe environmental conditions. Nevertheless, some FRC systems often do not meet any of the above requirements; in particular, decreased durability is one of the major concerns in civil structures that could be a drawback of FRC composites, due to the chemical and sulphate attack and alkali silica reactions that affect concrete. Suitable models that predict the durability of composites considering the interplay of cementitious materials and reinforcing fibres, especially in the case of natural fibres, have not yet been generated because of the complexity of the effects of interactions of chemical and mass transport, non-equilibrium cement chemistry, phases, temperature and humidity, volumetric changes and the changes in properties due to cracking. Therefore, durability of service life is still one of the unanswered questions, and further research is still needed in this area. On the basis of mechanical performance, FRC composites have demonstrated one of the highest values of strength-to-weight ratio. FRC composites are resistant to fire and do not contribute to fire spread; additionally, these materials will not rot, warp, crack or creep and are 100% recyclable [18]. For these reasons, the interest in the use of cementitious composites reinforced with natural fibres is continuously growing.

By using textiles instead of short, long or continuous unidirectional fibres, the mechanical properties of cementitious composites are improved. Indeed, unidirectional laminated composites exhibit excellent in-plane behaviour but poor interlaminar properties. The presence of fibre reinforcement in the direction perpendicular to the external solicitations improves damage tolerance. Fabric-reinforced cementitious matrix (FRCM) composites are a new class of materials with improved tensile strength and ductility. The technical guide ACI 549.4R-13 [20] states: "*Composite material consisting of a sequence of one or more layers of cement-based matrix reinforced with dry fibres in the form of open single or multiple meshes that, when adhered to concrete or masonry structural members, forms a FRCM system*". These materials have the potential for strengthening structural and non-structural elements. Their improved behaviour is mainly governed by the interfacial bond characteristics between the fabrics and

matrix. The tensile mechanical response of these composites revealed that micro-cracking and crack distribution are two main internal parameters that result in pseudo-ductility.

Repair and strengthening of masonry structures using composites reinforced with natural fibres is an application that has attracted the interest of researchers [17,21-23]. Brick was invented thousands of years ago and is the oldest construction material manufactured. The simplicity, strength and durability of brick resulted in extensive use in the construction of many historic buildings. Masonry can be used in a wide variety of architectural and structural applications, including walls (bearing, shear, structural, decorative), arches, domes and vaults, beams and columns (piers) [24]. Despite being a building material that is used in a simple manner, masonry exhibits a complex behaviour. The easier way to analyse and be able to correctly specify the mechanical behaviour of masonry is considering it as a composite material, which is constituted by solid elements (bricks) connected to a bonding material (mortar). Bricks have a high compressive strength with respect to mortars; both the tensile and flexural strength of masonry structures are significantly affected by the poor adhesive strength between the bricks and the bonding material, and therefore, masonry structures exhibit low resistance to tensile and out-of-plane loads. The tensile strength of masonry elements can be neglected in the study of their mechanical behaviour [25]. These concerns, in the case of ancient masonry, are increased due to degradation during the time of the bond between the materials. Moreover, taking into account that the vertical loads present in masonry structures may include destabilising effects, the overloads and the seismic events represent the main reason that causes the failure of such structural elements. Given the complexity of the structural problems observed in old and ancient masonry structures and the fact that they can cause non-compliance with current rules concerning seismic safety, there is a clear need for strengthening interventions [26]. FRCM composites have recently emerged as just such a system, offering great potential for strengthening masonry structures [27] due to a number of advantages in terms of compatibility with chemical, physical, and mechanical properties of masonry substrates, ease of installation, vapour permeability and good performance at elevated temperatures [20,28]. Thus, the development of an

FRCM system reinforced with natural fibres that allows for the strengthening of masonry structures was imposed as an aim of this thesis.

1.1 Thesis Scope and Objectives

There are two main parts in this thesis. The first part aims to develop a sustainable composite material based on a cementitious matrix and fabrics of natural fibres. Composite materials used for strengthening structures should demonstrate excellent mechanical properties and must interact properly with the substrate material of the structure. In addition, matrix materials must be compatible with the reinforcing fibres. Therefore, the durability of natural fibres in a cementitious matrix is a key feature and must be carefully addressed. For example, tests to evaluate the mechanical response of long-term aged samples should be conducted. Moreover, several factors can influence the mechanical performance of FRCM composites. The fibre content, interphase between fibres and the corresponding matrix material, textile architecture, fibre treatment and the anchorage capability of the fabrics in the matrix have significant effects on the tensile behaviour of FRCM composites.

The specific objectives of the first part of this work are as follows:

a) To conduct a physical and mechanical characterisation of the main properties of cementitious materials and natural fibres.
b) To manufacture FRCM composites using lime-based cementitious matrices and sisal and flax fabric strips.
c) To examine the durability of sisal and flax fibres by performing tensile tests on aged single yarns that were impregnated with cementitious matrices.
d) To experimentally study the tensile behaviour and crack propagation of sisal and flax FRCM composites and compare the results with cementitious composites reinforced with glass and PBO fabrics
e) To numerically analyse the tensile stress-strain response of sisal and flax FRCM composites.

The second part of this work aims to study the applicability of the sustainable FRCM composites developed in this thesis to strengthen and repair masonry elements. Unlike concrete structures, the strengthening

systems in masonry structures need not be as rigid as fibre-reinforced polymer (FRP) composites. Therefore, masonry elements built with clay bricks and lime-based mortar were studied. The mechanical behaviour of such elements is very different from that of the concrete elements. In masonry, the overall mechanical response governed by the bond strength between the mortar and bricks causes brittle behaviour and major resistance problems. Furthermore, the deformability of clay bricks is much higher than that of concrete. To address these issues, strengthening systems used in masonry structures should have a performance that allows for compatibility with the substrate.

The specific objectives of the second part are as follows:

a) To conduct physical and mechanical characterisation of the main properties of clay bricks and lime-based mortar used to build the masonry samples.
b) To experimentally study the mechanical behaviour of unreinforced and strengthened masonry elements by performing eccentric compression tests.
c) To evaluate the effectiveness of sustainable FRCM systems to repair masonry elements subjected to tensile tests.

1.2 Thesis synopsis

A review of the literature related to the general aspects of composite materials is given in *Chapter 2*. The particular characteristics and mechanical properties of composites and their constituent materials, the possible uses as reinforcing systems, their applicability to strength masonry structures and new regulations and technical guidelines are reviewed in this chapter.

In *Chapter 3*, the activities are presented to develop sustainable composites using cementitious matrices reinforced with untreated bi-directional fabrics of natural fibres, namely flax and sisal fibres. The fibres were mechanically characterised by tensile tests performed on both single yarns and fabric strips. Ageing effects due to fibre mineralisation in alkaline cement paste environments may cause a reduction in the tensile strength of natural fibres. The matrices used to study fibre durability were a natural

hydraulic lime-based mortar (NLM) mix with a low content of water-soluble salts and a lime-based grouting (NLG) mix containing natural pozzolans and carbonated filler. Tensile tests on impregnated single yarns subjected to wetting and drying cycles by exposure to external weathering were conducted at different ages to quantify these problems. Composite specimens were manufactured via the hand lay-up moulding technique using untreated fibre strips and an NLG matrix. The mechanical response of cementitious composites reinforced with natural fibres was measured under tension, and the effect of the matrix thickness was also addressed.

Chapter 4 presents an experimental analysis of the tensile behaviour of FRCM composites reinforced with natural fibres. The effects of the fibre type, the fabric geometry, the physical and mechanical properties of fabrics and the volume fraction of fibres on the tensile stress-strain response and crack propagation of composite samples reinforced with sisal and flax fabric strips were studied. To further examine the properties of the fibres, mineral fibres (glass) were also used to study the tensile behaviour of glass fabric-reinforced composites and contrast the results with those obtained for the natural fabric-reinforced composites. Composite samples were manufactured via the hand lay-up moulding technique using one, two and three layers of flax and sisal fabric strips and an NHL grouting mix.

In *Chapter 5,* the potential of sustainable composite systems to be applied for the repair and strengthening of masonry structures is evaluated. The results of an experimental study of the tensile behaviour of unreinforced and repaired masonry elements using flax-FRCM composite systems are given. The effectiveness of this composite system for improving the tensile bond strength of masonry elements is evaluated. To address the structural problems caused by eccentric loads in unreinforced masonry, three different types of masonry were prepared based on clay bricks bonded with a natural hydraulic lime mortar combined with a flax or polyparaphenylene benzobisoxazole (PBO) fabric-reinforced cementitious matrix (FRCM) composite. The mechanical behaviour, when subjected to concentric and eccentric loads, was studied by performing axial compression tests, with eccentric load tests only performed in instances of large eccentricities.

A numerical analysis of the tensile behaviour of sustainable FRCM composites is included in *Chapter 6*. To improve its application for

strengthening masonry elements such as wall panels and pier elements, the constitutive behaviour of the developed composite materials should be fully understood and accurately modelled. Using the ACK theory and Weibull model, the tensile stress-strain response was predicted. The well-known Aveston–Cooper–Kelly (ACK) theory is based on a tri-linear analytical approach and was used to define the theoretical stress–strain behaviour of the FRCM composites, which are based on a brittle matrix, considering that the fibre–matrix bond remains intact after the cracking of the matrix. By using the Weibull model, the transverse matrix crack spacing and change in debonding length between the fibre and the matrix are continuously monitored with increasing applied load. A detailed approximate stress analysis, together with failure statistics for fibre fracture, was used to determine the probability of fibre fracture and fibre fracture location in the composite.

Finally, concluding remarks and some suggestions for future work are given at the end of this thesis.

1.3 References

[1] Harris B. Engineering composite materials. 2nd ed. Cambridge: The Cambridge University Press; 1999.

[2] Wainwright SA, Biggs WD, Currey JD, Gosline JM. Mechanical design in organisms. Princeton University Press; 1982. p. 423.

[3] Gibson RF. Principles of composite material mechanics. New York: McGraw-Hill; 1994.

[4] Hull D, Clyne TW. An introduction to composite materials. 2nd ed. Cambridge, UK: Cambridge University Press; 1996.

[5] Rosa MF, Chiou B-s, Medeiros ES, Wood DF, Williams TG, Mattoso LHC, et al. Effect of fiber treatments on tensile and thermal properties of starch/ethylene vinyl alcohol copolymers/coir biocomposites. Bioresour Technol 2009;100:5196–202.

[6] Joshi SV, Drzal LT, Mohanty AK, Arora S. Are natural fiber composites environmentally superior to glass fiber reinforced composites? Compos Part A Appl Sci Manuf 2004;35:371–6.

[7] Virk AS, Hall W, Summerscales J. Failure strain as the key design criterion for fracture of natural fibre composites. Compos Sci Technol 2010;70:995–9.

[8] El-Sayed AA, El-Sherbiny MG, Abo-El-Ezz AS, Aggag GA. Friction and wear properties of polymeric composite materials for bearing applications. Wear 1995;184:45–53.

[9] Chand N, Dwivedi UK. High stress abrasive wear study on bamboo. J Mater Process Technol 2007;183:155–9.

[10] Hepworth DG, Vincent JFV, Jeronimidis G, Bruce DM. The penetration of epoxy resin into plant fibre cell walls increases the stiffness of plant fibre composites. Compos Part: A Appl Sci Manuf 2000;31:599–601.

[11] Chin CW, Yousif BF. Potential of kenaf fibres as reinforcement for tribological applications. Wear 2009;267:1550–7.

[12] Alawar A, Hamed AM, Al-Kaabi K. Characterization of treated date palm tree fiber as composite reinforcement. Compos Part B Eng 2009:601–6.

[13] Saha P, Manna S, Chowdhury SR, Sen R, Roy D, Adhikari B. Enhancement of tensile strength of lignocellulosic jute fibers by alkali-steam treatment. Bioresour Technol 2010;101:3182–7.

[14] Yousif BF, Ku H. Suitability of using coir fiber/polymeric composite for the design of liquid storage tanks. Mater Des 2012;36:847–53.

[15] Ienica. Interactive European Network for Industrial Crops and their Applications. 2012. <http://www.ienica.net/reports/BIGFIBRES.pdf>

[16] Knothe J., Schlösser Th. Natural fiber reinforced plastics in automotive exterior applications. In 3rd International Wood and Natural Fiber Composites Symposium. Kassel, September 1920; 2000.

[17] Olivito R, Cevallos O, Carrozzini A. Development of durable cementitious composites using sisal and flax fabrics for reinforcement of masonry structures. Mater Des 2014;57:258–68.

[18] Mobasher B. Mechanics of Fibre and Textile Reinforced Cement Composites. CRC Press. Taylor & Francis Group, Boca Raton, Fl; 2012.

[19] Zia P. State-of-the-Art of HPC: An International Perspective. In Proceedings PCI/FHWA International Symposium on High Performance Concrete. New Orleans; 1997.

[20] ACI 549.4R-13. Guide to Design and Construction of Externally Bonded Fabric-Reinforced Cementitious Matrix (FRCM) Systems for Repair and Strengthening Concrete and Masonry Structures. ACI, 2013.

[21] Olivito R, Codispoti R, Zuccarello F. Applicazione di materiali compositi in fibre naturali e malta cementizia a strutture murarie. In: XX Congresso Nazionale Associazione Italiana di Meccanica Teorica ed Applicata (AIMETA). Bologna; 2011.

[22] Larrinaga P, Chastre C, Biscaia HC, San-Jose JT. Experimental and numerical modeling of basalt textile reinforced mortar behavior under uniaxial tensile stress. Mater Des 2014;55:66–74.

[23] Olivito RS, Dubois F, Venneri A, Zuccarello FA. Experimental And Numerical Analysis Of Masonry Macroelements Reinforced By Natural-Fibre- Composite Materials. In: 6th international conference on FRP composites in civil engineering (CICE2012). Roma; 2012.

[24] RE.Klingner, Masonry structural design, McGraw-Hill Professional; 2010.

[25] M. Angelillo, PB. Lourenço, G. Milani. Mechanics of Masonry Structures. In CISM International Centre for Mechanical Sciences, CISM, Udine; 2014.

[26] Park J, Towashirapornb P, Craigc JI, Goodnod BJ. Seismic fragility analysis of low-rise unreinforced masonry structures. Eng Struct 2009;31(1):125–37.

[27] Papanicolaou CG, Triantafillou TC, Papathanasiou M, Karlos K. Textile-reinforced mortar (TRM) versus FRP as strengthening material of URM walls: out-of-plane cyclic loading. Mater Struct, RILEM 2008;41(1):143–57.

[28] Brameshuber W, editor. State-of-the-art report of RILEM technical committee 201 TRC: textile reinforced concrete (RILEM Report 36). Bagneux: RILEM Publications S.A.R.L.; 2006.

Chapter 2

LITERATURE REVIEW

2.1 Composite materials: Basic concepts

There are several acceptable definitions of composite materials; however, a composite material can be generally defined as "a heterogeneous mixture of two or more homogeneous phases which have been bonded together" [1]. Since the early modern man-made composite materials, the phases or constituent materials have been typically macroscopic and combined on a macroscopic scale via mechanical and chemical bonds, with an interface between them. However, it is possible to find new materials formed with nano-sized constituents, particularly the reinforcing materials, such as carbon nanoparticles, nanofibres and nanotubes. These types of composites, known as nanocomposites, are not part of this thesis.

A composite system can be considered as an anisotropic material with a prevalent linear elastic behaviour up to failure. The phases of the composite system should be present in appropriate proportions and be completely mixed and combined to result in a composite material with the expected

behaviour. Composites are generally used because they exhibit desirable properties that cannot be achieved by any of the constituents acting alone, and thus, the constituents have physical and mechanical properties quite different from each other [2]. Generally, composites are formed with inclusions suspended in a binder, and the most common example is the fibrous composite consisting of reinforcing fibres embedded in a matrix material. Both the matrix and the fibres preserve their characteristics in the composite structure.

Based on the scientific demonstrations performed by Griffith [3], fibrous reinforcements are very effective because materials are generally stronger and stiffer when they are in a fibrous form instead of a bulk form. Despite the fact that fibres alone cannot resist longitudinal compressive loads and their transverse performance is typically not as good as the corresponding longitudinal behaviour, fibres undoubtedly enable the maximum tensile strength and stiffness of a composite material. In addition, the use of reinforcing fibres in a brittle cementitious matrix increases the ductility and strength in terms of the tensile behaviour.

Many materials can be categorised as composites. Composite materials are one of the most widely used materials because of their adaptability to different situations and the relative ease of combination with other materials. Because of the excellent mechanical properties of the constituent materials, these materials can withstand severe loading stresses. In addition, composites are replacing traditional engineering materials in many industrial sectors, as shown in Fig. 2.1.

In the aircraft industry (see Fig. 2.1a), the use of fibre-reinforced composite materials has become an increasingly attractive alternative to conventional metals for many aircraft components, primarily due to their strength, durability, corrosion and fatigue resistance and damage tolerance. Composites also provide greater flexibility with regard to design requirements and offer significant advantages in weight. Carefully designed single composite pieces could be approximately 20 to 30% lighter than conventional metal counterparts. The composite materials used in the aircraft industry are generally reinforced fibres (commonly used carbon, aramid, glass and hybrid fibres) embedded in a resin matrix. The matrix material is generally an epoxy-based system that requires curing

temperatures between 120° and 180° C. Currently, the use of advanced composite materials includes a large number of aircraft components, both structural and non-structural, and considers various factors such as in-service loading, environmental conditions, etc. [8].

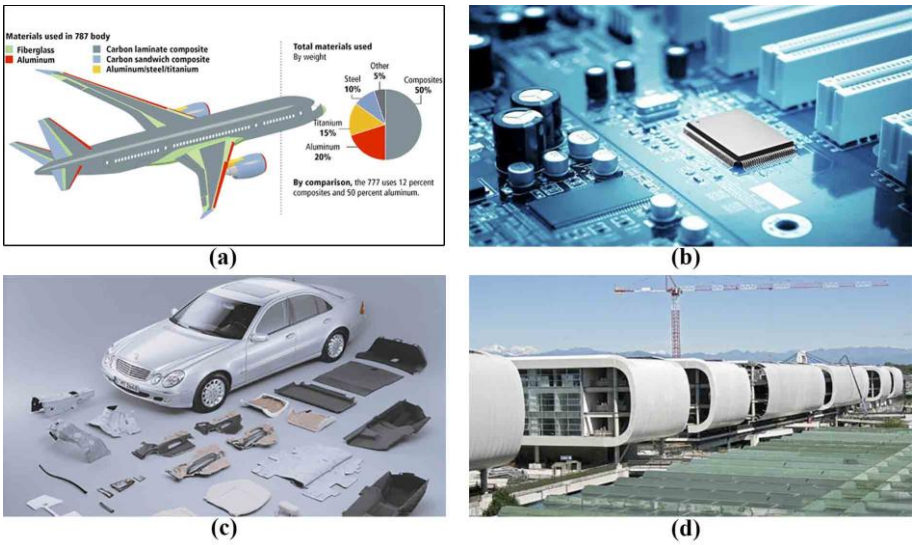

Fig. 2.1: Uses of composites materials in different industrial sectors: (a) aircraft industry [4]; (b) electronic industry [5]; (c) automotive industry [6]; and (d) construction industry [7].

Among the main materials for electrical connections are Sn-Pb alloys, which are used as solders. However, the difference in the coefficient of thermal expansion (CTE) between the two welded members causes thermal fatigue upon thermal cycling during operation, leading to the failure of the solder joint. Polymer matrix composites in paste form containing electrically conductive fillers are being developed to replace soldering. Another motivation for the use of composite materials in this area lies in the toxicity of lead used in the solder to improve the rheology of the liquid solder, and thus, lead-free solders are being developed. Similarly, copper is reinforced with carbon fibres, molybdenum particles, fillers, or other low CTE materials to improve performance to dissipate heat from electronics [9]. Some electronic components (see Fig. 2.1b) have been developed with metal-coated carbon materials, providing high levels of electromagnetic interference (EMI) shielding. These materials can be tailored to meet the

required attenuation values at certain specified frequencies. This technology can be used as-is or incorporated into a composite and offers a competitive lightweight and thermally stable alternative to traditional shielding options [5].

In the automotive industry, there is increasing interest in reducing weight to enable energy conservation and increased fuel economy. Because of the high cost of carbon or aramid fibre, most automotive applications involving glass-reinforced plastics (GRPs). A wide range of car and truck body mouldings, panels and doors is currently in service, including complete front-end mouldings, fascias, bumper mouldings, and various types of trim. There is considerable interest in the use of controlled-crush components based on the high energy-absorbing qualities of materials such as GRPs. Leaf and coil springs and truck drive shafts are also in service, and GRP wheel rims and inlet manifolds have been described in the literature. Selective reinforcement of aluminium alloy components, such as pistons and connecting rods, with alumina fibres is often discussed with reference to increased temperature capability [10]. The Mercedes C-class contains some 20 components made from natural material composites [6], as shown in Fig. 2.1c.

Fibre-reinforced composites have been widely used in the construction industry. Due to the high corrosion resistance and low weight of such composites, they have proven attractive for many applications. Applications range from non-structural elements to complete structural systems for construction supports, buildings, long-span roof structures, tanks, bridge components and complete bridge systems. The use of fibre-reinforced polymer (FRP) composites is gradually being introduced to the concrete reinforcement itself to replace conventional steel bars. For example, pultrusion, braiding, or braiding pultrusion techniques can be used to produce preforms for further processing [11]. Fig. 2.1 shows one innovative application of pultruded composites. The Sheraton Hotel Malpensa located in Milan is a quarter mile long, with units of three stories tall. The building has an area of 24750 m^2 and is at the top of an existing parking structure that was built over an underground railway. The roof of pultruded panels covers and wraps around a series of seven guest-room bay modules. The curved façades of the modulus face the Malpensa airport terminal. Composites

manufactured using an inorganic matrix instead of a polymer matrix are gaining in popularity in the construction industry to produce composite materials for strengthening and repair of concrete and masonry elements [12]. In addition, fibre cement spraying is one possible route for special uses and applications. Other critical applications of composites in the civil engineering area are:

- Tunnel and storage container supports
- Airport facilities (such as runways and aprons)
- Roads and bridge structures
- Marine and offshore structures
- Concrete slabs
- Power plant facilities
- Architectural features and structures (such as exterior walls, handrails, etc.)

2.1.1 Constituent materials

Composites can be prepared using a very wide range of materials and combinations. One of the main features of composites is the use of a reinforcing phase with different characteristics and mechanical properties of the matrix phase, which, when combined, provide unique properties to the resulting material.

2.1.1.1 Reinforcing phase

The reinforcing phase can be in many forms, such as short or continuous fibres or filaments, woven fibres or fabrics, particles or ribbons. The criteria for selecting the type and form of reinforcement will vary according to the design requirement for the composite. However, certain general attributes are desirable, including high strength and elastic modulus, low specific weight, environmental resistance, ductility, low cost, good workability and ease of fabrication. As mentioned in the previous section, due to the small section of fibres, these have a suitable structural performance that is combined with the intrinsic properties of the constituent materials for ensuring a linear elastic behaviour until failure. Commercial fibres are produced using very fine filaments and are available in different forms such

as "*monofilaments*", which have diameter sizes on the order of microns, packages of untwisted monofilaments called "*tows*", "*yarns*" formed with several hundred (even up to thousands) of continuous twisted monofilaments, and "*rovings*", which are sets of yarns or tows (see Fig. 2.2).

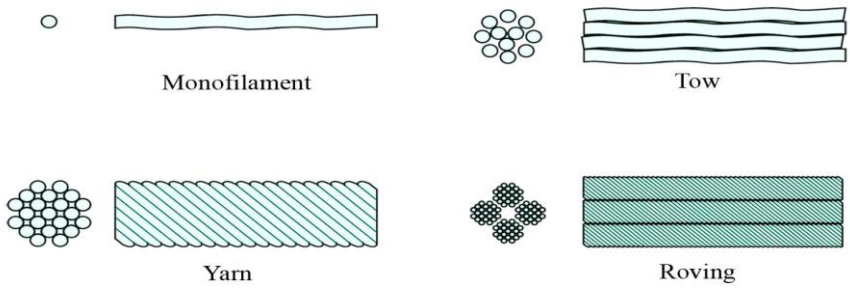

Fig. 2.2: Types of fibres [2].

Fibres such as S-glass, R-glass, and a wide range of carbon, boron, ceramic, polymeric, aramid and natural fibres have been used as reinforcement in composite materials [13]. These fibres are found in the following forms: continuous fibres arranged parallel in a plane, chopped fibres arranged in a plane with random orientation (MAT) or woven according to a warp and weft configuration, with single yarns arranged in a plane. In Figs. 2.3a and 2.3b, the typical stress-strain responses of man-made and natural fibres, respectively, are illustrated. In addition, Table 2.1 reports some of the key properties of reinforcing fibres used in composite systems. The evident differences in the mechanical properties of mineral and advanced synthetic fibres over natural fibres are presented in the table by comparing selected properties.

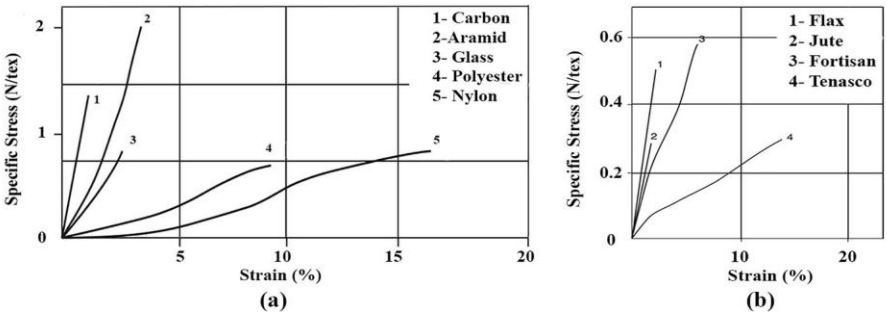

Fig. 2.3: Typical stress-strain curves: (a) man-made fibres; and (b) natural fibres [11].

Table 2.1: Selected properties of some reinforcing fibres [Adapted from 14-16].

Material	σ (GPa)	E (GPa)	ρ (g/cm^3)	σ/ρ	E/ρ	ε (%)
Glass Fibres						
E-glass	3.45	72	2.54	1.36	28.35	4.8
S-2 glass	4.89	87	2.46	1.99	35.37	5.7
PAN-Based Carbon Fibres						
AS4, 12K filaments	4.48	231	1.79	2.50	129.05	1.8
IM7, 12K	5.67	276	1.78	3.19	155.06	1.8
IM9, 12K	6.14	304	1.80	3.41	168.89	1.9
IM10, 12K	6.96	303	1.79	3.89	169.27	2.1
T-300, 12K	3.65	231	1.76	2.07	131.25	1.4
T650/35, 12K	4.55	248	1.70	2.68	145.88	1.8
T400H, 6K	4.41	250	1.80	2.45	138.89	1.8
M-40, 12K	2.74	392	1.81	1.51	216.57	0.7
T-700S, 12K	4.90	230	1.80	2.72	127.78	2.1
T-800S, 24K	5.88	294	1.80	3.27	163.33	2.0
T-1000G, 12K	6.37	294	1.80	3.54	163.33	2.2
Pich-Based Carbon Fibres						
P-55S, 2K	1.90	380	2.00	0.95	190.00	0.5
P-100S, 2K	2.10	760	2.13	0.99	356.81	0.2
P-120S, 2K	2.24	830	2.13	1.05	389.67	0.4
Polymeric Fibres						
Kevlar 29 Aramid	3.62	70	1.44	2.51	48.61	3.6
Kevlar 49 Aramid	3.62	112	1.44	2.51	77.78	2.4
Spectra 900/650 polyethylene	2.60	79	0.97	2.68	81.44	3.6
Spectra 2000/100 Polyethylene	3.34	124	0.97	3.44	127.84	3.0
Technora aramid	3.43	73	1.39	2.47	52.52	4.6
Zylon-As PBO	5.80	180	1.54	3.77	116.88	3.5
Dyneema SK60 polyethylene	3.50	110	0.97	3.61	113.40	
Other Fibres						
Boron 4.0 mil dia	3.60	400	2.54	1.42	157.48	0.8
SCS-6 silicon carbide	3.90	380	3.00	1.30	126.67	0.1
Carbon nanotubes	13-52	320-1470	1.3-1.4	-	-	-
Carbon nanofibres	2.7-7	400-600	1.8-2.1	-	-	-
Natural fibres						
Hemp	0.69	70	1.48	0.47	47.30	1.6
Cotton	0.27-0.60	5.5-12.6	1.5-1.6	191-398	3.7-8.4	7.0-8.0
Jute	0.39-0.77	26.5	1.30	302-595	20.38	1.5-1.8
Flax	0.50-1.5	50-70	1.4-1.5	357-1071	35.7-50	2.0-3.0
Ramie	0.40-0.94	61.4-128	1.50	267-625	40.9-85.3	3.6-3.8
Sisal	0.51-0.64	9.4-22.0	1.45-1.50	352-438	6.5-15.1	2.0-2.5
Coir	0.18	4.0-6.0	1.20	0.15	3.3-5.0	30.0

Note: σ = tensile strength, E = Young's Modulus, ρ = density, σ/ρ = specific strength (GPa/[g/cm^3]), E/ρ = specific modulus (GPa/[g/cm^3]), ε = ultimate strain

Glass fibres: Glass fibres have undoubtedly been the most common reinforcing elements in composite materials. In 1937, Owens-Illinois and Corning Glass developed a system for producing glass fibre from silica sand, limestone, boric acid, and other elements. The types of glass include E-glass, S-glass, C-glass, and Quartz.

Glass fibres used for the preparation of composite materials (see Fig. 2.4) are commercially distributed by a large number of companies specialising in the restoration and reinforcement of structures, offering a wide variety of fibre forms.

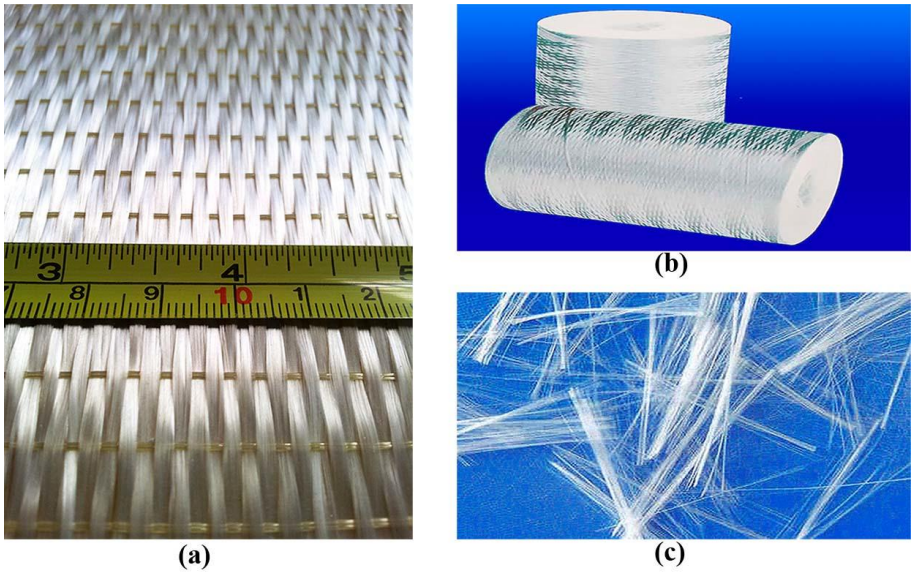

Fig. 2.4: Glass fibres: (a) unidirectional glass fabric; (b) rolls of yarns of glass fabrics [17]; and (c) single filaments of glass fibres [18].

Advantages of the use of glass fibres include:

- Applicable to a wide range of geometries and sizes
- Good strength and durability
- Lower tooling costs
- Increased design flexibility
- Minimal maintenance
- Corrosion resistant

Disadvantages of the use of glass fibres include:

- Mechanical properties are not as good as metals or other reinforcing fibres

Carbon fibres: In carbon fibres, the final strength is usually below the theoretical strength of the carbon-carbon chain [19]. However, by oxidising and pyrolysing a polyacrylonitrile (PAN) textile fibre (preventing it from shrinking in the early stages of the degradation process) and subsequently hot-stretching it, it is possible to convert PAN textile fibre to a carbon filament with an elastic modulus that reflects that of a crystal structure of graphite [10]. Fig. 2.5 shows some types of commercially available carbon fibres.

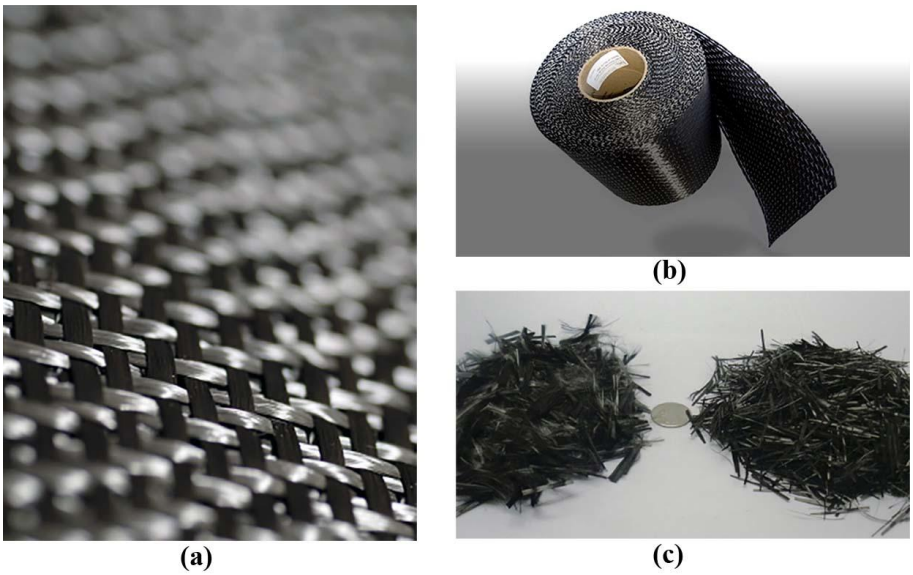

Fig. 2.5: Carbon fibres: (a) bi-directional carbon fabric [20]; (b) roll of carbon fabric [21]; and (c) short monofilaments of carbon fibres [22].

Prior to sale, fibres are usually surface-treated by chemical or electrolytic oxidation methods to improve the quality of adhesion between the fibre and the matrix in a composite. Furthermore, clean room methods of production are commonly used to increase the tensile strength of fibres.

The production of large amounts of carbon/graphite fibres began in the 1950s, and currently, such fibres are among the highest stiffness and highest strength material known today. Types of graphite fibres include:

- Polyacrylonitrile (PAN)-based Fibres
- Pitch-based Fibres
- Rayon-based Fibres

Advantages of the use of carbon fibres include:

- Excellent strength
- Excellent stiffness
- Excellent specific strength and stiffness
- Corrosion resistant

Disadvantages of the use of graphite fibres include:

- Significantly more expensive than glass fibres
- Brittle behaviour

Organic fibres: Bulk polymers are characterised by having a relatively low elastic modulus (less than 100 MPa), but if the polymer is spun into fibres and cold drawn to develop a high degree of molecular orientation, a substantial improvement in strength and stiffness can be achieved. In this process, both the crystalline and non-crystalline phases of the initially isotropic polymer are stretched out and aligned and there is an increase in crystal continuity, resulting in fibres with excellent mechanical properties.

One of the main advantages of these fibres over the inorganic fibres is the absence of a brittle behaviour. Fibres known as Kevlar-49 have been one of the major developments in organic fibres over the last three decades. These fibres have been produced using DuPont aromatic polyamide fibres, known as aramids [23]. Fibres such as Kevlar or aramid (see Fig. 2.6) have strengths on the order of 3.6 GPa and moduli up to 100 GPa (see Table 2.1). The mechanical properties of aramids are between those of carbon and glass fibres, whereas the ductility that these fibres exhibit offers an extra degree of flexibility in the composite design.

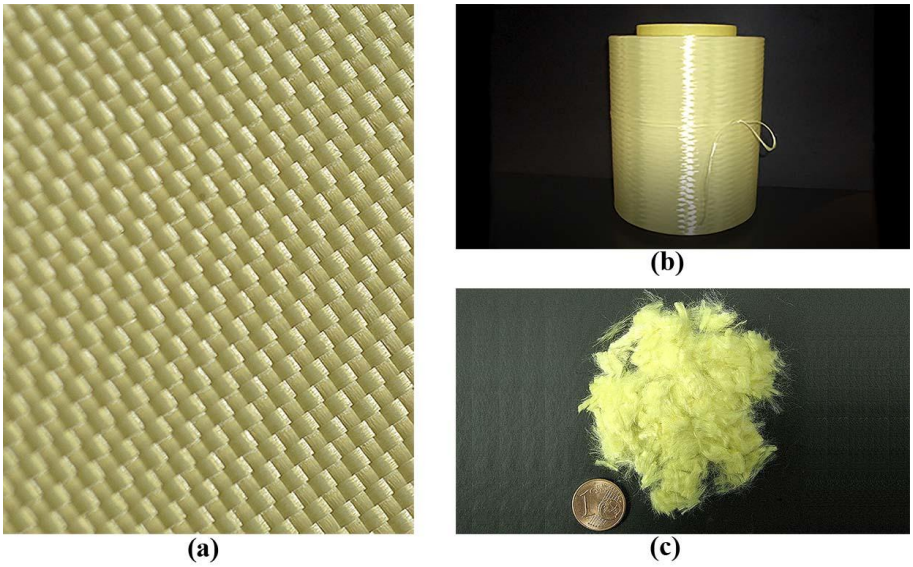

Fig. 2.6: Organic fibres: (a) bi-directional Kevlar fabric [24]; (b) roll of aramid single yarn [25]; and (c) short monofilaments of Kevlar fibres [26].

One important characteristic of these organic fibres is that they are extremely difficult to cut due to the fibrillar structure [10].

Organic fibres for structural applications were introduced for commercial applications in 1971. Graphite fibres are among the highest stiffness and highest strength materials known today. Types of organic fibres include:

- Kevlar Fibres
- Nomex Fibres
- Spectra (ultra-highly oriented polyethylene) Fibres

Advantages of the use of organic fibres include:

- Very high strength
- Very high stiffness
- Very high specific strength and stiffness
- Excellent impact resistance
- High toughness
- Corrosion resistant

Disadvantages for the use of organic fibres include:

- Significantly more expensive than glass fibres
- Properties may be affected by environmental factors (e.g., ultra violet radiation)

Natural fibres: Natural fibres can be defined as fibrous plant material produced as a result of photosynthesis. In the literature, these fibres could be referred to as plant, vegetable, or lignocellulose fibres. Natural fibres could also include hair, feather, wool and silk fibres. Sometimes, mineral fibres such as asbestos, basalt and glass are referred to as a natural material, but in the context of this thesis, only plant fibres will be covered as natural fibres. The use of natural fibres dates back over 10,000 years. Since approximately 8000 B.C. in the Middle East and China, natural fibres have been used for textile cellulosic materials [27]. For example, clothing made from flax fibre dates back to approximately 3000 B.C., and the Babylonians in 650 B.C. used flax for funerary purposes [28]. In the 21st century, the growing need to develop ecological materials that come from renewable sources has boosted the scientific research of natural fibres.

According to the botanical type, natural fibres can be classified into six types [15]: i) bast fibres (jute, flax, hemp, kenaf and ramie), ii) leaf fibres (banana, sisal, agave and pineapple), iii) seed fibres (coir, cotton and kapok), iv) core fibres (kenaf, hemp, jute), v) reed grass (wheat, corn and rice), and vi) all other types (wood, roots, etc.). Fig. 2.7 shows some types of commercially available natural fibres.

Advantages of the use of natural fibres include:

- Low cost
- Renewable resource
- Low density
- High specific properties and Young's modulus
- Good tensile strength
- Non-abrasive to tooling and modulus
- No risks to health
- CO_2 neutral
- Low energy consumption in production
- Biodegradable
- Worldwide availability

- Acoustic abatement capability
- Thermal incineration with high energy recovery
- Can be stored for a long time

Disadvantages of the use of natural fibres include:

- High moisture absorption
- Poor dimensional stability
- Poor microbial resistance
- Discontinuous fibre
- Anisotropic fibre properties
- Low transverse and compressive strength
- Demand and supply cycles
- Production efficiency dependent on environmental conditions
- Time required for fibre preparation with intensive work

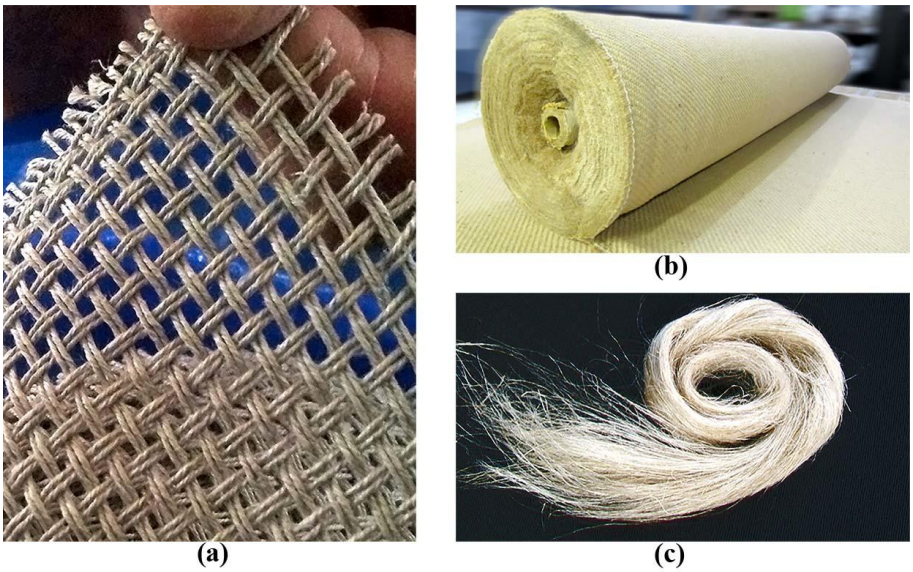

Fig. 2.7: Natural fibres: (a) bi-directional flax fabric; (b) jute fabric roll [29]; and (c) single filaments of flax fibres [30].

One of the most obvious drawbacks of natural fibres is the variability in their physical and mechanical properties, and this problem arises because many factors, such as climate, region of cultivation, age of the plant, growing season, etc., could affect the properties of the fibres. Unfortunately,

natural fibres also exhibit a strong hydrophilic character, which results in a strong sensitivity to water or moisture environments and a poor compatibility with the hydrophobic macromolecular matrices, thereby affecting their mechanical properties and interfacial adhesion. In spite of these disadvantages, the environmental benefits associated with the use of natural fibres appear to override the disadvantages.

The performance of natural fibres will always be compared to that of traditional fibres. The judgments regarding the use of sustainable materials allow researchers to continue the study of means to replace fibres such as carbon and glass in the production of composite materials. Many studies have been conducted in this field [31-34]. Table 2.2 provides a comparative analysis of different environmental parameters in the production of 1 kg of hemp and glass fibres.

Table 2.2: Environmental parameters in hemp and glass fibres production.

Parameters	Hemp fibre [a]	Glass fibre [b]
Power consumption (MJ)	3.4	48.3
CO_2 emissions (kg)	0.6	20.4
SO_x emission (g)	1.2	8.8
NO_x emission (g)	1.0	2.9
BOD (mg)	0.3	1.8

[a] Adapted from 33, [b] Adapted from 34.

Other reinforcing fibres: Alternative fibres such as boron fibres have a high Young's modulus and good strength. In the presence of high temperatures, different types of fibres may be used, such as ceramic fibres (*e.g.,* alumina fibres and silicon carbide fibres). Specialty reinforcements include:

- Boron
- Alumina
- Silicon Carbide
- Other fibres

These reinforcing fibres were originally developed in the 1960s. Advances in carbon and organic reinforcing materials coupled with the lower costs

associated with them have impacted the growth in applications for specialty reinforcements.

Advantages of the use of boron and silicon carbide fibres include:

- Very high strength
- Very high stiffness

Disadvantages of the use of boron and silicon carbide fibres include:

- Extremely high cost

2.1.1.2 Matrix phase

The matrix material binds the fibres together, keeping them aligned. Loads applied to the composite material are then transferred to the reinforcements through the matrix, and thus, composites can withstand tensile, bending and shearing forces. The ability of composites reinforced with fibres to resist these loads is dependent on the presence of a matrix with proper mechanical properties, and the efficiency of this load transfer is directly related to the quality of the fibre/matrix bond. The matrix must also isolate the fibres from each other; in this way, they can act as separate entities. Many reinforcing fibres are brittle solids with varying strengths. In the case of fibre-reinforced composites, the lack of dependence on the behaviour of the fibres prevents the occurrence of a catastrophic failure. The matrix should protect the reinforcing filaments from damage and from environmental attack. Through the interfacial bond strength, the matrix can also be an important means of increasing the toughness of the composite [10].

For several decades, thermoset resins have been the most commonly used matrices for production of fibre-reinforced composites. These matrices are generally in a fluid form or partially polymerised state with a pasty consistency, and when they are mixed with a proper reagent, they polymerise to become a solid, vitreous material. Thermosetting resins such as epoxy resin and polyester or vinylester resins have been widely used for civil engineering applications. Specialised personnel should always handle these types of matrices due to their toxicity [2]. These resins are beyond the scope of this thesis.

Cement-based matrices: The matrices used for FRCM composites must meet special demands regarding the production process, the mechanical properties of the composite and the durability of the reinforcement material. In most cases, small maximum grain sizes (< 2 mm) are used, and hence, these matrix systems can be considered as mortar. In addition, these matrices offer high performance properties in many respects and are used as a construction composite material, such that these matrix systems are also called fine grained concrete (or fine concrete) [35]. According to the ACI 549.4R-13 [36] standard, a cementitious matrix material is "*an inorganic hydraulic and non-hydraulic cementitious binder (mortar) that holds in place the structural reinforcement meshes in fabric-reinforced cementitious matrix (FRCM) composite material. If the mortar is polymer-modified, the maximum content of organic compounds (dry polymers) in the matrix is limited to 5 % by weight of cement.*"

Advantages of the use of ceramic matrix include:

- Dimensional stability at high temperatures
- High chemical stability
- High thermal stability
- Excellent mechanical properties (strength and stiffness)
- Resistant to moisture absorption
- Applicable to extreme temperatures (2000° to 4000°)

Disadvantages of the use of ceramic matrix include:

- Very brittle
- Very high consolidation pressures are required
- Very expensive to produce and maintain

2.1.2 Types of composite materials

On the basis of the type, geometry and orientation of the reinforcing phase, composites can be classified into three broad categories. Fig. 2.8 illustrates a typical composite classification.

Composites reinforced with fabrics or textiles are within the category of continuous fibre-reinforced composites. Alternatively, composite materials can be classified according to the physical, mechanical and long-term

properties and can also be designed according to the matrix type. Considering the latter, the most common composite designations are polymer matrix composites (PMCs), metal matrix composites (MMCs) and ceramic matrix composites (CMCs). Cementitious composites are within the classification of CMC composites. The characteristic that distinguishes CMC composites is the brittle nature of the matrix.

Therefore, their mechanical behaviour is different from that of PMC composites [12] (e.g., the ultimate strain in tension of these materials is considerably smaller than that of the fibres). In the literature, definitions such as textile-reinforced concrete (TRC), fibre-cement reinforced (FRC), textile-reinforced mortar (TRM), mineral-based composites (MBC), engineering cementitious composites (ECC), high performance fibre-reinforced cementitious (HPFRC) and fabric-reinforced cementitious matrix (FRCM) composites have been used to identify the different types and evolution of cement-based composites [35-39].

A composite laminate is a sheet of reinforcing fibres or fabrics embedded with a matrix paste [4]. These laminates could be stacked on top of each other in the same or in various orientations to form multilayer composites. Composites reinforced with fabrics or textiles (FRCM) are a rather new development of a composite material, where multi-axial fabrics are used in combination with fine-grained mortar. This approach allows for the production of very small thickness composites with a high compressive and tensile strength. Fig. 2.9 shows some fabric types with open constructions or meshes.

The use of fabrics that are placed in the main stress direction leads to a high effectiveness in comparison with the use of short fibres. However, because FRCM composite is an innovative material, further research is required for design optimisation and safe use for strengthening applications. FRCM composite systems evolved from Ferro-cement (metallic fibre-reinforced cement), and fabrics of dry fibres replaced the reinforcing fibres. Advances in the textile-engineering field consist of the use of two-dimensional fabrics and three-dimensional textiles as reinforcement options made from carbon, alkali-resistant (AR) glass, polymeric fibres, or hybrid systems.

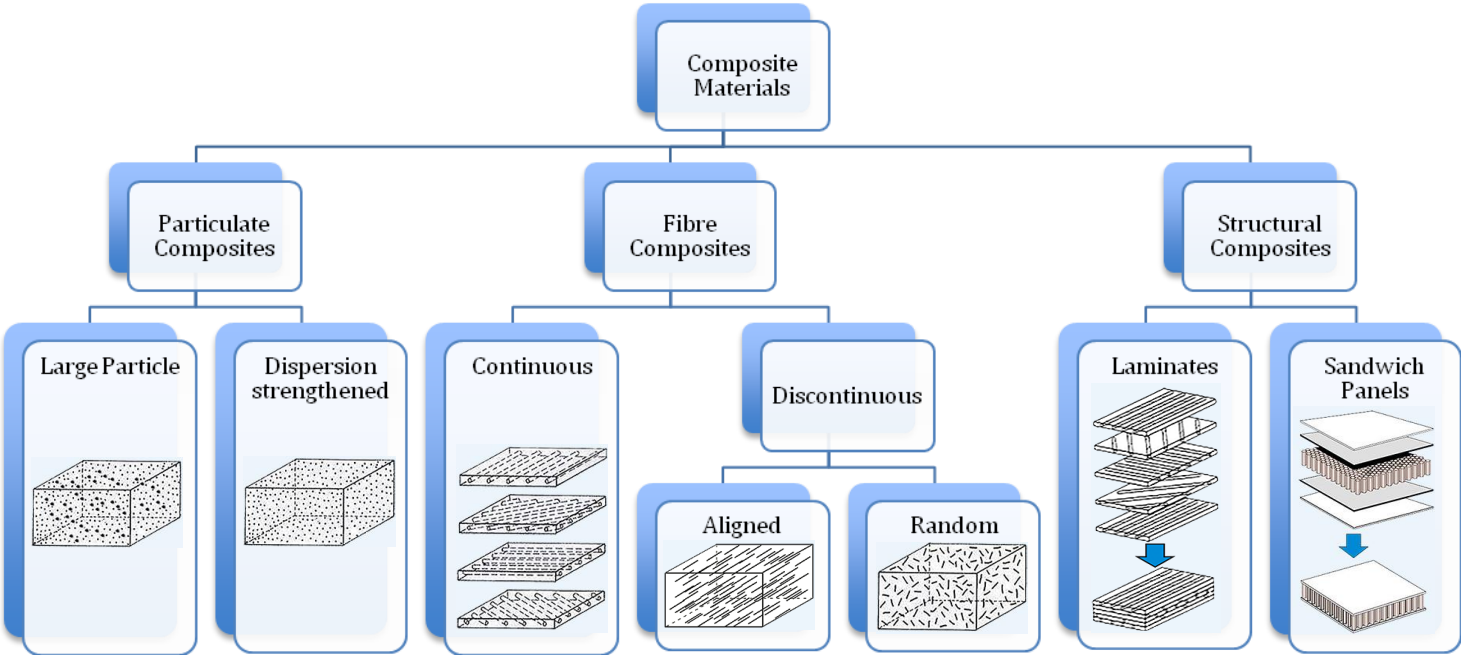

Fig. 2.8: Classification of composites by reinforcement shape and continuity.

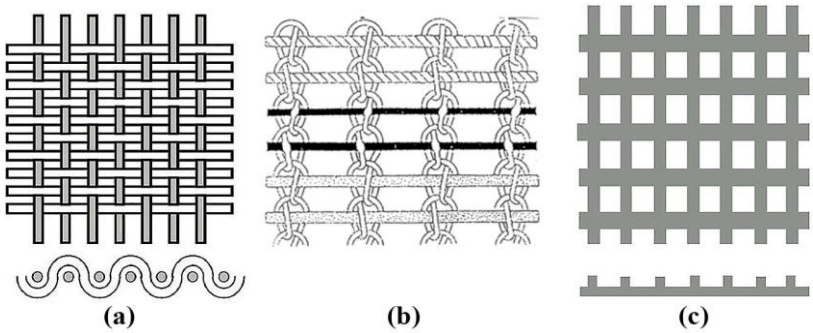

Fig. 2.9: Fabric types [36]: (a) woven; (b) knitted; and (c) bonded.

2.1.3 Properties and mechanical behaviour of FRCM composites

In fibre-reinforced composites, fibres are the constituents that play the role of supporting elements, and the mechanical properties of the composites, such as the stiffness and strength, are directly influenced by the contribution of the fibres to the mechanical integrity of the overall materials. The purpose of reinforcement in cementitious composites is to improve the tensile behaviour of cement-based matrices; for example, the tensile strength is approximately equal to 10–12% of the compressive strength [40], and the brittleness of this inorganic material affects its ductility. By incorporating reinforcing systems including fabric or textile structures, the flexural and tensile strength, the fracture toughness and post-cracking ductility are greatly improved; as a result, parameters such as the volume fraction of fibres and type of reinforcement determine the mechanical response of composites. The volume fraction of fibres (V_f) and the matrix content (V_m) are defined as:

$$V_f = \frac{v_f}{v_c} \tag{2.1}$$

$$V_m = \frac{v_m}{v_c} \tag{2.2}$$

where v_f is the volume of the fibres, v_m is the volume of the matrix, and v_c is the volume of the composite. If the composite is considered a non-porous material, the sum of the volume fractions is 1, and thus:

$$V_c = V_f + V_m \tag{2.3}$$

$$V_m = 1 - V_f \tag{2.4}$$

The main feature of composites is the transfer of stresses between the matrix and the fibres, which is the basis for studying their mechanical behaviour. For example, when tensile loads are applied, both the fibres and the matrix will stretch the same amount in the direction of loading (equal strains). If the fibres are stiffer than the matrix, then they will resist most stresses; in contrast, if the matrix is stiffer than the fibres, then the stresses will be greater in the matrix. Therefore, by considering the contributions of the phases with the overall load, the Young's modulus of the composites can be calculated using the well-known "rule of mixtures". The same concept is applied to calculate the resistance of the composite. Thus, the basic equations of the theory of composite materials are as follows:

$$\sigma_c = \sigma_m V_m + \sigma_f V_f \tag{2.5}$$

$$E_c = E_m V_m + E_f V_f \tag{2.6}$$

where σ_c, σ_m, and σ_f are the tensile strengths of the composite, matrix and fibre, respectively, and E_c, E_m, and E_f are the Young's moduli of the composite, matrix and fibre, respectively. From these equations, it is clear that a certain proportion of the load will be carried by the fibres and the remainder will be carried by the matrix. In the elastic range, these proportions are dependent on the volume fraction, shape and orientation of fibres and on the stiffness of both phases [12]. The matrix material in FRP composites exhibits more ductility than fibres. This characteristic leads to an elastic behaviour up to the point of failure when the fibres are elastic up to failure. In contrast, inorganic matrices in FRCM systems crack before reaching the maximum strain of the fabrics, and the reinforcement becomes effective at this cracking stage.

In cracked areas, the stresses are carried entirely by the reinforcing fabrics [41]. Therefore, there are two types of failure to consider; either the matrix or the reinforcement fails first (see Figs. 2.10a and 2.10b). In the case of cement-based composites, a low volume fraction of fibres increases the ductility of the matrix; however, neither the strength nor the stiffness of the composite is improved because it is the matrix that mainly provides the load-bearing capacity.

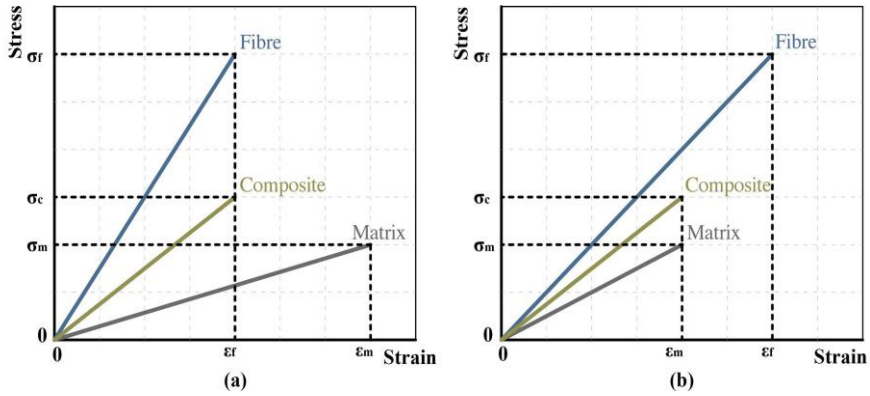

Fig. 2.10: Stress-strain relationship when the matrix strain capacity is higher than the fibres: (a) matrix dominated failure; and (b) fibre dominated failure.

By gradually increasing the volume fraction of fibres, the strength and the post-cracking ductility are remarkably improved in these composite systems, resulting in a fibre-dominated failure mode [12] (see Fig. 2.10b).

Considering FRCM composites, the tensile performance is directly influenced by the fabric/matrix interaction in terms of mechanical interlocking, physical bonds and chemical reactions as well as on the properties of the constituent materials, in particular:

- The ultimate tensile strength depends on the efficiency of the reinforcement.

- The cracking resistance and the so-called first crack load depend mostly on the matrix properties, which may be considerably improved if an efficient volume fraction of fibres is used.

- Generally, the compressive strength of FRCM systems is not assessed because local compressions are usually supported directly by the matrix.

- The penetration capability is achieved by the reinforcing phase in the matrix. A suitable penetration of the fabrics provides an improved anchorage and ability of the system to develop and maintain a bond. Therefore, the geometry of the fabrics is also a key parameter in the analysis of the mechanical behaviour of FRCM systems.

2.2 Natural fibre-reinforced cementitious composites

For almost three decades, the scientific community has directed its attention to the research of natural fibres to discover substitutes to asbestos fibres as well as traditional fibres such as glass and carbon fibres for producing composites and developing optimised production processes. One of the areas with the greatest interest is the use of cementitious matrices that increase the condition of sustainable material and allow for application in the construction industry. Natural fibre-reinforced cementitious (NFRC) composite is a generic name covering different realities because of the nature of the matrix, the nature of the fibre, and the treatment applied to the fibre [42].

The mechanical properties of natural fibres are inferior to those of glass or synthetic fibres, which will result in a lower composite strength and stiffness. Despite this, the mechanical performance levels that are exhibited by natural fibres are high enough for many applications, especially when considering the ability to increase the strain capacity offered by these fibres. The use of natural fibres is not intended to duplicate the mechanical performance of traditional composites; however, if the properties of these composites are properly exploited and their advantages such as higher strain capacity are taken into account in the design, then NFRC composites can be successfully used in applications that have typically been designed for FRP or FRC composites.

2.2.1 Production techniques

Production processes must ensure adequate bonding between the matrix and the reinforcement. Therefore, the characteristic of each technology is the means to bring together the matrix and reinforcing materials. For FRCM composites, the reinforcing phase may consist of chopped fibres, rovings, technical textiles or combinations thereof. Under laboratory conditions, or when small amounts of samples are examined, the production technique is often a manual technique. In addition, to produce fabric-reinforced composites, techniques for short-fibre-reinforced cement or combined techniques with other production processes have been typically used. Moreover, the most common production techniques for FRP composites can

also be used to produce natural fibre-reinforced polymer (NFRP) composites. The same can be applied to the case of natural fibre-reinforced cementitious (NFRC) composites, and some of the production technologies that are currently available may be classified as follows:

Premix process: Process in which the fibres are combined with the cementitious matrix in a mixer. The fibres are treated simply as an extra ingredient in the most common method of producing a cementitious mix. However, because the fibres reduce the workability, only up to approximately 2% fibres by volume can be introduced into the mix using this method.

Spray-up process: This process has been used primarily with glass fibre-reinforced cement. Chopped natural fibres and cement slurry are sprayed simultaneously onto the forming surface to produce thin sheets. With this technique, substantially higher fibre volumes, up to approximately 6%, can be incorporated into the NFRC.

Premix/spray process: Using a modification of normal shotcreting techniques, this process is a combination of both methods previously discussed. Chopped strands are added to the matrix, and that mix is sprayed into the mould. Usually, a fibre content of approximately 2 vol.-% is used, but often, additional textile reinforcement is used to increase the load-bearing capacity [43]. With this method, the lining of tunnels and stabilisation of rock slopes has been found to be possible.

Pulp-type processes: For cellulose or other fibres used as a replacement for asbestos, the fibres are dispersed in cementitious mortar, which is then dewatered to produce thin sheet materials. These sheets can be built up to the required thickness by layering. This process yields fibre contents of typically from 9% to over 20% by volume.

Hand lay-up process: Layers of fibres in the form of mats or fabrics can be placed in moulds, impregnated with a cementitious mortar, and then vibrated or compressed to produce dense materials with very high fibre contents.

Pultrusion process: This technique is used to produce fabric-cement laminate composites by passing the fabrics through a slurry infiltration

chamber and then pulling them through a set of rollers to squeeze the cementitious matrix in the openings of the fabric, which should be sufficiently fluid to enable the fabric to transfer through the cement mortar but dense enough so that it will remain on the fabric. This methodology removes excessive paste and forms composite laminates.

Extrusion process: Injection moulding and compression moulding refer to short-fibre-reinforced cementitious composites. However, these methods are listed because they can be combined with the production techniques described in [35] for FRCM systems, including Wellcrete technology (low pressure extrusion) and a module process technology.

2.2.2 Durability of natural fibres in cementitious composites

The fibre/matrix interface is a key parameter in the development of the properties of FRC composites, and its microstructure has a significant impact on durability. In the reference sources, a summary of the findings from many studies can be found that addresses these issues [44,45]. Based on these studies, degradation with ageing was found to occur in FRC composites produced with fibres that are known to be immune to alkali attack (e.g., carbon-FRC systems) [46], and in most cases, it is concluded that the degradation of the composite mechanical properties is attributed to densification, bond enhancement and bundle filling/mineralisation effects.

The application of natural fibres as reinforcement of cementitious materials involves potentially deleterious effects on certain species of fibres. In this context, most of the plant fibres are formed from lignin, cellulose and hemicellulose, which have interfacial adverse reactions when in contact with cementitious matrices. In particular, reactions between an ordinary Portland cement (OPC) matrix and the lignin cause degradation in the composite strength. [47]. This degradation occurs because the alkaline pore water dissolves the lignin and hemicellulose existing in the middle lamellae of the fibres, thus weakening the link between the individual fibre cells [48]. An additional mechanism is the alkaline hydrolysis of cellulose molecules, which causes degradation of molecular chains, therefore leading to a reduction in the degree of polymerisation and lower tensile strength [47]. Another aspect to consider in cementitious composites reinforced with

natural fibres is carbonation, which induces mineralisation [49] and microstructural changes and modifies the interface from being open and porous to more dense and homogenous [50] (see Fig. 2.11), contributing to the increase in the first crack strength and reduction in toughness, by reducing the deformability of fibres. On the basis of a chemical analysis conducted by Tolêdo Filho et al. [48], a considerable transport of cement chemicals, mainly calcium products, to the fibres during the cycles of wetting and drying confirms the mineralisation of natural fibre.

To enhance the durability of NFRC composites, several approaches have been studied [51-53]. Treatments such as modifications to the Portland cement matrix through the addition of undensified silica fume and blast-furnace slag, carbonation of the cementitious matrix, pre-impregnation of the fibres in slurry silica fume, fibre coating with latex, among others, have decreased aging effects in natural fibres, but it seems that the most favourable approach is that of reducing or replacing the OPC portion in the matrix.

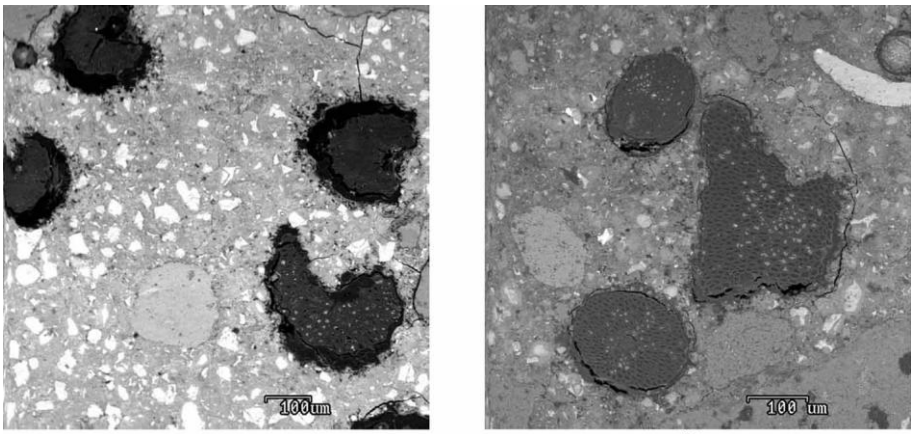

Fig. 2.11: SEM images of the cross-section of coconut fibre reinforced cement composite [48]: (a) 28 day specimen; (b) specimen submitted to 25 cycles of wetting and drying

The durability problems of natural fibres are increased when moisture is present. Natural fibres are very sensitive to changes in moisture content, which affect both the mechanical properties of the fibre and its dimensions in terms of the cross-sectional area. When natural fibre absorbs moisture, it

loses stiffness and gains ductility. The dimensional changes observed in natural fibres during wetting and drying may lead to changes in the contact pressure across the interface, causing variations in the bond. As a result, the overall properties of the composite are very sensitive to moisture content, and most of the moisture sensitivity of plant fibre composites can be attributed to the hygroscopic nature of the fibres.

2.3 FRCM composites in construction applications

According to ACI 549.4R-13 [36], at least three manufacturers produce commercial FRCM systems for the repair and strengthening of concrete and masonry structures. These systems are based on carbon, AR-glass, basalt and polyparaphenylene benzobisoxazole (PBO) fibres, and in all cases, the manufacturers provide premixed mortar powders.

The potential of these innovative systems has been evaluated in numerous applications involving the repair and strengthening of structural and non-structural elements in the construction sector. As documented in the literature, FRCM composites have been used to repair roof-openings for high temperature ducts. These ducts were to be operated at temperatures considered too high for conventional FRP repair systems.

Another application that should be highlighted is the strengthening of a railroad bridge (see Fig. 2.12) along the Rome-Formia railway line in Italy [54,55].

Fig. 2.12: Strengthening of railway bridge: (a) & (b) installation of the FRCM systems [54,55].

After a complete characterisation of the constituents of the system and a detailed analysis and design, using a limit state analysis, the application of reinforcement was then performed. The concrete surface was cleaned and rebuilt in locations that exhibited signs of deterioration. A first matrix layer was then applied, followed by the first phase of the reinforcement. In this project, the use of a two-layer FRCM system was planned.

To reinforce concrete and masonry structures, FRCM composites have also proven effective in other applications such as the following: strengthening of reinforced concrete tunnel lining along the Egnatia Odos Motorway in Greece [56]; strengthening a trestle of a railway bridge base confinement in New York [56]; confinement of a concrete support base of a piece of equipment in an industrial plant in the Midwestern United States, which shall remain at a temperature of 82 °C (180 °F); strengthening of reinforced concrete bridge piers of a structure located in Novosibirsk, Russia [56]; strengthening of the unreinforced masonry chimney part of the now-closed sawmill François Cuny complex located in the municipality of Gerardmer in France [56]; school building strengthening in Karystos, Greece [57]; and the masonry dome strengthening in the old church of Panaghia Crina in the island of Chios, Greece [57].

FRC composites reinforced with natural fibres are already commercially available [58]. Polyvinyl alcohol (PVA) fibres and a combination of cellulose and short PVA fibres have also been proposed for asbestos replacement [59]. In addition, many efforts have been made to use sisal and coconut fibres in the construction industry; these results have been reported in [48,52,60-62]. Natural fibres such as sisal, jute and coconut have been used as reinforcement of cementitious matrices in the form of short filament fibres [48,63]. These composites presented a softening behaviour with low tensile strength, which directs their use for non-structural applications. To produce a composite reinforced with natural fibres that presents strain-hardening behaviour, long natural fibres must be used; as a result, natural fabric-reinforced composites can provide the required performance for load-bearing applications. A cementitious composite system produced using natural fabrics was developed as part of an extensive research project carried out in the University of Calabria, and the results are reported in this thesis.

Currently, research projects such as the NATEX project have focused on the development of textiles suitable for structural applications. The NATEX project is funded under the European Commission 7th Framework Programme. Possible application areas for these textiles include the transportation sector, e.g., rail and road, and the repair and strengthening of masonry structures.

It seems unlikely that natural fibre composites will ever compete with fabric composites reinforced with advanced fibres; nevertheless, in the case of glass-fibre-reinforced material or in specific conditions where the low density or higher strain capacity of cellulose fibres is an obvious advantage, the situation might be different.

2.4 Technical guides for the strengthening with FRCM composites

FRCM is a system that has emerged in recent years; only since 2003 has the new International Code Council Evaluation Services (ICC-ES) acceptance criteria for masonry and concrete strengthening using fibre-reinforced cementitious matrix composite systems (AC434) [39] been available (since 2013, the AC434 changes the term *fibre* for *fabric* in the FRCM system definition), and these criteria were updated by the Evaluation Committee in October 2011. Properties evaluated under such criteria include flexural and shear capacities, performance under environmental exposures, performance under exposure to fire conditions, and structural design procedures. In addition, the acceptance criteria have been prepared to provide interested parties with guidelines for demonstrating compliance with performance features of the codes referenced in the criteria. However, the reason for the development of the criteria is not to provide requirements for testing and determination of structural capacity, reliability and serviceability of these composite systems. In 2013, this document was expanded and superseded by AC434-13, which provides guidance for evaluation and characterisation of FRCM systems. AC434-13 was developed in consultation with industry, academia, and other parties. In June 2013, the College of Engineering, Structures and Materials Laboratory, Department of Civil, Architectural and Environmental Engineering of the University of Miami performed a study of an Italian company specialised in products for the strengthening and repair of structures in which FRCM systems are

evaluated using the theoretical design calculations and analysis criteria reported in AC434. Design criteria for reinforced concrete (RC) and unreinforced wall specimens are detailed in this document, such as the following: wall shear test specimens made from concrete masonry units and clay bricks, wall flexural test specimens made from concrete masonry units and clay bricks, RC slab flexural test specimens for nominal high and low strength concretes, RC beam flexural test specimens for nominal high and low strength concretes, RC beam shear test specimens for nominal high and low strength concretes, and RC column flexural test specimens for nominal high and low strength concretes.

In early 2014, the American Concrete Institute (ACI) published the technical document ACI 549.4R13 [36] "Guide to Design and Construction of Externally Bonded FRCM Systems for Repair and Strengthening Concrete and Masonry Structures". This guide covers FRCM composite systems used to strengthen existing concrete and masonry structures, providing the following: background information and field applications; FRCM material properties; axial, flexural, and shear capacities of the FRCM-strengthened structures; and structural design procedures. The guide idealises the FRCM tensile stress-strain curve as a bilinear curve (un-cracked and cracked segments). The initial segment of the curve corresponds to the FRCM linear elastic behaviour. The second linear segment is characterised by the cracked tensile modulus of elasticity. The design approach for flexure and shear strengthening considers an effective usable strain of the FRCM composite. Once the effective strain is defined, the design procedure of FRCM strengthening systems is similar to the design procedure using FRP composites [64].

2.5 References

[1] Kelly A, editor. Concise Encyclopedia of Composite Materials. Pergamon; 1994.

[2] CNR-DT 200 R1. Istruzioni per la Progettazione, l'Esecuzione ed il Controllo di Interventi di Consolidamento Statico mediante l'utilizzo di Compositi Fibrorinforzati. Commissione di Studio per la Predisposizione e l'Analisi di Norme Tecniche relative alle costruzioni – CNR; 2013.

[3] Griffith A. The phenomena of rupture and flow in solids. In: Philosophical Transactions of the Royal Society 1920;221A:163–198
[4] Vlot A, Gunnink JW. Fibre Metal Laminates, Kluwer Academic Publishers, Dordrecht, The Netherlands; 2001.
[5] Technical Fibre Products Inc. Consumer Electronics. 2014, New York, USA. <http://www.tfpglobal.com/applications/consumer-electronics/>.
[6] The Engineer website. Lightening the load: new materials for automotive. 2014, London, England. <http://www.theengineer.co.uk/automotive/in-depth/lightening-the-load-newmaterials-for-utomotive/101296
9.article>.
[7] Composites World. Hotel wrap: Curvilinear pultrusions. 2010, Cincinnati, USA. <http://www.compositesworld.com/articles/hotel-wrap-curvilinear-pultrusions>.
[8] Nicolais L, Meo M, Milella E. Composite materials: a vision for the future. Springer London, Limited; 2011.
[9] Chung D.L. Composite Materials: Functional Materials for Modern Technologies. Springer, London; 2003.
[10] Harris B. Engineering composite materials. 2nd ed. Cambridge: The Cambridge University Press; 1999.
[11] Fangueiro R, editor. Fibrous and composite materials for civil engineering applications. Woodhead Publishing; 2011.
[12] Mobasher B. Mechanics of Fibre and Textile Reinforced Cement Composites. CRC Press. Taylor & Francis Group, Boca Raton, Fl; 2012.
[13] Hollaway LC. A review of the present and future utilisation of FRP composites in the civil infrastructure with reference to their important in-service properties. Constr Build Mater 2010;24:2419–45.
[14] Bos HL. The potential of flax fibres as reinforcement for composite materials. Ph.D. Thesis, TUEindhoven 2004.
[15] Pickering K. Properties and performance of natural-fibre composites. CRC Press; 2008.
[16] Gibson RF. Principles of composite material mechanics. New York: McGraw-Hill; 1994.

[17] Textile engineer blogspot. Some Common Man-Made Fibres. 2010. <http://textileengineerr.blogspot.it/2010/10/some-common-man-made-fibers.html>.

[18] Textile information Blog For Student. Introduction of Glass Fiber | Types of Glass Fiber | Properties of Glass Fiber | Manufacturing Processes of Glass Fiber | Uses of Glass Fiber or Glass Yarn. 2014. <http://texnoteblog.wordpress.com/2014/01/15/introduction-of-glass-fiber-types-of-glass-fiber-properties-of-glass-fiber-manufacturing-processes-of-glass-fiber-uses-of-glass-fiber-or-glass-yarn/>.

[19] Watt W. Discussion Meeting on Strong Fibrous Solids, Proc Roy Soc Lond 1970; A319: 5-15.

[20] Innovation in Textiles. Toray to develop carbon fibre car parts with Daimle. 2010, Nantwich, UK. <http://www.innovationintextiles.com/toray-to-develop-carbon-fibre-car-parts-with-daimler/>.

[21] Kimia. Kimitech CB320 data sheet. Kimia S.p.A. 2009, Perigia, Italy. <http://www.kimia.it/default/prodotti.action?idCategoria=10&searchType=categoria&idLingua=3>.

[22] Reinforcing Plastics. Launching the carbon fibre recycling industry. Elsevier Ltd. 2010, Kidlington, UK. <http://www.reinforcedplastics.com/view/8116/launching-the-carbon-fibre-recycling-industry/>.

[23] Yang HH. Kevlar Aramid Fibre. John Wiley. Chichester; 1993.

[24] Army technology. Fibre Armour: Stronger than Steel. 2014. <http://www.army-technology.com/features/feature98985/feature98985-4.html>.

[25] Smart Rigging. Aramid (Twaron) The performance fibre. 2014, Joure, Netherlands.<http://www.smartrigging.com/index.php?page=17&item=22>.

[26] Outdoors NB. Materials and Construction. 2014, Saint John, Canada. <http://outdoorsnb.com/Kayak-Materials.php>.

[27] Railey K. The amazing hemp plant (Cannabis satavi L.). H&B Online &content, 1993-2001 Chet Day, 2001. <htt://chetday.com/hemp.html.

[28] Mikuriya, T.H., 'Marijuana: Medical papers', in Medi-Comp Press, Oakland, California, 1973, pp xiii-xxvii.

[29] Composite evolution. Biotex Jute. 2014, Chesterfield, UK. <http://www.compositesevolution.com/Products/Biotex/BiotexJute.aspx>.

[30] The felting and fiber studio. Natural Wools and Natural Fibers. 2012. <http://feltingandfiberstudio.com/2012/02/28/natural-wools-and-natural-fibres/>.
[31] Joshi SV, Drzal LT, Mohanty AK, Arora S. Are natural fiber composites environmentally superior to glass fiber reinforced composites. Compos A Appl Sci Eng 2004;35(3):371–6.
[32] Wambua P, Ivens J, Verpoest I. Natural fibres: can they replace glass in fibre reinforced plastics. Compos Sci Technol 2003;63:1259–64.
[33] Shahzad A. Impact and Fatigue Properties of Natural Fibre Composites. VDM Verlag Dr. Müller, Saarbrücken, Germany, 2010.
[34] Mougin. G. Natural Fibre Composites – Problems and solutions. JEC Composites 2006;25:32–5.
[35] Brameshuber W, editor. State-of-the-art report of RILEM technical committee 201 TRC: textile reinforced concrete (RILEM Report 36). Bagneux: RILEM Publications S.A.R.L., 2006.
[36] ACI 549.4R-13. Guide to Design and Construction of Externally Bonded Fabric-Reinforced Cementitious Matrix (FRCM) Systems for Repair and Strengthening Concrete and Masonry Structures. ACI, 2013.
[37] Blanksvärd T, Täljsten B. Strengthening of concrete structures with cement based bonded composites. J Nordic Concr Res 2008:133–54.
[38] Matsumoto T, Mihashi H. DFRCC Terminology and Application Concepts. Committee Report. Journal of Advanced Concrete Technology 2003;1(3):335-40.
[39] AC434-13 Acceptance Criteria For Masonry And Concrete Strengthening Using Fiber Fabric-Reinforced Cementitious Matrix (Frcm) Composite Systems. AC434, 2013.
[40] Brandt AM. Cement-based composites: materials, mechanical properties and performance. New York: E and FN Spon, 1995.
[41] Larrinaga P, Chastre C, Biscaia HC, San-Jose JT. Experimental and numerical modeling of basalt textile reinforced mortar behavior under uniaxial tensile stress. Mater Des 2014;55:66–74.
[42] Arsène MA, Savastano JH, Allameh SM, Ghavami K, Soboyejo WO. Cementitious composites reinforced with vegetable fibers. In Anais da 1st Inter American Conference On Nonconventional Materials And

Technologies In The Ecoconstruction And Infrastructure. João Pessoa-PB, 2003.

[43] Pachow. U. Textile Reinforced Concrete - New Manufacturing Technologies and Applications. In: 12th International Techtextil Symposium for Technical Textiles, Nonwovens and Textile Reinforced Materials. Frankfurt; 2003.

[44] Majumdar A.J, Laws V. Glass Fibre Reinforced Cement. BSP Professional Books, Oxford 1991. p. 197.

[45] Bentur A, Mindess S. Fibre Reinforced Cementitious Composites. Elsevier Science Publishers Ltd. UK Barking 1990. p. 449.

[46] Katz A, Bentur A. Effect of matrix composition on the aging of CFRC. Cement and Concrete Composites 1995;17:87-97.

[47] Gram HE. Durability of natural fibres in concrete. Swedish Cement and Concrete Research Institute, Research Fo. 1:83, Stockholm, 1983.

[48] Toledo Filho RD, Scrivener K, England GL, Ghavami K. Durability of alkali sensitive sisal and coconut fibres in cement based composites. Cement Concr Compos 2000;6(22):127–43.

[49] Bentur A, Akers S.A.S. The microstructure and ageing of cellulose fibre reinforced cement composites cured in a normal environment. International Journal of Cement Composites and Lightweight Concrete 1989;11:99–109.

[50] MacVicar R, Matuana L.M, Balatinecz J.J. Aging mechanisms in cellulose fiber reinforced cement composites. Cement and Concrete Composites 1999;21:189-196.

[51] Toledo Filho RD, England GL, Ghavami K, Scrivener K. Development of vegetable fibre–mortar composites of improved durability. Cem Concr Comp 2003;25:185–96.

[52] Canovas MF, Selva NH, Kawiche GM. New economical solutions for improvement of durability of Portland cement mortars reinforced with sisal fibers. Mater Struct 1992;25:417–22.

[53] Juárez C, Durán A, Valdez P, Fajardo G. Performance of "Agave lechuguilla" natural fiber in Portland cement composites exposed to severe environment conditions. Build Environ 2007;42:1151–7.

[54] Berardi F, Focacci F, Mantegazza G, Miceli G. Rinforzo di un Viadotto Ferroviario con PBO-FRCM. In Proceedings 1st Convegno Nazionale Assocompositi, Milán, Italy; 2011.

[55] D'Ambrisi A, Focacci F, Caporale A. Strengthening of masonry–unreinforced concrete railway bridges with PBO-FRCM materials. Compos Struct 2013;102:193–204.

[56] Nanni A. A New Tool in the Concrete and Masonry Repair. Concrete International 2012; 34(4):43–9.

[57] Triantafillou T.C. Textile-Reinforced Mortars (TRM) versus Fibre-Reinforced Polymers (FRP) as Strengthening and Seismic Retrofitting Materials for Reinforced Concrete and Masonry Structures. In: International Conference on Advanced Composites in Construction (ACIC07), University of Bath, 2007.

[58] Coutts R.S.P. Wood fibre reinforced cement composites. In: Natural Fibre Reinforced Cement and Concrete. Vol. 5. London, 1988, p.1–62.

[59] Hikasa J, Genba T, Mizobe A, Okazaki M. Replacement for asbestos in reinforced cement products – "Kuralon" PVA fibers, properties, structure. In: International Man-Made Fibers Congress, Dornbirm, 1986.

[60] Toledo Filho RD, Joseph K, Ghavami K, England GL. The use of sisal fiber as reinforcement in cement based composites. Braz J Agric Environ Eng 1999;3:245–56.

[61] Berhane Z. Performance of natural fiber reinforced mortar roofing tiles. Mater Struct 1999;27:347–52.

[62] Toledo Filho RD. Natural fiber reinforced mortar composites: experimental characterisation. PhD thesis, DEC-PUC-Rio, Brazil; 1997.

[63] Ramakrishna G, Sundararajan T. Impact strength of a few natural fibre reinforced cement mortar slabs: a comparative study. Cem Concr Comp 2005;27:547–53.

[64] Structure Magazine. The Second Generation of Externally-Bonded Composite Systems for Strengthening of Concrete and Masonry Structures. 2014. <http://www.structuremag.org/?p=5446>.

Chapter 3

FLAX AND SISAL-FRCM COMPOSITES

3.1 Introduction

Natural fibres are one of the most studied materials, and because fibres such as sisal, henequen, coconut (coir), flax, bamboo, hemp, jute, wood and palm are strong, lightweight, cheap and non-polluting, they have become attractive alternatives to conventional fibres, e.g., glass, aramid and carbon fibres, as reinforcements in composite materials [1,2]. Furthermore, unlike brittle or mineral fibres, natural fibres exhibit a high degree of flexibility that enables them to bend rather than fracture when processed or being intensively mixed with a matrix. This study focussed on sisal and flax fibres. These fibres, due to their good mechanical properties, may have important implications for many different applications [3-5].

It is well known that cement is the most important building material and is mainly used as a binder in concrete production, but due to its brittleness, low tensile strength and poor resistance to crack opening and propagation, bars or fibres are used for reinforcement. In recent years, scientific interest

has been directed toward natural fibre reinforced cementitious (NFRC) composites, and scientists have studied their performance in construction applications. In particular, short fibres, long fibres and textile laminates of cellulosic fibres have been investigated using inorganic matrices [6-8].

Despite encouraging results, some deficiencies in the durability of NFRC composites have been observed. It was observed that composites produced with an OPC (ordinary Portland cement) matrix undergo an accelerated ageing process due to fibre mineralisation and alkali attack related to variations in humidity and are subject to a reduction in post-cracking strength and toughness [9,10]. Furthermore, fibre degradation leads to an increase in fibre fracture and a decrease in fibre pull-out. Several methods have been developed to improve the durability of natural fibres reinforcing cement matrices without yielding satisfactory results. Pre-treating fibres with sodium silicate, sodium sulphite, magnesium sulphate, barium, iron or copper compounds and sulphite salts have not prevented fibre degradation [11]. Impregnating fibres with water-repellent agents and incorporating fly-ash in cement matrices has been observed to reduce fibre mineralisation in "Agave Lechuguilla" and "Hemp" fibres [12,13]; however, studies conducted by Gram using polyvinyl acetate, amide wax, silicone oil, tar, rubber latex, asphalt and stearic acid have shown that various methods of fibre impregnation are ineffective for improving durability [11]. Impregnating fibres with organic compounds has been shown to slightly reduce the brittleness of aged fibres [10]. The best results have been achieved by matrix modification. Both sealing the pores of a matrix by adding small amounts of zinc stearate powder or wax in fresh cement paste and impregnating the hardened matrix with sulphur have been shown to preserve the long-term properties of natural fibres [11]. Similarly, reducing matrix alkalinity by adding silica fume, slag, natural pozzolans or using both high-alumina cement and magnesium phosphate cement does not affect the toughness of composites or the bond between matrices and fibres [11,14,15].

To produce flax or sisal FRCM composites with improved durability, this study focussed on the use of hydraulic lime-based matrices instead of a Portland cement matrix. The matrices were a natural hydraulic lime-based mortar (NLM) mix with a low content of water-soluble salts specially created for strengthening masonry structures and a lime-based grouting

(NLG) mix containing carbonate filler and pure pozzolan with a high content of reactive silica (fly-ash family). These matrices meet the requirements BS EN 998/2 [16] for M15 mortars used in masonry structures. Using natural hydraulic lime (NHL) mortars guarantees the absence of any OPC binder and therefore the absence of harmful amounts of water-soluble salts, such as calcium sulphates, that are inevitably found in any OPC binder. From a mechanical point of view, the low modulus of elasticity that such binding materials have favours a natural compatibility with existing masonry structures and to an even greater extent with historical buildings and monuments. Moreover, unlike OPC binders, lime-based mortars develop their final mechanical properties after more than 28 days, allowing them to better adapt to masonry structure deformations during the hardening phase.

The use of sustainable FRCM composites in civil infrastructure systems is currently rather limited; however, potentially relevant applications such as repair and retrofit structures, strengthening of unreinforced masonry (URM) walls and beam-column connections are currently being developed [6,17-19]. Consequently, a deeper understanding of fundamental mechanisms that govern the mechanics of these systems is important for analysis, modelling and design.

The fibre durability was examined by conducting tensile tests on single yarns, which were impregnated with both matrices and they were subjected to environmental wetting and drying cycles. An extensive physical and mechanical characterization of sisal and flax fabrics and the two cementitious matrices was performed. The composites were prepared with untreated bi-directional sisal and flax fabric strips and the NLG matrix; their tensile strength and the effect of matrix thickness were also investigated. A significance level of 5% (95% confidence interval) was considered to indicate statistical significance.

3.2 Experimental programme

The experimental programme was as follows:

a) Study of the physical and mechanical properties of flax and sisal fibres.
b) Determination of the mechanical behaviour of mortars.

c) Assessment of fibre durability.
d) Composite sample preparation and study of tensile behaviour.

All results were validated by statistical analysis focussing on the variability of the measured values.

3.2.1 Materials

Flax, also known as linen (Linaceae family), is an erect annual plant that grows 0.5–1.25 m tall with a stem diameter of 16–3.2 mm. Bast fibres are separated from inner bark by retting, and the ultimate fibre length is between 9 and 70 mm. The use of flax for linen cloth production dates back at least to ancient Egyptian times. Flax grows in moderate climates, and currently, the main flax-producing countries are China, France and Belarus [20]. There are two types of flax: fibre flax and seed flax, which produce thin strong fibres and coarser fibres, respectively [5]. The fibres studied were produced in Italy and supplied as rolls of bi-directional fabric, as shown in Figs. 3.1a and 3.1c.

Like banana, agave and pineapple fibres, sisal fibres are obtained from the leaves of monocotyledonous plants. Sisal plant, or *Agave sisalana*, grows sword-shaped leaves measuring 1.5–2 m tall. The name of the plant is derived from the Yucatan port of Sisal, from which the plant was exported to the world. Each leaf is approximately 1–2 m long, 10–15 cm wide and 6 mm thick, and an average of 1000 fibres can be obtained from a single leaf. Sisal leaf fibres are bundles that measure 1–2 m long, and the ultimate sisal fibre length is 1–8 mm [20]. Sisal fibres are traditionally used in making twine, rope and woven fabrics for manufacturing bags to transport agricultural products. The sisal fibres studied were extracted from sisal plants cultivated in Colombia. Samples were obtained from transporting bags, and the fabric type and geometry are shown in Figs. 3.1d and 3.1f. A random sampling of fabrics from three different producers was performed, and experimental errors caused by varying the plant source and the fibre morphology were considered.

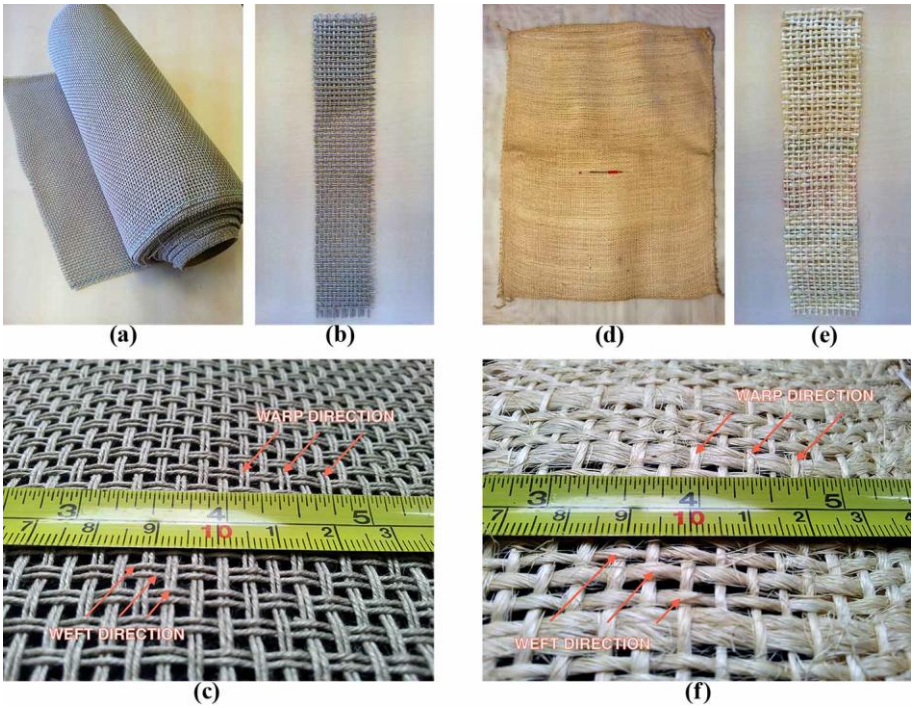

Fig. 3.1: Sisal and Flax bi-directional fabrics: (a) roll of flax fabric; (b) strip of flax fabric; (c) thread and pick distribution in a plain fabric of flax fibres; (d) transporting bag made of sisal fibres; (e) strip of sisal fabric; and (f) thread and pick distribution in a plain fabric of sisal fibres.

The matrices used were premixed NHL-based mortars that are CE-marked and comply with the European standard BS EN 459 [21]. The matrices can be classified as masonry mortars type M15 according to BS EN 998/2 [16] and were supplied by specialists in producing and trading materials for building recovery and restoration in Italy. The NLM matrix is a mortar mix with a low water-soluble salt content; there is no presence of chromium VI, and the mortar must be mixed with approximately 22% water according to the product data sheet. Due to its mechanical strength, the NLM matrix can be used for the consolidation of masonry structures and for fibre reinforced cementitious mortar (FRCM) applications. The NLG matrix is a grouting mix with added natural pozzolan and carbonate filler; the matrix must be mixed with approximately 30% water according to the product data sheet and can be used for the recovery and pre-consolidation of ancient brick or stone walls.

The main properties of the matrices, provided by the supplier and determined by flexural and compression tests, are presented in Table 3.1.

Table 3.1: Technical characteristics and mechanical properties of the cementitious matrices.

	Characteristic	**Typical value**
NLM	Particle size distribution UNI EN 1015-1 (passing 2.00 mm)	100%[a]
	Apparent volumetric mass of fresh mortar UNI EN 1015-6	1940 kg/m^3[a]
	Consistency of fresh mortar UNI EN 1015-3	150 mm[a]
	Water Absorption Coefficient due to capillary UNI EN 1015-18	0.20 kg/(m^2.min$^{1/2}$)[a]
	Flexural Strength (MPa)	3.27 ± 0.22
	Compressive Strength (MPa)	11.67 ± 1.09
NLG	Particle size distribution UNI EN 1015-1 (passing: 0.09 mm – 0.06 mm)	100% – 90%, respectively[a]
	Resistance to sulphates	No loss of strength for specimens immersed for 90 days in 5% Na_2SO_4 solution[a]
	Fluidity UNI 8997	70 – 80 cm[a]
	Apparent Volumetric Mass of fresh mortar UNI EN 1015-6	1930 ± 50 kg/m^3[a]
	Workability time of mortar UNI EN 1015-9	195 ± 30 minutes[a]
	Water Absorption Coefficient due to capillary UNI EN 1015-18	0.40 kg/(m^2.min$^{1/2}$)[a]
	Flexural Strength (MPa)	4.87 ± 0.62
	Compressive Strength (MPa)	14.62 ± 1.38

[a]Data extracted from the product data sheets

3.2.2 Fibre characterisation

Physical properties such as fibre *diameter*, yarn *density* and *linear density*, yarn *area* and fabric *mass per unit area* were studied. By SEM analysis (see Fig. 3.2), it was possible to quantify the diameter of single-fibre samples.

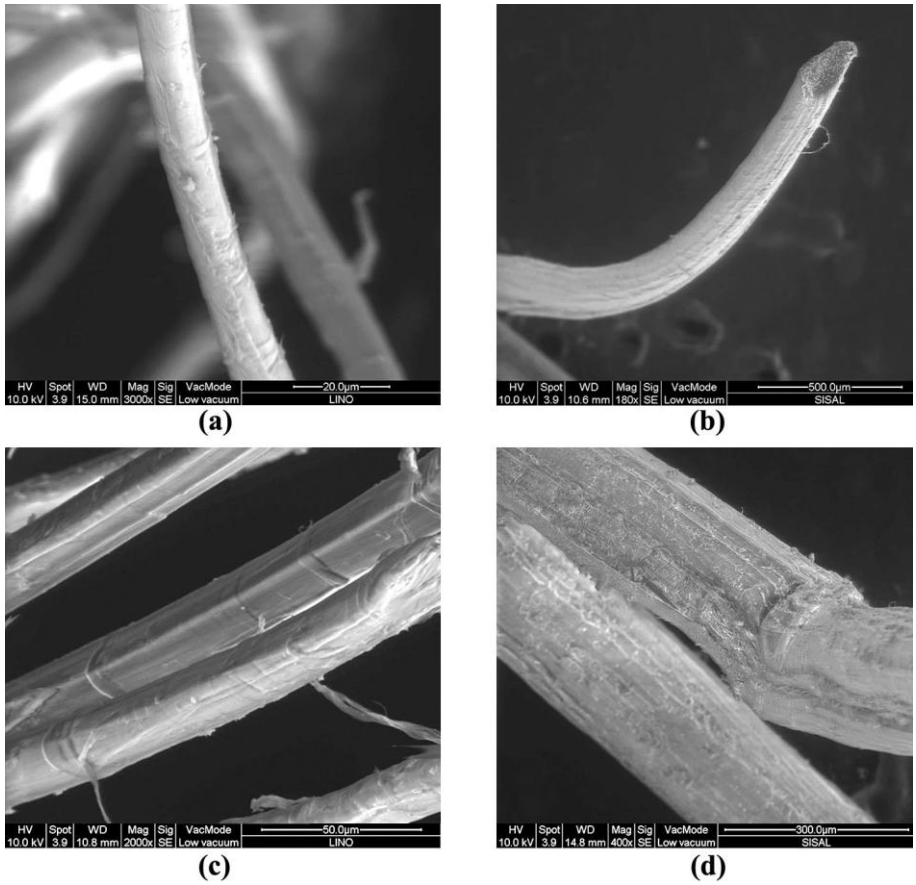

Fig. 3.2: SEM images of the single-fibre samples: (a) & (c) flax fibres; and (b) & (d) sisal fibres.

The testing procedures specified in ASTM: D 792-08 were used to determine the yarn density (ρ) of specimens weighing 1 to 5 g immersed in distilled water. The yarn linear density (T_X) was measured in accordance with EN ISO 1889:2009 [22] and using samples measuring 1 m in length (see Fig. 3.3a). To determine the yarn area (A_y), the fabric area (A_f) was calculated by *Eq. 3.1* [23] and divided by the number of yarns (*Eq. 3.2*):

$$A_f = \frac{b_f \times T_X \times N_1}{10^4 \times \rho} \tag{3.1}$$

$$A_y = \frac{A_f}{N_{yarns}} \tag{3.2}$$

where b_f is the width of the fabric in centimetres and N_f is the number of threads observed in one centimetre of fabric. According to ISO 3374:2000 (E) [24], the fabric mass per unit area ρ_A was determined using specimens measuring 50 mm x 50 mm, using different weft yarns (see Fig. 3.3b).

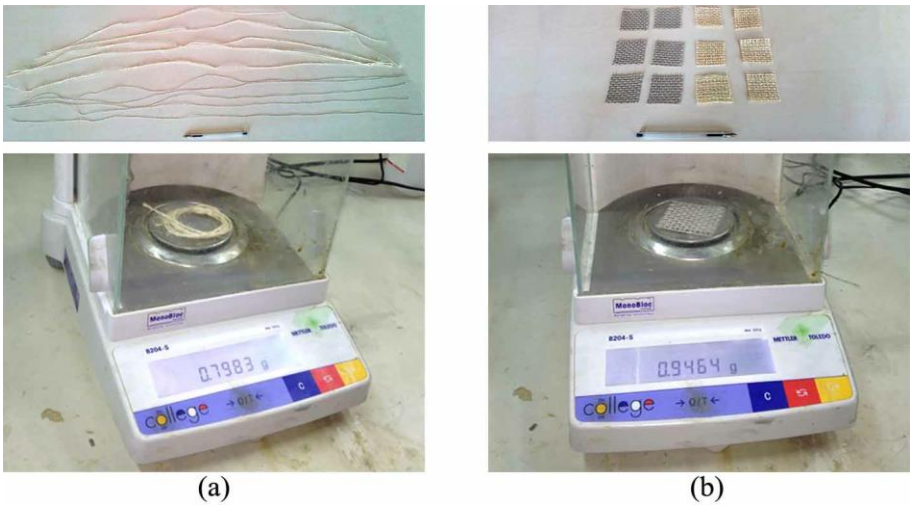

Fig. 3.3: Weight measurements in natural fibre samples: (a) single yarn of sisal and flax fibres; and (b) fabric sample of sisal and flax fibres.

After completing the physical characterisation, mechanical properties such as the tenacity, tensile strength, Young's modulus and the strain to failure of single yarns and fabric strips were determined using A Zwick Roell Z020 20-kN universal testing machine to apply tensile loads.

To study the tensile behaviour of single yarns according to ISO 2062:2009 (E) [25], specimens measuring 300 mm in length were cut from the linear density test samples. To prevent slipping during the test, Plexiglas plates were glued to the specimen ends. The constant rate of extension (CRE) of the moving clamp was set to 250 mm/min, and a preload of 2 N was applied. All data were automatically recorded using an autographic force/deformation recording device (FDRD). The number of specimens tested depended on the type of fracture obtained; those specimens that broke in the jaws zone were discarded, and at least five tests with a proper break (see Fig. 3.4b) were considered for statistical validation.

Furthermore, to study the tensile behaviour of the fabrics, both sisal and

flax fabric strips were cut with scissors in the warp and weft directions to the desired dimensions of 300 mm in length x 50 mm in width (see Figs. 3.1b and 3.1e). No specimens were cut from within 150 mm of either edge of the global sample, and the same threads (warp direction) and picks (weft direction) were not contained in another fabric strip. The clamping system used in this study was composed of sets of 0.5-mm aluminium plates fixed to specimen ends. The specimens tested with this system had no internal slippage on the threads. Tests were performed with a CRE of 20 mm/min and a preload of 5 N; the test set-up is shown in Fig. 3.4a. After an analysis of the maximum loads and the type of sample break, the specimens with "jaw breaks" and results that fell below the lowest result with "normal break" were excluded, in accordance with BS EN ISO 13934-1:2013 [26]. All data were automatically recorded using an FDRD device.

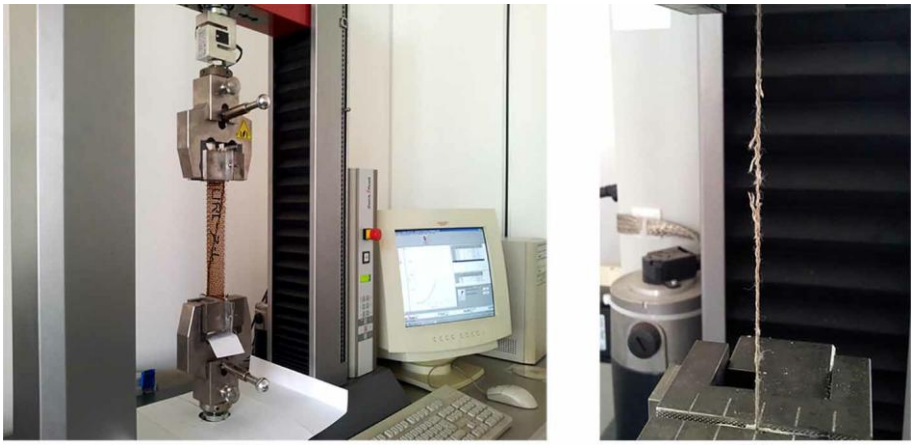

Fig. 3.4: Set-up for the tensile tests: (a) fabric strip tensile test; and (b) single yarn tensile test.

3.2.3 Compression and Flexion test on cementitious matrices

The mortars used to study fibre durability and composite production were mixed with water amounts described in the product data sheet according to BS EN 196-1 [27]. The powder mortars were not modified by the addition of any other component. Samples were cast in four prismatic moulds with dimensions of 40 mm x 40 mm x 160 mm, in accordance with BS EN 1015-11:1999 [28]. The internal faces of the moulds were pre-coated with mineral oil to facilitate de-moulding. To preserve curing humidity conditions, the

samples were stored indoors and covered with plastic sheets for 28 days. An Instron 5582 100-kN universal testing machine was used to perform the tests, in accordance with BS EN 1015-11:1999 [28]. The flexural strength (see Table 3.1), studied by three-point bending tests, was determined by using a span of 100 mm and a deflection rate of 5 mm/min. The compressive strength reported in Table 3.1 was determined on the two sample parts resulting from the three-point bending tests, and a displacement-controlled load was applied at a uniform rate of 3 mm/min. All loads applied, deflections and deformations were digitally recorded using automatic data acquisition software.

3.2.4 Fibre impregnation and durability

Flax and sisal single yarns measuring 300 mm long were obtained in the warp direction through a random sampling process from several sections of the fabrics according to ISO 2062:2009 (E) [25] and then carefully immersed in the fresh mortar mixes. A total of 21 specimens were prepared for each type of fibre and matrix. The samples were cured for 48 hours and then stored under external weathering conditions until the tensile tests were performed. The environmental conditions to which the samples were exposed for 84 days of ageing were obtained from weather reports.

To prevent slipping during the test, Plexiglas plates were glued to the specimen ends. For each type of fibre-matrix combination, seven specimens were tested at three different ages (28, 56 and 84 days). A Zwick Roell Z020 20-kN universal testing machine was used to perform the tensile test on the impregnated single yarns, in accordance with ISO 2062:2009 (E) [25].

3.2.5 Tensile properties of composite materials

The size and arrangement of the reinforcing fibres (only warp direction) were the same as those used in the mechanical characterisation of the fabrics. NLG matrices were mixed with 30% water according to BS EN 196-1 [27]. Wooden moulds were used to prepare specimens measuring 300 mm long x 65 mm wide by the hand lay-up moulding technique, as shown in Fig. 3.5a. All composite specimens were reinforced with one fabric layer, and the final thicknesses of the samples were 5 and 8 mm. Four different types of

FRCM composites were studied, and a total of 32 composite specimens were prepared.

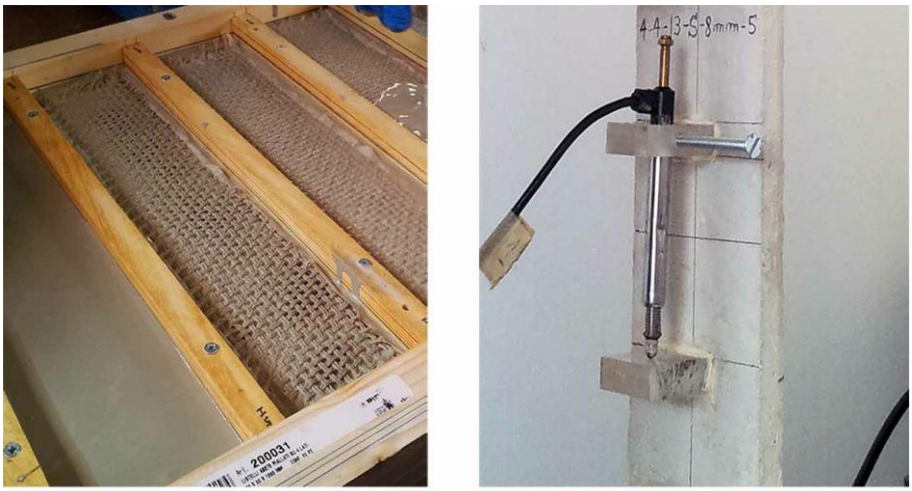

Fig. 3.5: FRCM composites: (a) preparation using the hand lay-up moulding technique; and (b) displacement transducer applied to the composite samples.

The specimens were removed from the moulds after 48 hours and cured for 28 days under the cover of plastic sheets. To prevent any eccentric axial loads, two 4-mm-thick parallel steel plates were bonded to the specimen ends. The same testing machine used in the fibre characterisation was used to perform the direct tensile test on the composite samples. The CRE was set to 0.5 mm/min. One displacement transducer with a nominal measuring length of 10 mm was fixed to the centre of the specimens (see Fig. 3.5b). Load, extension and strain data were automatically recorded using an FDRD device.

3.3 Results and discussion

3.3.1 Materials Characterisation

There are many scientific reports that describe the physical and mechanical properties of natural fibres. Table 3.2 shows data extracted from studies conducted on cellulosic fibres. Clearly, there are significant differences among each report, and in this case, the use of different fibres,

different moisture conditions and different testing methods resulted in an expanded range of physical and mechanical properties than that observed in the relevant literature. Furthermore, the composition, pulping characteristics, structure and strength of natural fibres are related to plant maturity, growth location and stages of plant growth [20,29,30].

Table 3.2: Properties of natural fibres [Adapted from 5,20,31].

	Cotton (*Gossypium sp.)*	**Jute (*Corchorus capsularis*)**	**Flax (*Linum usitatissimum*)**	**Sisal (*Agave sisalana*)**
Diameter (μm)	12–35	5–25	10–80	100–300
Density (g/cm^3)	1.5–1.6	1.3	1.4	1.45
Elongation (%)	7.0–8.0	1.5–1.8	2.0–3.0	2.0–2.5
Tensile strength (MPa)	287–597	393–773	500–1500	511–635
Young's modulus (GPa)	5.5–12.6	26.5	50–70	9.4–22.0

The physical and mechanical properties of the reinforcing fibres were determined. Studying single filaments of sisal fibres, Belaadi et al. [30] have observed brittle behaviour with a sudden load drop following a slight softening when fibre failure occurs during tensile test. This characteristic can be caused by mechanical interactions between internal cell walls present in natural fibres or due to the brittle nature of primary cell walls [5]. In this study, samples of single yarns had similar behaviour (see Fig. 3.7), but since yarns are an assemblage of twisted filaments and fibres into a continuous length, they exhibited higher softening and strains at break than single filaments.

In fabrics, the brittleness problem of single filaments was not present, strains at break were higher and there was a clear softening effect, as shown in Fig. 3.6. It was also noted that the ductility in fabric strip samples increases as the number of yarns in the test direction increases.

The results of tests conducted on samples of single yarns are reported in Table 3.3. The single fibre diameter determined by SEM analysis (see Fig. 3.2) shows higher coefficients of variation due to the irregular geometry of natural fibres.

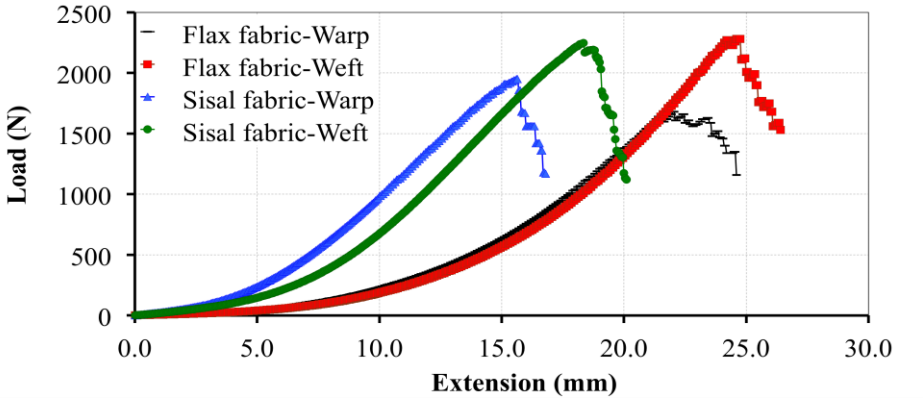

(a)

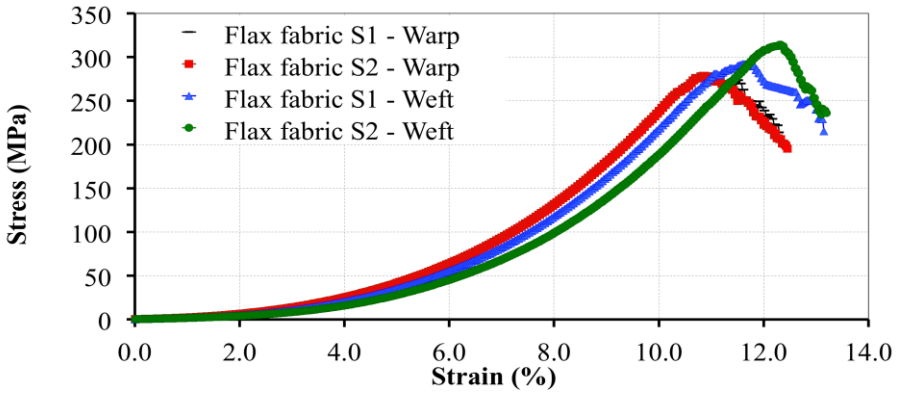

(b)

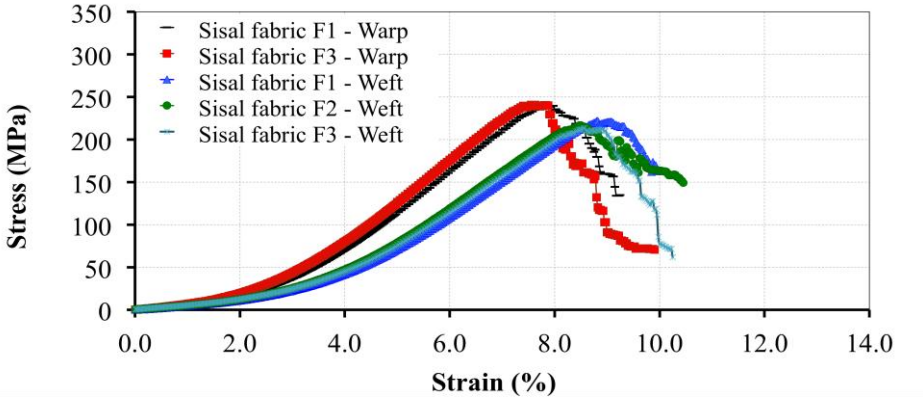

(c)

Fig. 3.6: Tensile behaviour of fabric strips: (a) load-extension curves of representative specimens of sisal and flax fabric strips; (b) mean stress-strain curves of flax fabric strips; and (c) mean stress-strain curves of sisal fabric strips.

Table 3.3: Single yarn properties of sisal and flax fibres.

	Sisal		Flax	
	Mean	**Std. Dev.**	**Mean**	**Std. Dev.**
Fibre diameter (μm)	170.27	62.35	12.69	4.39
Density (g/cm^3)	1.46	0.06	1.4	0.04
Linear Density (Tex)	921.86	131.41	352.54	14.81
Area (mm^2)	0.6311	-	0.2455	-
Young's Modulus (GPa)	8.06	1.7	9.94	1.15
Tenacity (N/Tex)	0.22	0.02	0.28	0.02
Strain to failure (%)	4.94	0.7	4.59	0.71
Tensile Strength (MPa)	323.32	32.5	396.59	24.36

The yarn area was not determined from the geometry of the samples; instead, the formula specified in CNR-DT 200/2013 [23], which considers the density and linear density of fibres, was used to obtain this parameter. The values of diameter and fibre density (see Table 3.3) fall in the ranges reported in previous studies (see Table 3.2). Flax and sisal fibres have shown similar tensile mechanical behaviour, but for both fibres, the results differ from those reported in Table 3.2. It is necessary to consider that the variability of the data reported in the literature also depends on the method used to quantify the mechanical properties and even the arrangement or geometry of the specimens tested. For this reason, it is generally not appropriate to compare data from different investigations until approaches to measure the mechanical properties of natural fibres are standardised. Therefore, special attention was directed toward obtaining the tensile properties of fabric strips. Fig. 3.6a shows load-extension curves of representative specimens, and Figs. 3.6b and 3.6c present mean stress-strain curves of flax and sisal fabrics studied in both directions.

The experimental design depended on variables such as fibre growth location and fabric supplier. Thus, in the case of flax, the tensile performance was evaluated by considering two different series of specimens obtained from two bulk samples (lots), whereas in the case of sisal, the results were obtained by considering three different suppliers.

Table 3.4 reports the fabric mechanical characterisation results obtained by studying the variability of the means by one-way ANOVA. All sisal warp

and weft fabric samples had 12 threads and 15 picks, respectively, whereas the flax fabric samples had 24 threads (warp) and 28 picks (weft). In Table 3.4, the fabrics are grouped according to series (S1 and S2) or fabric supplier (F1, F2 and F3). The table shows that the results do not vary significantly with respect to flax series or sisal supplier between groups and the levels of p values, being high (> 0.05), demonstrate confidence intervals greater than 95% in all cases. However, the uneven distribution of the sisal yarns in the weft direction (see Fig. 3.1f) produces a high dispersion of values compared with the results obtained for the flax fabrics. It should be noted that sisal fabric samples supplied by F2 were considered only in the weft direction. By including the F2 supplier in the warp-fabric study, the variability analysis results overcome the 5% maximum experimental error considered in this study. The F2 fabric supplier was not used in the following stages of the study.

Table 3.4: Mechanical characterisation of sisal and flax fabrics.

Sample/Direction		No.	P_u (N)	Tensile Strength				Young's Modulus				Strain to failure			
				Mean (MPa)	CoV (%)	*p* Value	CI (%)	Mean (GPa)	CoV (%)	*p* Value	CI (%)	Mean (%)	CoV (%)	*p* Value	CI (%)
Flax fabric-S1	Warp	8	1722.5	292.34	3.22	0.9653	99.82	3.77	3.42	0.5050	97.39	10.99	2.41	0.8242	99.07
Flax fabric-S2	Warp	8	1721.25	292.13	3.34			3.73	2.21			11.03	2.6		
Flax fabric-S1	Weft	8	2167.66	315.33	3.33	0.3299	96.47	3.9	4.61	0.8832	99.39	11.86	3.44	0.0587	95.05
Flax fabric-S2	Weft	8	2205	320.76	3.44			3.89	7.35			12.19	1.58		
Sisal fabric-F1	Warp	8	1892.5	249.9	10.74	0.8852	99.4	4.39	10.24	0.8067	98.98	8.05	5.08	0.0540	95.02
Sisal fabric-F3	Warp	8	1881.25	248.42	3.93			4.34	3.53			7.69	3.25		
Sisal fabric-F1	Weft	5	2180.78	230.38	3.39	0.5315	97.53	3.62	3.34	0.8252	99.08	9.14	2.97	0.1541	95.55
Sisal fabric-F2	Weft	5	2156.82	227.85	10.86			3.68	9.46			8.75	5.91		
Sisal fabric-F3	Weft	5	2076.18	219.33	4.12			3.6	2.91			8.65	3.97		

*N*o=Number of valid test, P_u= Maximum load, CI=Confidence interval.

Table 3.5: Statistical analysis of the variability of the tensile properties of single yarns between four groups (No AE, 28-days, 56-days, 84-days).

	Tensile Strength			Young's Modulus			Strain to failure			Tenacity		
	F	*p* Value	F_{critic}	*F*	*p* Value	F_{critic}	*F*	*p* Value	F_{critic}	*F*	*p* Value	F_{critic}
Flax - NLM matrix	89.95	0.00000	3.86	24	0.00001	3.41	7.57	0.00353	3.41	69.69	0.00000	3.41
Flax - NLG matrix	0.57	0.64193	3.2	4.37	0.01870	3.2	12.33	0.00016	3.2	0.56	0.64806	3.2
Sisal - NLM matrix	97.72	0.00000	3.29	15.28	0.00008	3.29	6.34	0.00545	3.29	97.72	0.00000	3.29
Sisal - NLG matrix	0.22	0.88421	3.41	0.06	0.98018	3.41	0.73	0.55054	3.41	0.22	0.88421	3.41

F = Ratio of the variance calculated among the means to the variance within the samples.

The final physical and mechanical properties of the fabrics are summarised in Table 3.6. The results are grouped according to the direction of the fabric threads; only the mass per unit area does not change in the warp and weft direction. The decrease in the mechanical properties of fabric samples subjected to tensile loads with respect to the results obtained for single yarn samples (see Table 3.3) is attributable to the effects of perpendicular picks and an irregular load distribution throughout the fabric threads, and the results show that both the tensile strength and Young's modulus decrease in fabric samples. Moreover, the presence of irregular arrangements of threads and picks or a greater number of microstructural defects in thicker fabrics decreases the mechanical performance of the fabrics. In studies conducted by Korte (2006) [32], the variation in the Young's modulus and tensile strength of hemp fibre was determined as a function of fibre bundle diameter, and a decrease in these properties was observed with increasing bundle diameter.

Table 3.6: Fabric properties of sisal and flax fibres.

Property/Direction		**Sisal**		**Flax**	
		Mean	**Std. Dev.**	**Mean**	**Std. Dev.**
Mass per unit area (g/m^2)		388.34	24.35	374.61	5.28
Fabric area (mm^2)	Warp	7.57	-	5.89	-
	Weft	9.47	-	6.87	-
Yarn count (No/cm)	Warp	2	-	4.4	-
	Weft	2.4	-	5.2	-
Young's Modulus (GPa)	Warp	4.36	0.32	3.75	0.11
	Weft	3.63	0.21	3.43	1.4
Strain to failure (%)	Warp	7.87	0.38	11.01	0.27
	Weft	8.84	0.42	10.4	4.24
Tensile Strength (MPa)	Warp	249.16	19.53	292.23	9.26
	Weft	225.85	15.47	318.05	10.77

The tensile properties presented in Table 3.3 and Table 3.6 provide a good indication of the high performance potential of sisal and flax fibres in fibre reinforced composite applications.

3.3.2 Ageing effects

Vegetable fibres are subject to an accelerated ageing process when exposed to humid environments and temperature changes that induce hemicellulose and lignin decomposition. In related studies [33], a reduction in tensile strength of more than 50% was observed when coir and sisal fibres were immersed in solutions with a pH of approximately 12. This decomposition problem limits the use of these fibres as reinforcements in cement-based composites.

An alternative method for quantifying ageing effects on natural fibres using tensile tests on single yarns impregnated with fresh cementitious matrices is presented in this study. The tests performed before and after cycles of wetting and drying were carried out by exposing the fibres to temperatures and environmental humidity levels ranging from 1.9 to 37.7 °C and from 15 to 80%, respectively. The matrices used were NHL mortars with physical and mechanical characteristics, specially recommended for strengthening masonry structures, ancient brick or stone walls and for fibre reinforced cementitious mortar (FRCM) applications.

The one-way ANOVA presented in Table 3.5 was performed to determine the variability of the yarn tensile properties during the three months of ageing and demonstrates the significant effects of the NLM matrix on all tensile properties of sisal and flax fibres, whereas the NLG matrix slightly affected the elasticity and strain of flax fibres but did not affect any of the tensile properties of the sisal fibre samples. Significance levels above 97% in all cases verified that no statistically significant differences occurred between the control and aged samples studying both the tensile strength of sisal and flax fibres and the rest of the mechanical properties of sisal fibres.

Table 3.7 shows the results of tensile tests conducted on samples impregnated both in a lime-based mortar (NLM) matrix and a lime-based grouting (NLG) matrix and exposed to 28, 56 and 84 days of ageing.

Table 3.7: Tensile properties of single yarns **subjected to ageing.**

Fibre	Matrix	Age	Tensile Strength (MPa)		Young's Modulus (GPa)		Strain to failure (%)		Tenacity (N/Tex)	
			Mean	(%CoV)	Mean	(%CoV)	Mean	(%CoV)	Mean	(%CoV)
Flax	-	No ageing effects	396.59	(6.14)	9.94	(11.55)	4.59	(15.47)	0.28	(6.14)
Flax	NLM	28-days ageing effects	333.67	(8.32)	6.71	(18.72)	6.33	(10.95)	0.23	(8.32)
Flax	NLM	56-days ageing effects	248.47	(5.53)	4.76	(26.65)	6.05	(17.66)	0.17	(5.53)
Flax	NLM	84-days ageing effects	190.97	(14.02)	4.9	(13.82)	4.42	(5.8)	0.13	(14.02)
Flax	NLG	28-days ageing effects	389.13	(6.39)	7.93	(13.68)	6.51	(7.71)	0.27	(6.39)
Flax	NLG	56-days ageing effects	411.74	(10.2)	8.41	(9.41)	5.82	(9.09)	0.29	(10.2)
Flax	NLG	84-days ageing effects	395.85	(5.19)	8.07	(11.48)	6.45	(6.9)	0.28	(5.19)
Sisal	-	No ageing effects	323.32	(10.05)	8.06	(21.1)	4.94	(14.1)	0.22	(10.05)
Sisal	NLM	28-days ageing effects	193.95	(13.23)	4.32	(19.44)	6.97	(17.34)	0.13	(13.23)
Sisal	NLM	56-days ageing effects	116.85	(5.09)	3.47	(44.49)	4.7	(37.41)	0.08	(5.09)
Sisal	NLM	84-days ageing effects	92.56	(17.8)	3.36	(20.45)	3.9	(22.11)	0.06	(17.8)
Sisal	NLG	28-days ageing effects	323.22	(13.98)	8.38	(32.2)	5.11	(2.69)	0.22	(13.98)
Sisal	NLG	56-days ageing effects	307.69	(10.51)	7.87	(19.91)	4.84	(16.88)	0.21	(10.51)
Sisal	NLG	84-days ageing effects	310.2	(14.44)	8.16	(4.56)	4.4	(14.19)	0.21	(14.44)

Because the sampling procedures and specimen characteristics of the single yarns subjected to ageing were the same as those used in the single yarn characterisation, the results for the control samples (No AE) were taken from Table 3.3. The NLM matrix showed detrimental effects on the durability of flax and sisal single yarns; the reduction in tensile strength (see Figs. 3.7a and 3.7c), Young's modulus and tenacity was marked. On the other hand, the NLG matrix did not affect the tensile strength of single yarns even after 84 days of ageing, as shown in Table 3.7 and Figs. 3.7b and 3.7d; however, in the case of flax fibres, by comparing the tensile property results with those reported for the control samples, slight changes in the tensile behaviour such as lower Young's moduli and greater strains to failure were observed, as shown Fig. 3.7b.

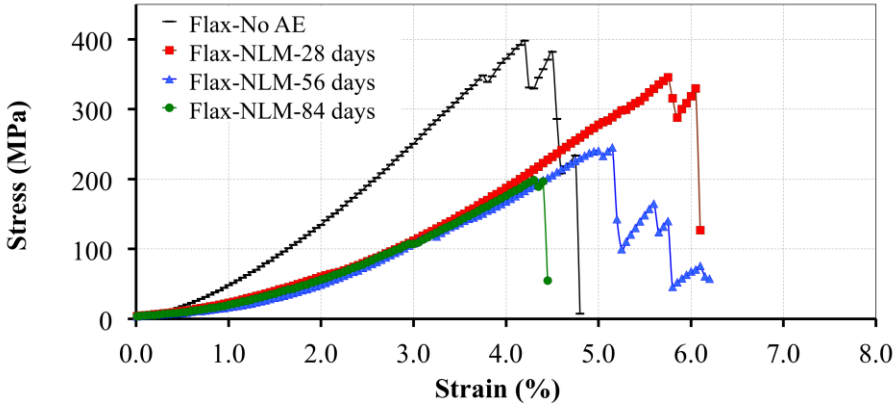

(a)

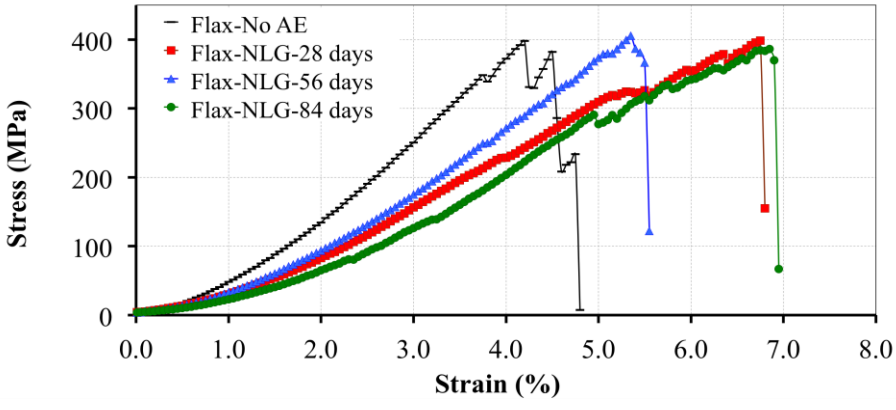

(b)

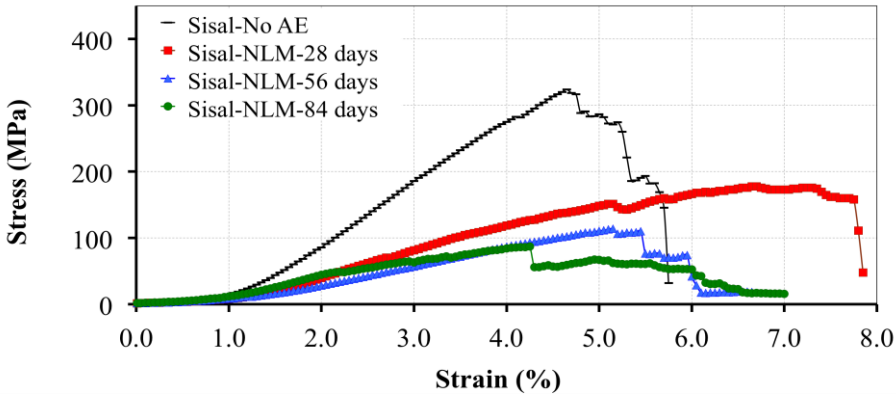

(c)

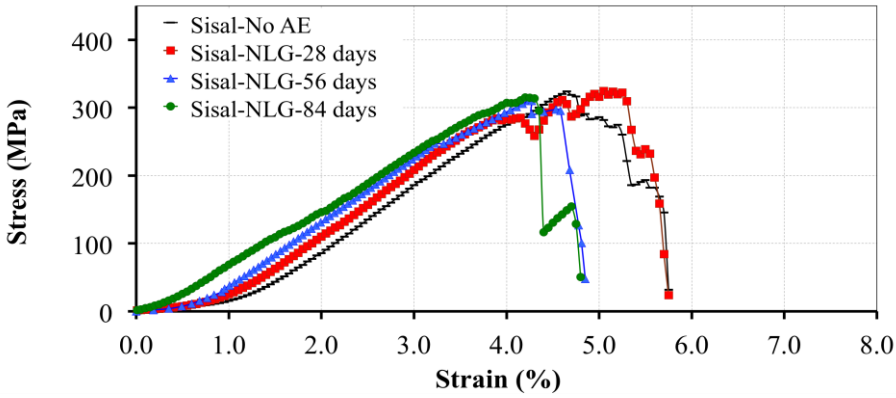

(d)

Fig. 3.7: Tensile behaviour of sisal and flax fibres subjected to ageing: (a) stress-strain curves of flax yarns aged in an NLM matrix; (b) stress-strain curves of flax yarns aged in an NLG matrix; (c) stress-strain curves of sisal yarns aged in an NLM matrix; and (d) stress-strain curves of sisal yarns aged in an NLG matrix.

Sisal fibres were more strongly affected than flax fibres when exposed to ageing effects in the NLM matrix. It should be noted that the tensile strength was reduced by more than 71% and 51% in sisal and flax fibres, respectively, after 84 days of ageing (see Table 3.8).

Fig. 3.8 summarises the results obtained by studying the durability of natural fibres impregnated with cementitious matrices. The results corresponding to each of the fibre-matrix combinations are compared, and the ageing effects produced over three months are shown with their standard deviations.

Table 3.8: Reduction in the tensile strength of fibres subjected to ageing.

	Flax-NLM	Flax-NLG	Sisal-NLM	Sisal-NLG
No AE	0.00%	0.00%	0.00%	0.00%
28-days	-15.86%	-1.88%	-40.01%	-0.03%
56-days	-37.35%	3.82%	-63.86%	-4.83%
84-days	-51.85%	-0.19%	-71.37%	-4.06%

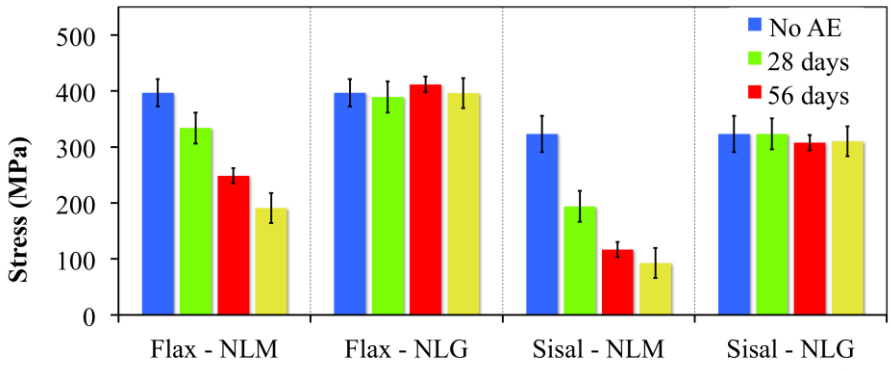

Fig. 3.8: Variation with age of the tensile strength of impregnated sisal and flax fibres.

3.3.3 Tensile tests on flax and sisal FRCM composites

By identifying the durability problems of fibres impregnated with NLM matrices, FRCM composite samples were moulded using an NLG matrix with one reinforcing layer of natural fabric strips. To study the mechanical behaviour of the composite system, the direct tensile test was selected, making possible to determine the potential of using this composite material in strengthening applications. The effect of the matrix thickness on the composite tensile behaviour was also addressed. All tests were conducted at 28 days of ageing. Fig. 3.9 shows the test set-up and the cracks that formed at the end of the tests. The arrangement of the displacement transducer used, with a gage length of 60 mm, is also presented (see Fig. 3.9b).

Fig. 3.9: Test set-up and cracks formation during the tensile tests conducted on FRCM composite samples: (a) 5-mm-thick composite specimen reinforced with flax fabrics; and (b) 8-mm-thick composite specimen reinforced with sisal fabrics.

In Table 3.9, the properties of the FRCM composites are grouped according to the fibre used and the thickness of the matrix. The fibre type is denoted by the letters F or S for flax or sisal, respectively. The tensile stress values were obtained from the normalisation of the tensile load with respect to the composite cross-sectional area [23]. The results show that the tensile strength of the composites is slightly altered when varying the reinforcing fibres. Thus, flax and sisal fibre composites measuring 5 mm thick achieved tensile strengths of 3.83 and 3.87 MPa, respectively, whereas flax and sisal fibre composites measuring 8 mm thick achieved tensile strengths of 2.22 and 2.37 MPa, respectively. FRCM composites reinforced with sisal fabric strips reached strains to failure lower than those reached by flax composites reinforced with fabric strips; this matrix effect on flax fibre performance was also noted in the durability study in which tensile tests were performed on impregnated single yarns. Figs. 3.10a and 3.10b shows the tensile behaviour of the composites studied; for clarity, only the stress-strain curves as a function of matrix thickness of representative specimens are shown.

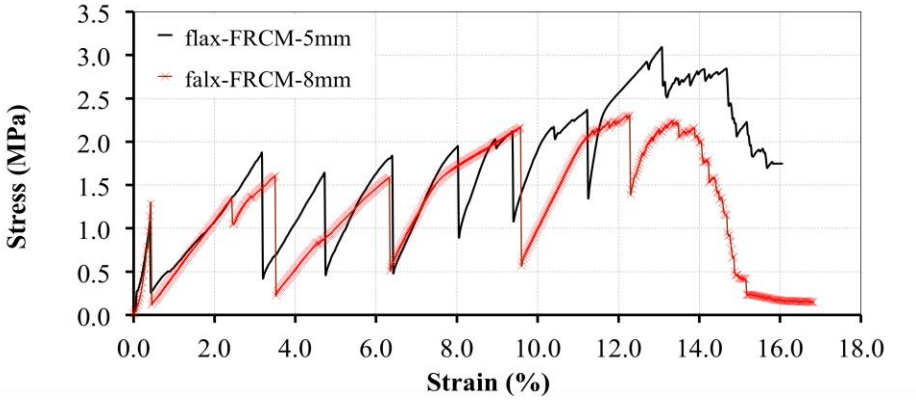

(a)

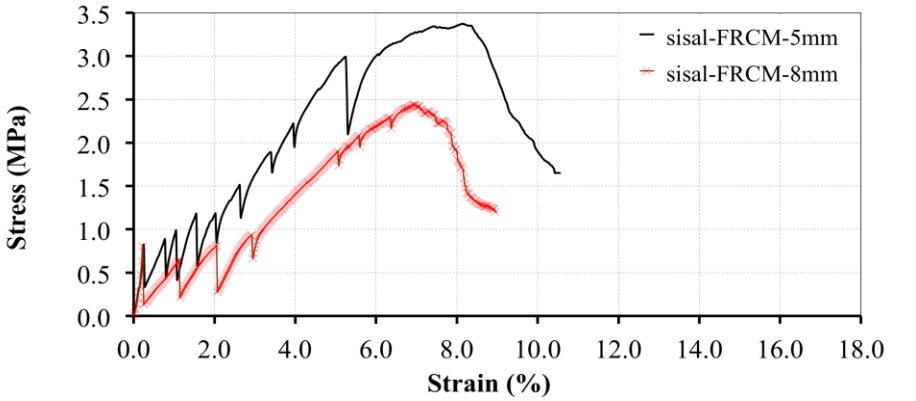

(b)

Fig. 3.10: Tensile performance of sustainable FRCM composites: (a) stress-strain curves of 5-mm-thick and 8-mm-thick flax-FRCM composite samples; and (b) stress-strain curves of 5-mm-thick and 8-mm-thick sisal-FRCM composite samples.

Three zones that describe the tensile behaviour can be identified and these will be discussed in *Chapter 4*. The stress-strain responses show a multiple clacking behaviour. Similar cement-based composite behaviour has been observed in previous studies conducted by Silva et al. [34], in which sisal fibre reinforced cement composites achieved ductile behaviour through crack distribution by sisal fibres; however, the tensile strengths of these composites were higher due to the higher volume fraction of the fibres that have been used. Maximum loads and extensions of composites reinforced with the same type of fibre are not significantly affected by the thickness of

the matrix (see Table 3.9), but due to their larger cross-sectional area, the 8-mm-thick composites samples exhibited lower tensile strengths.

Table 3.9: Tensile properties of flax and sisal FRCM composites.

Specimen		P_u (N)	Def_u (mm)	σ_u (MPa)	ε_u (%)	E_I (GPa)	E_{II} (GPa)	E_{III} (GPa)
NFRC-F-5mm	1	1319.58	23.25	4.06	11.63	0.123	0.214	0.061
	2	1420.78	27.8	4.37	13.9	0.474	0.126	0.096
	3	1004.36	26.15	3.09	13.08	0.217	0.104	0.053
	4	1049.58	31.75	3.23	15.88	0.341	0.171	0.06
	5	1036.17	29.85	3.19	14.93	0.369	0.11	0.035
	6	1304.8	26.2	4.01	13.1	0.297	0.096	0.047
	7	1584.34	29.05	4.87	14.53	0.416	0.114	0.057
Mean		*1245.66*	*27.72*	*3.83*	*13.86*	*0.32*	*0.13*	*0.06*
(%Co.V)		*(17.8)*	*(10.13)*	*(17.8)*	*(10.13)*	*(37.42)*	*(32.4)*	*(32.24)*
NFRC-F-8mm	1	1202.98	26.35	2.31	13.18	0.387	0.055	0.038
	2	1174.27	28.05	2.26	14.03	0.373	0.055	0.036
	3	1040.03	15	2	7.5	0.143	0.038	0.029
	4	1198.39	24.55	2.3	12.28	0.393	0.064	0.029
	5	1154.26	24.45	2.22	12.23	0.238	0.055	0.039
Mean		*1153.99*	*23.68*	*2.22*	*11.84*	*0.31*	*0.05*	*0.03*
(%Co.V)		*(5.78)*	*(51.59)*	*(5.78)*	*(21.42)*	*(36.37)*	*(17.68)*	*(15.03)*
NFRC-S-5mm	1	1389.07	14.4	4.27	7.2	0.3699	0.1277	0.0784
	2	1423.76	14.65	4.38	7.33	0.2462	0.1433	0.0826
	3	1287.05	13.75	3.96	6.88	0.2025	0.159	0.0715
	4	1256.54	15.65	3.87	7.83	0.3208	0.1686	0.0606
	5	1242.23	17.05	3.82	8.53	0.3463	0.1237	0.0578
	7	1096.01	16.25	3.37	8.13	0.3535	0.1793	0.0654
	8	1100.8	13.2	3.39	6.6	0.1243	0.1048	0.0658
Mean		*1256.49*	*14.99*	*3.87*	*7.5*	*0.35*	*0.14*	*0.07*
(%Co.V)		*(14.96)*	*(9.22)*	*(10.1)*	*(9.22)*	*(32.84)*	*(18.6)*	*(13.25)*
NFRC-S-8mm	2	1093.36	16.7	2.1	8.35	0.377	0.0379	0.0334
	4	1253.23	13.9	2.41	6.95	0.2663	0.0666	0.0428
	6	1194.66	18.15	2.3	9.08	0.2094	0.0529	0.0414
	7	1350.33	17.75	2.6	8.88	0.1966	0.0542	0.0467
	8	1267.86	13.9	2.44	6.95	0.2688	0.0772	0.0454
Mean		*1231.89*	*16.08*	*2.37*	*8.04*	*0.26*	*0.06*	*0.04*
(%Co.V)		*(7.74)*	*(12.81)*	*(7.74)*	*(12.81)*	*(27.04)*	*(25.8)*	*(12.39)*

P_u= Maximum load, Def_u= Maximum extension, σ_u= Tensile Strength, ε_u= Strain to failure, E_I = Young's Modulus - first zone, E_{II} = Young's Modulus – second zone, E_{III} = Young's Modulus – third zone.

The clearest effect produced by varying the matrix thickness is that on the distribution of stresses in the composite samples, as indicated by the number of cracks formed in the composite matrix.

Fig. 3.11 shows the crack pattern of FRCM composites moulded with different matrix thicknesses. In studies conducted by Wang [35] and Ratna Prasad [36] in various composite materials, it was observed that the tensile behaviour increases with the volume fraction. Volume fractions of 10% in sisal fibre reinforced cement based composites [34] and 40% and 60% in jowar fibre reinforced polyester composites and coir fibre reinforced rubber composites, respectively [35,36], were used studying the volume fraction effect in sustainable composite materials. In this study, the volume fractions used were: 2.9% and 2.1% for sisal and flax fibre reinforced composite materials, respectively. At the end of the test, the 5-mm-thick composite samples were characterised by the presence of a larger number of matrix cracks relative to the number observed in the 8-mm-thick composite samples, which indicates higher ductility. In the 8-mm-thick composite samples, due to the low volume fraction of fibres, the composite stiffness is mainly affected by the matrix properties. In both cases, the ductility of the composite material can be improved by increasing the volume fraction of reinforcing fibres, using more layers of fabric strips.

Fig. 3.11: Crack patterns of 5-mm-thick and 8-mm-thick sisal-FRCM composites: (a) front view; and (b) lateral view.

3.4 References

[1] Wambua P, Ivens J, Verpoest I. Natural fibres: can they replace glass in fibre reinforced plastics. Compos Sci Technol 2003;63:1259–64.

[2] Faruk O, Bledzki AK, Fink H, Sain M. Biocomposites reinforced with natural fibers: 2000–2010. Prog Polym Sci 2012;37:1552–96.

[3] Dittenber DB, GangaRao HVS. Critical review of recent publications on use of natural composites in infrastructure. Compos Part A – Appl S 2012;43:1419–29.

[4] Brandt AM. Fibre reinforced cement-based (FRC) composites after over 40 years of development in building and civil engineering. Compos Struct 2008;86:3–9.

[5] Bos HL. The potential of flax fibres as reinforcement for composite materials. Ph.D. Thesis, TUEindhoven 2004. p. 3,12.

[6] Olivito RS, Codispoti R, Zuccarello FA. Applicazione di materiali compositi in fibre naturali e malta cementizia a strutture murarie. In: XX Congresso Nazionale Associazione Italiana di Meccanica Teorica ed Applicata (AIMETA). Bologna; 2011.

[7] Savastano Jr H, Agopyan V, Nolasco AM, Pimentel L. Plant fibre reinforced cement components for roofing. Constr Build Mater 1999;13:433–38.

[8] Mobasher B, Pivacek A, Haupt GJ. Cement based cross-ply laminates. J Adv Cement Based Mater 1997;6:144–52.

[9] Toledo Filho RD, Scrivener K, England GL, Ghavami K. Durability of alkali sensitive sisal and coconut fibres in cement based composites. Cement Concr Compos 2000;6(22):127–43.

[10] Canovas SK. New economical solutions for improvement of durability of portland cement mortars reinforced with sisal fibres. Mater Struct 1992;25:417–22.

[11] Gram HE. Durability studies of natural organic fibre in concrete, mortar or cement. Stockholm, Sweden: Swedish Cement and Concrete Research Institute; 1986.

[12] Juárez C, Durán A, Valdez P, Fajardo G. Performance of ‘‘Agave lechuguilla” natural fiber in Portland cement composites exposed to severe environment conditions. Build Environ 2007;42:1151–7.

[13] Asprone D, Durante M, Prota A, Manfredi G. Potential of structural pozzolanic matrix–hemp fiber grid composites. Constr Build Mater 2011;25:2867–74.

[14] John VM, Agopyan V, Derolle A. Durability of blast furnace- slag-based cement mortar reinforced with coir fibres. In: Second International Symposium on vegetable plants and their fibres as Building Materials, RILEM Proc 7. London: Chapman and Hall; 1990. p. 87–97.

[15] Li, Z., Z. Ding and Y. Zhang. Development of sustainable cementitious materials. In: Proceedings of the International Workshop on Sustainable Development and Concrete Technology. Beijing; 2004.

[16] BS EN 998/2. Specification for mortar for masonry. Masonry mortar. BSI; 2010.

[17] Olivito RS, Dubois F, Venneri A, Zuccarello FA. Experimental And Numerical Analysis Of Masonry Macroelements Reinforced By Natural-Fibre- Composite Materials. In: 6th International Conference on FRP Composites In Civil Engineering (CICE2012). Roma; 2012.

[18] Codispoti R, Oliveira DV, Fangueiro R, Olivito RS. Lourenço PB. Study on natural fiber based composites for strengthening of masonry structures. In: XLI Convegno Nazionale Associazione Italiana per l'Analisi delle Solicitazione (AIAS). Vicenza; 2012.

[19] Venneri A, Taforel P, Dubois F. Modelli di Pannelli Murari Rinforzati con Fibre Naturali: Analisi Numerica e Sperimentale. In: XL Convegno Nazionale AIAS - Associazione Italiana per l'Analisi delle Sollecitazioni. Palermo; 2011.

[20] Pickering K. Properties and performance of natural-fibre composites. CRC Press; 2008.

[21] BS EN 459. Building lime. Definitions, specifications and conformity criteria. BSI; 2010.

[22] BS ISO 1889. Reinforcement yarns. Determination of linear density. BSI; 2009.

[23] CNR-DT 200 R1. Istruzioni per la Progettazione, l'Esecuzione ed il Controllo di Interventi di Consolidamento Statico mediante l'utilizzo di Compositi Fibrorinforzati. Commissione di Studio per la

Predisposizione e l'Analisi di Norme Tecniche relative alle costruzioni – CNR; 2013.

[24] ISO 3374. Reinforcing Products – Mats and Fabrics – Determination of mass per unit area. International Organization for Standardization; 2000.

[25] ISO 2062. Textiles – Yarn from packages – Determination of single-end breaking force and elongation at break using constant rate of extension (CRE) tester. International Organization for Standardization; 2009.

[26] BS EN ISO 13934-1. Textiles. Tensile properties of fabrics. Determination of maximum force and elongation at maximum force using the strip method. BSI; 2013.

[27] BS EN 196-1. Methods of testing cement: determination of strength. BSI; 2005.

[28] BS EN 1015-11. Methods of test for mortar for masonry: determination of flexural and compressive strength of hardened mortar. BSI; 1999.

[29] Chand N, Hasmi SAR. Effect of plant age on structure and strength of sisal fibre. Metal Mater Proc 1993;5(1):51–8.

[30] Belaadi A, Bezazi A, Bourchak M, Scarpa F. Tensile static and fatigue behaviour of sisal fibres. J Mater Des 2013;46:76–83.

[31] Mukherjee KG, Satyanarayana KG. Structure and properties of some vegetable fibres. Part 1: sisal fibre. J Mater Sci 1984;19:3925–34.

[32] Korte S. Processing–Property Relationships of Hemp Fibre. ME Thesis; University of Canterbury; 2006.

[33] Agopyan, V. Vegetable Fibre Reinforced Building Materiales - Development in Brazil and Other Latin American Countries. In: Swamy, R.N., editor. Natural Fibre Reinforced Cement and Concrete, Glasgow; 1988. p. 208–42.

[34] Silva FA, Mobasher B, Toledo Filho RD. Cracking mechanisms in durable sisal fiber reinforced cement composites. Cement Concr Compos 2009;31:721–30.

[35] Wang Wei, Huang Gu. Characterisation and utilization of natural coconut fibres composites. J Mater Des 2009;30:2741–4.

[36] Ratna Prasad AV, Mohana Rao K. Mechanical properties of natural fibre reinforced polyester composites: jowar, sisal and bamboo. Mater Des 2011;32:4658–63.

Chapter 4

TENSILE BEHAVIOUR OF SUSTAINABLE FRCM SYSTEMS

4.1 Introduction

Composites reinforced with natural fibres, also known as bio-composites or green composites, have the potential to serve as next-generation materials for many applications [1-4].

Using an inorganic matrix such as cement favours the effective bonding between reinforcing fibres and the matrix and also between the composite material and substrate [5,6]. If all of the positive aspects associated with the use of a cement matrix are evaluated in combination with the advantages of using natural fibres in the production of fabric cementitious composites, then the use of these materials to solve problems of sustainability in the construction industry is revealed to be a promising area of research [7-10].

Several factors can influence the mechanical performance of fibre-reinforced composites. The fibre length, weight ratio, fibre orientation and

interphase between fibres and the corresponding matrix material have significant effects on the tensile, flexural and fatigue behaviour [11-13]. Gassan [14], studying polymer composites reinforced with natural fibres, observed significant effects on crack propagation and fibre-matrix adhesion by considering factors such as textile architecture and fibre treatment. Similarly, in fabric-reinforced composites, the stiffness and the strength are controlled by the fibre and matrix properties, bond interphase and the anchorage of the fabrics in the matrix [15]. When considering cementitious composites reinforced with natural fabrics, both the mechanical response and the parameters affecting their behaviour are less well understood than those of other composite systems due to the lack of systematic and detailed information available.

This chapter deals with the tensile behaviour and crack propagation of fabric-reinforced cementitious matrix (FRCM) composites produced with natural fibres. The effects of different fabric parameters on the tensile behaviour of cementitious composites produced with layers of reinforcing fabric strips were studied. Composite samples were produced using one, two or three layers of flax and sisal fabric strips. Because of their good mechanical properties compared to those of other natural fibres, flax and sisal fibres have been used to produce composite materials with great potential for strengthening structures [4,5,8,16]. All composite samples were subjected to direct tensile tests. Various physical and mechanical properties of fabrics, such as the fabric geometry, mass per unit area, linear density, Young's modulus, tensile strength and strain to failure, were analysed. The effects of these fabric parameters, including the volume fraction of fibres, on the tensile behaviour and crack propagation of flax and sisal fabric composites were studied. Furthermore, to evaluate the effect of fibre type, mineral fibres (glass) were also considered, and glass fabric-reinforced composites were prepared and tested using the same test setup.

Composites produced with an OPC (ordinary Portland cement) matrix undergo an accelerated ageing process due to fibre mineralisation and alkali attack related to variations in humidity [17,18]. Hence, using natural hydraulic lime (NHL) mortars guarantees the absence of any OPC binder and therefore the absence of harmful amounts of water-soluble salts. As discussed in *Chapter 3*, the NLG matrix used to manufacture flax- and sisal-

FRCM composites, which contains carbonate filler and pure pozzolan with a high content of reactive silica, improved the ductility of the reinforcing fibres.

4.2 Experimental programme

4.2.1 Materials

The matrix employed was a natural hydraulic lime grouting (NLG) mix with added natural pozzolan and carbonate filler. The water content used for mixing this matrix was 240 kg/m^3, and was not modified by the addition of any other component. The mechanical characterization of six prismatic specimens (160 mm x 40 mm x 40 mm) of the NLG matrix was conducted according to BS EN 1015-11:2007 [19]. The samples were cured for 28 days and then tested in bending and compression. Since its compression strength and flexural strength was 15 MPa (9.47% coefficient of variation (CoV)) and 5 MPa (12.79% CoV), respectively, this matrix can be classified as a masonry mortar type M15 according to BS EN 998/2 [20]. The particle size distribution of this cementitious material was 100% passing 0.09 mm and 90% passing 0.06 mm according to BS EN 1015-1 [21]. Its fluidity [22] (70–80 cm) and workability time [23] (195 ± 30 min) improve impregnation and simplify the arrangement of the reinforcing fibres. In addition, both its water absorption coefficient due to capillary (0.40 kg / m^2 . min$^{1/2}$), measured according to BS EN 1015-18 [24], and low water-soluble salt content (< 1.5%, of which chlorides are < 0.03%) increase compatibility between the NLG matrix and masonry structures.

Bi-directional woven fabrics made from single yarns of natural fibres were used as raw material to produce the composite samples. Their architecture makes these fabrics lighter, compact and more suitable than unidirectional fabrics for specific applications requiring optimised structural weight. Since the natural fabrics used are woven fabrics, the resulting materials exhibit good stability in both directions (warp and weft) and a high yarn packing density in relation to the fabric thickness. The plain-fabric structure presented in Fig. 4.1a is one of the most common weave structures. Both the flax and sisal fabrics were symmetrically woven with a plain type structure using single yarns. In the sisal fabric (see Fig. 4.1b), each warp

yarn passes alternately under and over each weft yarn, whereas it can be noted that the flax fabric structure (see Fig. 4.1c) was formed with two single yarns arranged in both directions.

Table 4.1 summarises the physical and mechanical properties of both the glass and natural fabrics considered in the study and described in *Chapter 3*. In contrast to the flax fabrics, the sisal fabrics showed an irregular distribution of the yarn bundle size, mainly in the weft direction (see Fig. 4.1b), and the manual production processes used to weave these fabrics resulted in a wider variation in their physical and mechanical properties (see Table 4.1) [5].

Over the past several decades, glass fibres have been widely used for producing composite materials based on polymers (FRPs) [25]. The high mechanical properties of these fibres are comparable to those of carbon fibres [26]; however, their low strain capacity generally results in glass fibre-reinforced cement (GFRC) composites with a typical brittle behaviour [27]. The glass fabrics used (see Fig. 4.1d) were produced in Italy and were supplied as rolls of unidirectional fabrics. According to the product data sheet, these fabrics are designed to produce composite materials with a low weight and reduced thickness and to carry out strengthening interventions in structures.

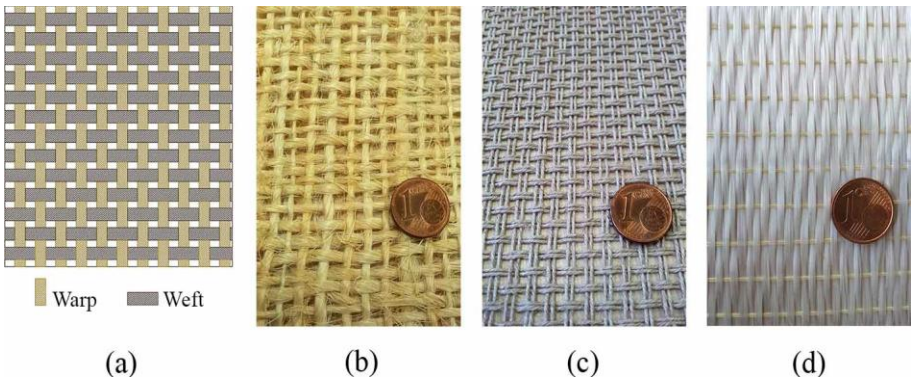

Fig. 4.1: Reinforcing fabrics: (a) plain fabric-structure; (b) bi-directional sisal fabric; (c) bi-directional flax fabric; and (d) unidirectional glass fabric.

Table 4.1: Physical and mechanical properties of the flax, sisal and glass fibres.

Type of fibre	Property	Flax		Sisal		Glass
Single yarn	Linear density (Tex)	353	(4.2%)	922	(14.3%)	593[a]
	Density (g/cm^3)	1.4	(3.0%)	1.46	(3.9%)	1.60[a]
Fabric strip (warp direction)	Design thickness (mm)	0.108	-	0.126	-	0.123
	Fabric area (mm^2)	5.94[b]	-	6.94[b]	-	6.77[b]
	Mass per unit area (g/m^2)	375	(1.4%)	388	(6.3%)	320[a]
	Yarn count (No/cm)	4.4	-	2	-	5
	Young's modulus (GPa)	3.8	(2.8%)	4.4	(7.4%)	71[a]
	Strain to failure (%)	11	(2.4%)	7.9	(4.8%)	4.50[a]
	Tensile strength (MPa)	292	(3.2%)	249	(7.8%)	2900[a]

[a] Data extracted from the product data sheet.
[b] Fabric area of 55-mm-wide fabric strips.
The coefficients of variation (CoV %) are reported in brackets.

4.2.2 Sample preparation

The composite specimens were manufactured by the hand lay-up moulding technique using strips of untreated fabrics and the NLG matrix. To produce flax- and sisal-FRCM composites with different volume fractions of fibres, the specimens were moulded with one, two or three reinforcing layers, as shown in Fig. 4.2a. Both the arrangement and the symmetry of the fabric strips were uniform throughout the cross-sectional area. The thickness of the composite samples produced was 8 mm, and thus, the study of the tensile properties was carried out considering a normal composite thickness, which can be practically used to produce composite systems for strengthening structures.

The glass-FRCM composites were prepared with one layer of fabric strips and moulded under the same conditions used to produce the natural fabric-reinforced composites. In addition, unreinforced specimens (300 mm long x 65 mm wide x 8 mm thick) of the NLG matrix were cast to examine the tensile properties of the cementitious material.

Fig. 4.3 depicts the stress-strain response of a representative unreinforced specimen. All of the specimens were cured for 28 days and then tested by direct tensile tests.

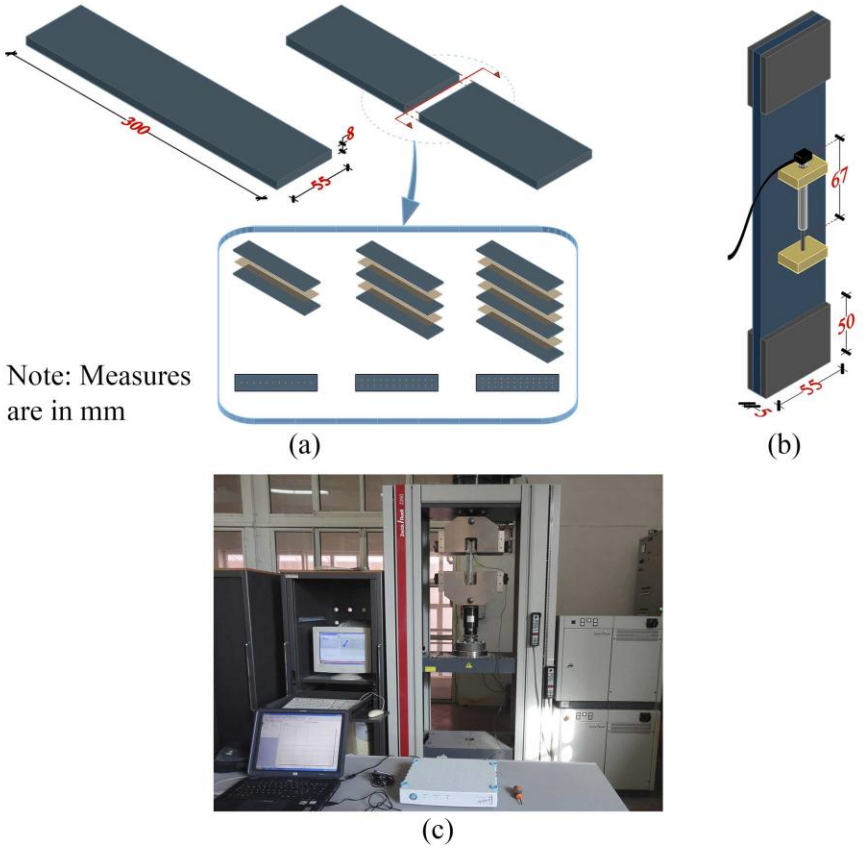

Fig. 4.2: Composites samples: (a) geometry and dimensions of the samples and arrangement of the reinforcing fibres; (b) specimens preparation; and (c) tensile test set-up.

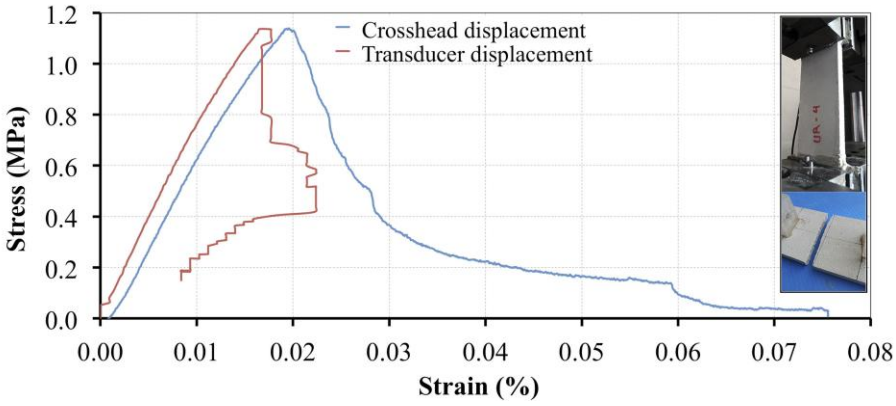

Fig. 4.3: Stress-strain curves of representative unreinforced specimen (NLG matrix).

4.2.3 Tensile test

A total of 50 composite specimens were tested. The results were not considered when the tensile tests were affected by slippage of the specimens in the clamping device of the testing machine, or when the failure of the specimens occurred in the zone of the jaws. To validate the results of the tensile tests, the means of two sets of the same type of specimens were compared using a one-way analysis of variance (one-way ANOVA). At least five results were considered for statistical validation. In the case of composite specimens, two different sets were produced with the same type and number of reinforcing fabrics, whereas for the unreinforced specimens, two sets of specimens were produced with the NLG matrix. Two 4-mm-thick parallel steel plates were attached to the specimen ends to produce a secure grip between the samples and the jaws of the testing machine and to prevent the application of eccentric and torsional loads when the samples were tested. The specimens were accurately positioned on a Zwick Roell Z250 250-kN universal testing machine, and the tensile tests were performed using a constant rate of extension of 0.5 mm/min without any pre-load applied. Additionally, one digital displacement transducer with a nominal measuring length of 10 mm was fixed to the centre of the specimens, as shown in Fig. 4.2b. Fig. 4.2c presents the test setup; all loads applied and extensions were digitally recorded using an autographic force/deformation recording device and processed using automatic data acquisition software.

Crack growth was analysed by taking photographs of the specimens during the tensile tests, which were correlated with the recorded response in terms of stress-strain behaviour. A gradient filter for grey-scale mapping was applied to the images to create digital images that provide a clear contrast between the cracked areas and the matrix. To perform a visual examination of the interaction between the matrix and reinforcing fabrics, the tested samples were prepared and then macroscopically analysed using an 8-Dioptre macro-scan conversion lens.

4.3 Results and discussion

In fabric-reinforced cementitious matrix (FRCM) composites, in addition to protecting the reinforcing fibres, the main role of the cementitious matrix

is to act as a medium for transferring stresses and strains between the fibres and between the composite and the substrate material to be reinforced. The latter can be achieved only if an appropriate fibre-matrix interaction exists and the bond interphase as well as the anchorage of the fabrics in the matrix are strong enough to spread the external loads throughout all internal fibres.

In this study, both natural and glass fabric-reinforced composites were experimentally examined by direct tensile tests. The tensile behaviour of the composite samples is comprehensively analysed in section 4.3.1, and then a detailed discussion of the fabric parameters affecting the tensile behaviour of the fabric-reinforced composites is provided in sections 4.3.2, 4.3.3, and 4.3.4.

4.3.1 Composite performance

As expected, the tensile performance of the natural fabric-reinforced composites was characterised by high ductility and by the formation of multiple cracks in the cementitious matrix. In Figs. 4.4 and 4.5, the representative stress-strain curves of composite samples reinforced with flax and sisal fabrics are presented. In these figures, the letters F or S and 1S, 2S or 3S denote the type of fibre and the number of reinforcing layers used, respectively.

By studying the tensile response of FRCM composites, researchers have clearly identified three main stages [28-31]. The *first stage* is characterised by linear or quasi-linear behaviour. This stage ends with the formation of the first crack in the matrix. In general, crack development in FRCM composites is a complex phenomenon characterised by the formation of matrix cracks over time intervals, which depends on the load and the strain applied [32,33]. In the *second stage*, composites exhibit both non-linear behaviour and a sudden change in stiffness. During this stage, multiple matrix cracks occur, releasing the elastically stored energy and causing an instantaneous decrease in stress by the formation of new matrix cracks. In the *third stage* (post-cracking stage), the reinforcing fabrics govern the tensile behaviour of the composite materials, and the matrix contribution can be neglected. This phase ends when the maximum load that causes the failure of the composite material is reached. In addition, by analysing the entire stress-strain curve of

cementitious composites, a *fourth stage* could be identified. This stage begin when the maximum tensile load is reached and is maintained with a progressive decrease in the accumulated tension, which takes place due to the gradual failure of the reinforcing fibres.

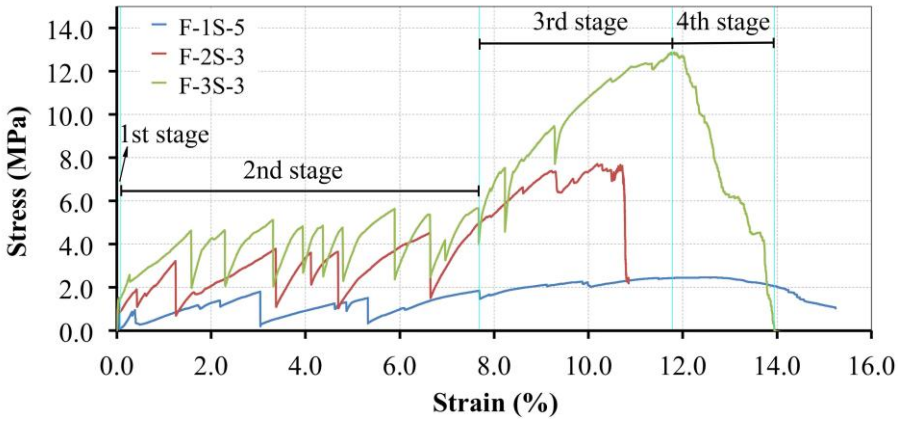

Fig. 4.4: Stress-strain curves of representative composite specimens reinforced with one, two and three layers of flax fabrics.

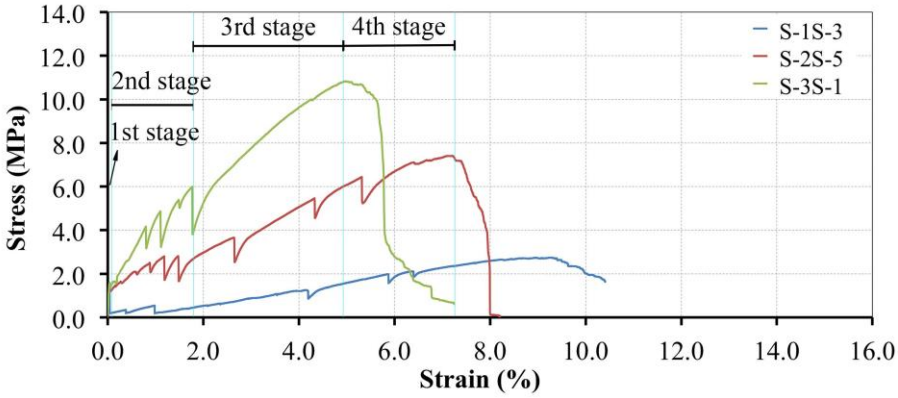

Fig. 4.5: Stress-strain curves of representative composite specimens reinforced with one, two and three layers of sisal fabrics.

The natural fabric-reinforced composites examined in this study exhibited a similar behaviour during the first and second stages (see Figs. 4.4 and 4.5). However, the first stage was less visible than that of the glass fabric composites by considering the overall stress-strain curve. This

behaviour was due to the high ductility of the flax and sisal fabrics. After the first stage, the tensile behaviour of both natural fabric cementitious composites was characterised by the formation of matrix cracks; however, in several specimens, the multiple cracking behaviour was also manifested during the third stage, which resulted in significant reductions in strength. This specific behaviour suggests the ability of the NLG matrix to store energy even when the stiffness of the composite is mainly affected by the stiffness of the natural fabrics. Therefore, the contribution of the matrix to the mechanical behaviour in the third stage should not be neglected in these composite systems with high ductility, contrary to what is assumed in conventional models [32]. These stages in the behaviour of the specimens are illustrated in Figs. 4.4 and 4.5. To provide clear images, only the stages of the specimens produced with three layers of fabrics were included.

As shown in Figs. 4.6a and 4.7a, the failure of the natural fabric-reinforced composites was a result of crack widening, leading to fibre pull out in the sisal fabric composites.

Fig. 4.6: Crack pattern of sisal fabric-reinforced composites produced with high volume fraction of fibres: (a) failure of the S-3S-4 specimen during the tensile test; and (b) crack pattern of the S-3S-5 specimen.

Fig. 4.7: Crack pattern of flax fabric-reinforced composites: (a) failure of the F-2S-2 specimen; and (b) macrograph showing the failure of the flax fabrics (fabric stability in the cementitious matrix and no fibre/matrix debonding).

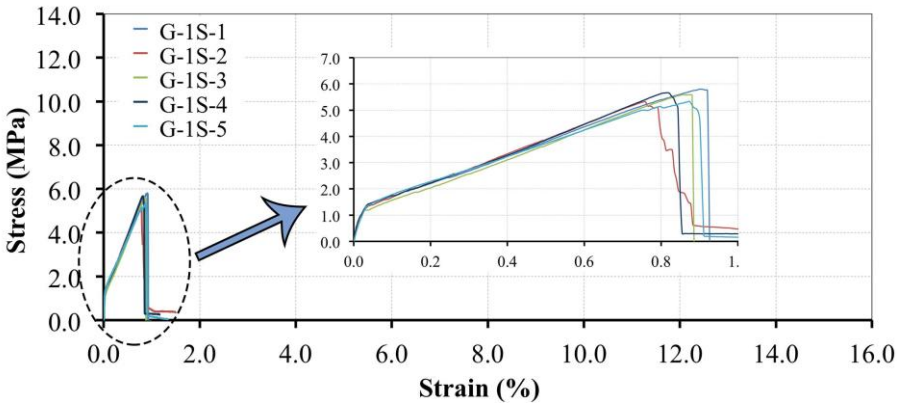

Fig. 4.8: Stress-strain curves of cementitious composites reinforced with one layer of glass fabrics.

The tensile behaviour of the glass fabric cementitious composites is presented in Fig. 4.8. The figure shows the stress-strain curves of the five composite specimens considered for statistical validation. A marked difference observed between the behaviour of the natural and glass fabric composites was the ability to produce multiple cracks. As shown in Fig. 4.8, the release of elastically stored energy by producing matrix cracks in the

glass fabric composites was absent or much lower in extent than that observed for the composites reinforced with natural fabrics, and only in some specimens were discrete load drops recorded after the first stage. These reductions in strength were attributed to the development of micro-cracks in the matrix and the debonding of the glass fabrics.

A considerable amount of information regarding the study of the mechanical properties of composite materials can be found in literature; however, most of these reports do not specify how these properties were evaluated. From a mechanical point of view, composite systems can be classified in terms of their elastic modulus and tensile strength. According to the Italian technical guide CNR-DT 200 R1/2013 [26], related to the design of systems for the repair and strengthening of structures with composite materials, both stiffness and strength can be evaluated, in the case of preformed systems, by considering the entire area of a composite (fibre and matrix):

$$\sigma_u = \frac{P_u}{A_c} \tag{4.1}$$

$$A_c = b \times t \tag{4.2}$$

were σ_u is the tensile strength of the composite specimen, P_u is the maximum load, A_c is the composite cross-sectional area, b and t are the composite width and thickness, respectively. In contrast, for systems constructed in situ, the mechanical properties can be evaluated by considering only the area of the fibres.

$$\sigma_u = \frac{P_u}{A_f} \tag{4.3}$$

For bidirectional fabrics, the area of the fibres can be evaluated using *Eq. 3.1*, whereas for unidirectional fabrics:

$$A_f = \frac{p_t \times b_f}{10^3 \times \rho} \tag{4.4}$$

where b_f is the width of the fabric in centimetres, T_X is the linear density of the yarn, ρ is the fibre density, N_f is the yarn count and p_t is the mass per unit area of the fabric.

The mechanical behaviour of these composite systems must be analysed by considering the proposed application and limitations of the materials. Clearly, the differences in the results obtained using either approach are considerable; however, the fact that the results are referenced to the design thickness should not be neglected. In this study, the tensile strengths and Young's moduli that can be obtained using these two different approaches were evaluated; the results are reported in Table 4.2. The data are grouped according to the fabric type and number of reinforcing layers. In addition, it can be noted that the data show an acceptable level of reproducibility despite the varying nature and characteristics of these materials, which typically cause large scatter in test results.

4.3.2 Effects of geometry and physical properties of the fabrics

The bonding in composite materials is essential to achieving an appropriate mechanical performance and depends on various factors such as the hydrophilic and hydrophobic nature of the fibres, the characteristics of the matrix and the anchorage ability of the fibres [34].

In the case of FRCM composites, the anchorage is developed and maintained by the penetration capacity of the matrix between the fabric openings. The penetration capability was assessed by analysing the fabric geometry and its relationship with physical properties such as the linear density and the mass per unit area. The geometry of the fabric is a key factor to improving the bonding in these composite systems. As previously discussed, the natural fabrics used have been produced with a bidirectional plain structure, whereas the glass fabric featured a unidirectional structure with fixed reinforcements arranged in the perpendicular direction (see Fig. 4.1).

Table 4.2: Tensile properties of natural and glass fabric-reinforced composites according to the method of calculation.

Specimen	P_u (N)	Def_u (mm)	Impregnated systems method				Preformed systems method			
			σ_u (MPa)	E_I (GPa)	E_{II} (GPa)	E_{III} (GPa)	σ_u (MPa)	E_I (GPa)	E_{II} (GPa)	E_{III} (GPa)
F-1S-1	1264.06	26.88	212.76	263.4	1.8	1.58	2.87	3.56	0.02	0.02
F-1S-2	1116.05	25.81	187.85	274.26	2.18	1.46	2.54	3.7	0.03	0.02
F-1S-3	1114.11	21	187.52	274.26	3.34	1.78	2.53	3.7	0.05	0.02
F-1S-4	1259.25	23.08	211.95	291.24	2.45	1.85	2.86	3.93	0.03	0.02
F-1S-5	1085.13	24.94	182.65	248.44	1.78	1.47	2.47	3.35	0.02	0.02
Mean	*1167.72*	*24.34*	*196.55*	*270.32*	*2.31*	*1.63*	*2.65*	*3.65*	*0.03*	*0.02*
Std. dev.	*86.64*	*2.33*	*14.58*	*15.77*	*0.64*	*0.18*	*0.2*	*0.21*	*0.01*	*0*
F-2S-1	3700.24	18.06	311.41	133.4	3.34	3.45	8.41	3.6	0.09	0.09
F-2S-2	3519.09	18.7	296.16	110.44	3.05	3.17	8	2.98	0.08	0.09
F-2S-3	3392.69	20.38	285.53	169.33	2.53	2.8	7.71	4.57	0.07	0.08
F-2S-4	3902.29	20.06	328.41	158.96	3.52	3.27	8.87	4.29	0.1	0.09
F-2S-5	3757.6	22.25	316.24	132.81	2.53	2.84	8.54	3.59	0.07	0.08
Mean	*3654.38*	*19.89*	*307.55*	*140.99*	*2.99*	*3.11*	*8.31*	*3.81*	*0.08*	*0.08*
Std. dev.	*200.62*	*1.63*	*16.88*	*23.37*	*0.46*	*0.28*	*0.46*	*0.63*	*0.01*	*0.01*
F-3S-1	5550.8	23.45	311.43	84.38	2.18	2.66	12.62	3.42	0.09	0.11
F-3S-2	5638.13	20.3	316.33	104.34	2.58	3.12	12.81	4.23	0.1	0.13
F-3S-3	5669.31	23.64	318.08	115.66	2.26	2.69	12.88	4.69	0.09	0.11
F-3S-4	5822.52	18.71	326.68	89.67	2.62	3.49	13.23	3.63	0.11	0.14
F-3S-5	5646.82	22.37	316.82	137.99	2.54	2.83	12.83	5.59	0.1	0.11
Mean	*5665.52*	*21.7*	*317.87*	*106.41*	*2.44*	*2.96*	*12.88*	*4.31*	*0.1*	*0.12*
Std. dev.	*98.65*	*2.13*	*5.54*	*21.52*	*0.2*	*0.35*	*0.22*	*0.87*	*0.01*	*0.01*
S-1S-1	1172.93	17.03	168.97	270.68	1.88	1.97	2.67	4.27	0.03	0.03
S-1S-2	1178.68	12.79	169.8	268.77	3.18	2.66	2.68	4.24	0.05	0.04
S-1S-3	1207.02	18.51	173.88	247.37	1.83	1.88	2.74	3.9	0.03	0.03
S-1S-4	1242.74	16.69	179.02	222.16	3.2	2.14	2.82	3.5	0.05	0.03
S-1S-5	1320.28	14.18	190.2	197.13	2.57	2.7	3	3.11	0.04	0.04
Mean	*1224.33*	*15.84*	*176.37*	*241.22*	*2.53*	*2.27*	*2.78*	*3.81*	*0.04*	*0.04*
Std. dev.	*60.36*	*2.31*	*8.7*	*31.51*	*0.67*	*0.39*	*0.14*	*0.5*	*0.01*	*0.01*

Table 4.2 Continued

Specimen	P_u (N)	Def_u (mm)	Impregnated systems method				Preformed systems method			
			σ_u (MPa)	E_I (GPa)	E_{II} (GPa)	E_{III} (GPa)	σ_u (MPa)	E_I (GPa)	E_{II} (GPa)	E_{III} (GPa)
S-2S-1	3276.73	11.96	236.02	120.47	5.76	3.95	7.45	3.8	0.18	0.12
S-2S-2	3703.28	11.14	266.74	156.13	7.42	4.79	8.42	4.93	0.23	0.15
S-2S-3	3325.23	11.3	239.51	105.91	5.83	4.24	7.56	3.34	0.18	0.13
S-2S-4	3044	12.06	219.25	138.3	4.93	3.64	6.92	4.36	0.16	0.11
S-2S-5	3260.03	14.41	234.81	160.68	4.93	3.26	7.41	5.07	0.16	0.1
Mean	*3321.85*	*12.18*	*239.27*	*136.3*	*5.77*	*3.97*	*7.55*	*4.3*	*0.18*	*0.13*
Std. dev.	*239.04*	*1.31*	*17.22*	*23.27*	*1.02*	*0.58*	*0.54*	*0.73*	*0.03*	*0.02*
S-3S-1	4762.05	9.89	228.67	86.13	7.17	4.62	10.82	4.08	0.34	0.22
S-3S-2	4950.03	10.8	237.69	76.6	5.9	4.4	11.25	3.63	0.28	0.21
S-3S-3	4009.84	11.11	192.55	106.81	4.78	3.47	9.11	5.06	0.23	0.16
S-3S-4	4780.07	12.14	229.53	90.17	7.34	3.78	10.86	4.27	0.35	0.18
S-3S-5	4950.03	10.75	237.69	90.19	6.77	4.42	11.25	4.27	0.32	0.21
Mean	*4690.4*	*10.94*	*225.23*	*89.98*	*6.39*	*4.14*	*10.66*	*4.26*	*0.3*	*0.2*
Std. dev.	*390.88*	*0.81*	*18.77*	*10.92*	*1.06*	*0.49*	*0.89*	*0.52*	*0.05*	*0.02*
G-1S-1	2551.49	1.81	376.92	272.62	-	41.71	5.8	4.19	-	0.64
G-1S-2	2339.73	1.52	345.64	236.97	-	45.5	5.32	3.65	-	0.7
G-1S-3	2459.74	1.72	363.37	267.29	-	42.29	5.59	4.11	-	0.65
G-1S-4	2491.91	1.63	368.12	248.15	-	45.13	5.66	3.82	-	0.69
G-1S-5	2347.27	1.75	346.76	260.9	-	39.69	5.33	4.01	-	0.61
Mean	*2438.03*	*1.68*	*360.16*	*257.19*		*42.87*	*5.54*	*3.96*		*0.66*
Std. dev.	*92.4*	*0.11*	*13.65*	*14.53*		*2.44*	*0.21*	*0.22*		*0.04*

P_u = maximum load, Def_u = maximum extension, σ_u = ultimate tensile strength, E_I = Young's modulus (Stage 1), E_{II} = Young's modulus (Stage 2), E_{III} = Young's modulus (Stage 3). For impregnated systems, the tensile strengths were calculated by: $\sigma_u = P_u / (n \,.\, A_f)$, were n is the number of reinforcing layers of fabric strips.

The interlocking mechanisms produced by the bi-directional woven fabrics of natural fibres were more robust than those produced by the unidirectional glass fabrics due to the presence of weft yarns. In addition, the lack of reinforcing yarns in the perpendicular direction led to a low damage tolerance in the glass fabric composites characterised by a brittle failure of the specimens (without multiple cracking behaviour), as shown in Figs. 4.9 and 4.12g.

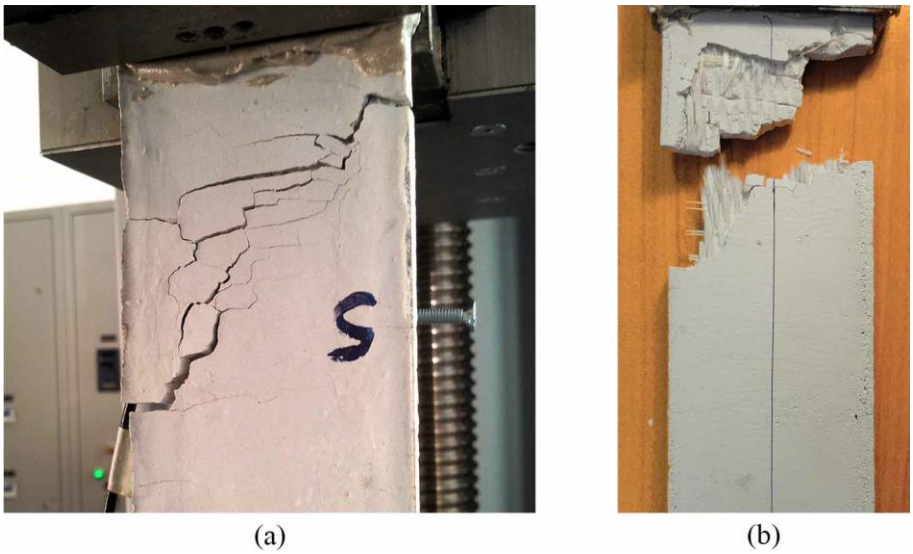

Fig. 4.9: Crack pattern of glass fabric-reinforced composites: (a) failure of the G-1S-5 specimen during the tensile test; and (b) crack pattern of the G-1S-4 specimen.

Studying the effects of woven fabric geometry on the bonding performance of cementitious composites reinforced with polyethylene fabrics, Peled et al. [35] observed a connection between the number of yarns and the bonding performance. Similarly, in this study, the number of yarns in both directions also affected the tensile behaviour of the natural fabric-reinforced composites. As shown in Fig. 4.1c, the flax fabric was produced using a twin-yarn plain structure, and the yarn count per centimetre of fabric in the warp and weft directions was greater than that for the sisal fabric (see Table 4.1). For perpendiculars yarns (picks), a greater number thereof indicated a greater number of joints between the fabric and the matrix, which served as anchorage points. Thus, the higher anchorage ability of the flax

fabrics reduced the fibre/matrix debonding and pull out of the fibres during the tensile tests (see Fig. 4.7a). In addition, the greater number of yarns in the loading direction reduced the lateral deformations of the perpendiculars yarns and therefore improved the overall fabric stability during the loading process (see Fig. 4.7).

Physical parameters such as the mass per unit area of the fabric (g/m^2) and the linear density of the yarns (TEX) were also considered and, for the natural fibres, correlated to the geometry of the fabrics. As shown in Table 4.1, the masses per unit area of the flax and sisal fabrics are quite similar, but the linear density of the sisal yarns (921.86 TEX) is almost three times that of the flax yarns (352.54 TEX). Therefore, considering that the densities of flax and sisal fibres are comparable (1.40 g/cm^3 - 1.46 g/cm^3), there must be a greater number of yarns in the flax fabric to obtain a similar mass per unit area. This assumption is consistent with the yarn count values reported in Table 4.1. Nevertheless, the fact that a greater number of yarns occurred in both directions did not mean that the flax fabric had a narrower structure. On the contrary, the higher linear density of the sisal yarns reduced the size of the fabric openings, despite having a smaller yarn count, and thus, by analysing the mass per unit area and the linear density of the natural fabrics, it is possible to note that the flax fabric provided penetrability than the sisal fabrics (see Figs. 4.10a and 4.10b). In the sisal fabric composites, both the dimensional irregularity of the yarns and the higher bundle size affected the anchorage of the fabric in the last stage of the tensile test when the fibre volume fraction was increased, resulting in the detachment of the matrix in areas where the pull out of the fabrics occurred (see Fig. 4.6b).

The glass-fabric structure showed no penetration capacity (see Fig. 4.10c), forming a barrier between the two layers of the matrix, limiting the stress transfer, and thus, adhesion could be achieved in the glass fabric composites by reduced matrix impregnation in the outer filaments of the yarns and by chemical bonding. In this composite system, the debonding clearly affected the tensile behaviour. Fig. 4.10d shows an area of the cementitious matrix in which the glass fabric was pulled out from the matrix during the loading process.

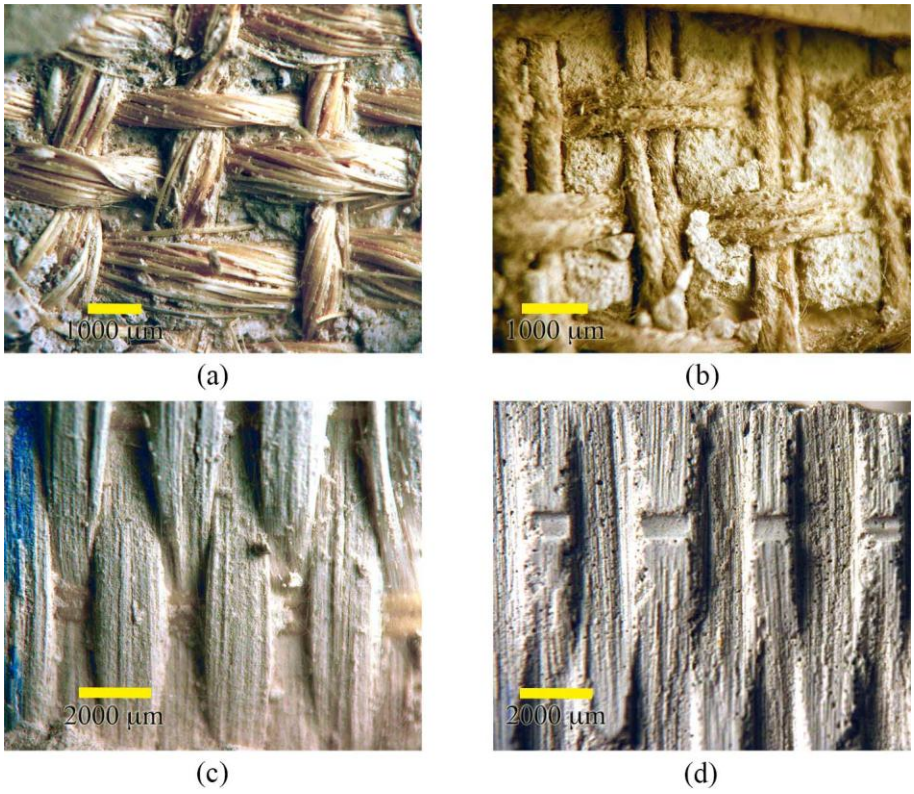

Fig. 4.10: Macrographs of fabric embedment in the NLG matrix: (a) sisal fabric-reinforced composite; (b) flax fabric-reinforced composite; (c) glass fabric-reinforced composite; and (d) area of the cementitious matrix where the glass fabric was pulled out.

4.3.3 Effects of mechanical properties of the fabrics

To quantify the effects of the mechanical properties of the fabrics on the tensile behaviour of the natural and glass fabric-reinforced composites, properties such as the tensile strength, Young's modulus and strain to failure were considered. In Table 4.3, the mechanical properties of the fabrics used in this study are presented and compared with those of the cementitious composites produced with one layer of fabric strips. In this table, the data are grouped according to fabric type. To perform a comparative analysis of the values of stiffness and strength, the tensile strength and stiffness per unit width (N/mm) of the composites were evaluated considering the method for impregnated systems [26].

Table 4.3: Tensile properties of fabric strips and fabric-reinforced cementitious composites.

FRCM (1S)	Properties of fabrics				Properties of composites (one layer)					
	σ_f MPa	$\sigma_f \cdot t_f$ N/mm	$E_f \cdot t_f$ N/mm	ε_f %	σ_u MPa	$\sigma_u \cdot t_f$ N/mm	E . t_f N/mm	ε_I %	ε_{II} %	ε_{III} %
Flax	292.23	31.57	404.76	11.01	196.55	21.23	2.16	0.038	6.20	12.16
Sisal	249.16	31.45	550.9	7.872	176.37	22.26	5.05	0.032	3.22	7.93
Glass	2900	356.92	8738.5	4.5	360.16	44.33	81.23	0.034	-	0.84

σ_f = tensile strength of fabrics, $\sigma_f \cdot t_f$ = tensile strength per unit width of fabrics, $E_f \cdot t_f$ = Young's modulus per unit width of fabrics, ε_f = strain to failure of fabrics, σ_u = ultimate tensile strength of composites, $\sigma_u \cdot t_f$ = tensile strength per unit width of composites, E . t_f = Young's modulus per unit width of composites (third stage), ε_I, ε_{II}, ε_{III} = strain capacity of composites at first, second and third stages, respectively.

As shown in Table 4.3, the mechanical properties of the reinforcing fabrics affected the tensile behaviour of the composites. The higher properties of the glass fabrics were transferred to the composites, and both the tensile strength and stiffness of the glass fabric-reinforced composites were greater than those of the natural fabric-reinforced composites. Similarly, when the Young's modulus and strain capacity of the natural fabrics are considered, the stiffness and ductility of the flax and sisal fabrics were reflected in the composite behaviour. Indeed, the strains to failure (ε_{III}) of these composites were quite similar to those of the fabrics (approximately 12% for the flax fabric composites and 8% for the sisal fabric composites). The higher strains observed in these ductile composite systems were achieved by the formation of multiple cracks in the matrix and by the crack widening. For the sisal fabric composites, the crack widening began at a strain level of less than 3.5%, whereas, for the flax fabric composites, it was observed at higher strains (approximately 6%).

Studying the effects of warp knitted fabrics made from multifilament cement-based composites, Cohen et al. [36] observed that the use of glass fabrics as a reinforcement for cementitious composite systems can lead to brittle behaviour. Similarly, in this study, the stiffness and brittleness of the glass fabrics affected the composite ductility, and the values of strain to failure achieved by the glass fabric composites are within the ranges reported by Majumddar et al. (0.6-1.2%) [27]. However, it should be noted that the low anchorage ability developed by the glass fabrics and the absence of cracks in the matrix also affected the composites' strain capacity.

In previous sections, the stress-strain response of the natural fabric composites was discussed; indeed, in their tensile behaviour, multiple stages were observed. For the glass fabric-reinforced composites, the first stage was also characterised by linear or quasi-linear behaviour in which the mechanical properties of the cementitious matrix governed the composites' response. Unlike in the natural fabric composites, a crack in the matrix that denotes the end of the first stage was not observed; however, a marked change in the stiffness of the composite indicated a change in stage. During this new phase, the stiffness of the glass fabric composites depended mainly on the stiffness of the fabric. This stiffness remained constant throughout this stage and nearly up to the maximum tensile strength of the composite (see Fig. 4.8). Upon reaching the ultimate strength, the glass fabric composites suffered brittle failure, manifested by the formation of a large crack, as shown in Fig. 4.9.

Despite these drawbacks, it was observed that the stiffness of the glass fabrics allowed for high stress values to be attained at relatively low strains. Indeed, when the tensile behaviour of the composites at low strain levels (e.g., 0.5%) is analysed, the glass fabric composites can be determined to have strengths of approximately 4 MPa, whereas the flax and sisal fabric composites, at the same strain level, barely reached (in the second stage) strengths of 0.8 MPa and 0.9 MPa, respectively. Even the composites reinforced with three layers of natural fabrics did not reach the strengths achieved by the glass fabric composites reinforced with one layer when the strains were below 0.5%. These results suggest that for low-strain applications, the glass fabric-reinforced composites are more suitable than the composites reinforced with natural fabrics.

4.3.4 Effects of volume fraction of fibres:

Due to the different physical properties exhibited by the flax and sisal fabrics, the volume fraction of fibres in these two composite systems varied with the number of fabric layers used in each natural fabric composite. In Table 4.4, the volume fractions (%) of the fibres considered in this study are reported. Note that only the natural fabric composites were used to quantify the effects of the volume fraction of fibres on the tensile behaviour. As expected for composite materials, the Young's modulus and the tensile

strength of the samples were clearly enhanced with the increase in the volume fraction of fibres (see Table 4.2).

Table 4.4: Volume fraction of fibres used to produce the cementitious composites reinforced with natural fabrics.

Composites	**Volume fraction o fibres**			
	0 layers	One layer	Two layers	Three layers
Flax fabric composites	0%	1.35%	2.70%	4.05%
Sisal fabric composites	0%	1.58%	3.16%	4.73%

Fig. 4.11 shows the tensile strength of the natural fabric composites as a function of the volume fraction of fibres. For specimens without reinforcing fibres, reported values are referenced to the tensile strength of the NLG matrix (unreinforced matrix). It can be noted that the additional bearing capacity achieved by the flax and sisal fabric composites reinforced with one layer showed lower pronounced increase than the other two composite systems (see Fig. 4.11).

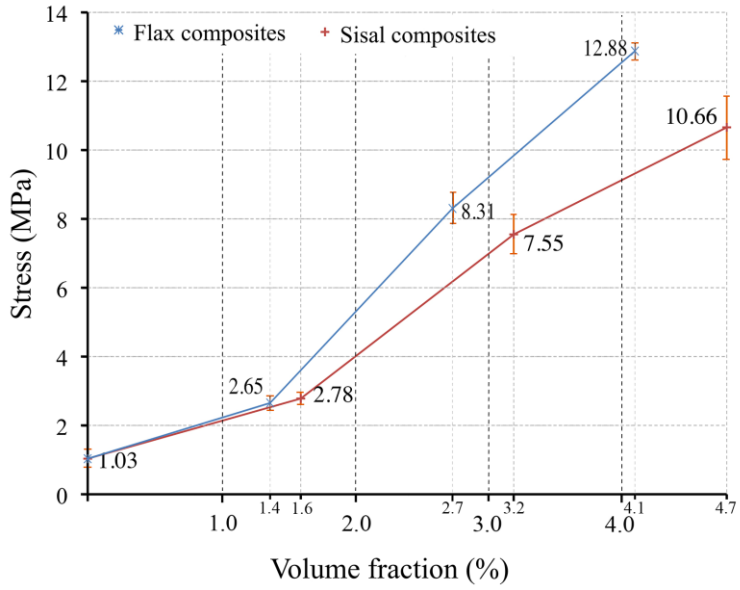

Fig. 4.11: Effects of the volume fraction of fibres on the tensile strength of cementitious composites reinforced with natural fabrics.

Furthermore, the fibre content at which the reinforcement began to be effective was approximately 3% for both natural fabric composites. On the other hand, some drawbacks related to the use of higher fibre contents were manifested in the sisal fabric composites. Indeed, as previously discussed, both debonding of fabrics and detachment of the matrix were observed in sisal fabric composites reinforced with three layers (see Fig. 4.6b).

The strain capacity of the natural fabric composites was also affected by the volume fraction of the fibres (see Figs. 4.4 and 4.5). In the sisal fabric composites, this effect was more evident, and can be attributed to the changes in stiffness experienced by the composites with the increase in the number of reinforcing layers (the stiffer composites achieved their ultimate tensile strength at strains that were lower than those obtained by the composites produced only with one layer of reinforcing fabrics).

Fig. 4.12 depicts the crack pattern of the natural fabric-reinforced composites. Clear differences in the number of cracks and crack spacing between the composites reinforced with flax and sisal fabrics were observed. Additionally, the crack pattern of the glass-FRCM composites is included.

The flax-FRCM composites developed fewer cracks than did the sisal-FRCM composites. This disparity was due to the lower volume fraction of fibres in the flax fabric composites. By increasing the number of reinforcing layers (stronger and stiffer composites), the amount of energy stored was greater and more rapidly accumulated during the multiple-cracking phase; therefore, composites produced with three reinforcement layers developed more cracks in the matrix than composites reinforced with one or two layers. The formation of new cracks in these composite systems also depended on the ability to transfer stresses throughout the material; thus, a greater number of reinforcing layers indicated a greater number of stress-transfer channels. The volume fraction of fibres was the parameter that directly affects the crack patterns of the flax and sisal fabric composites.

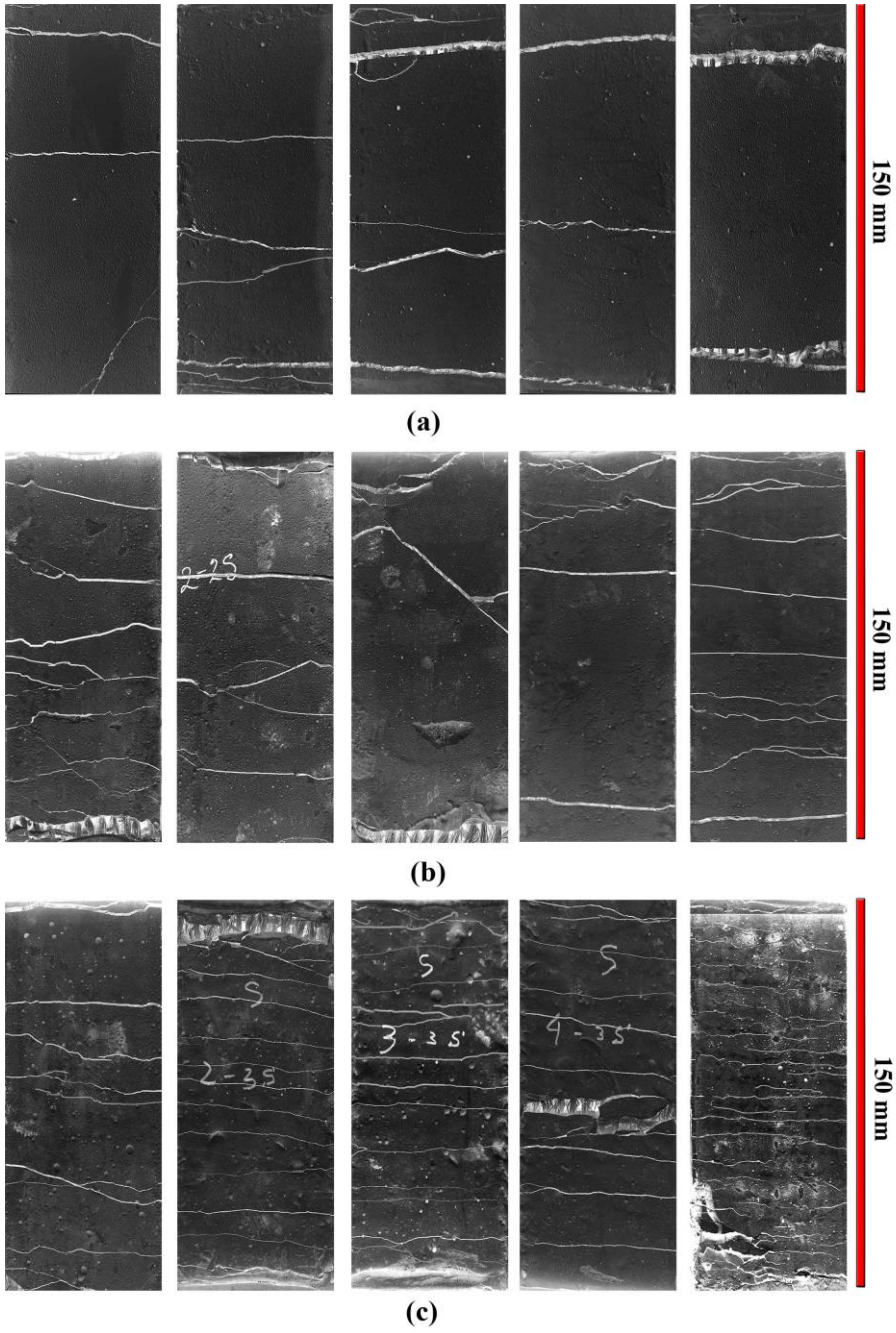

Fig. 4.12 Crack pattern of the fabric-reinforced cementitious composites: (a) sisal fabric composites reinforced with one layer; (b) sisal fabric composites reinforced with two layers; and (c) sisal fabric composites reinforced with three layers. *Continue...*

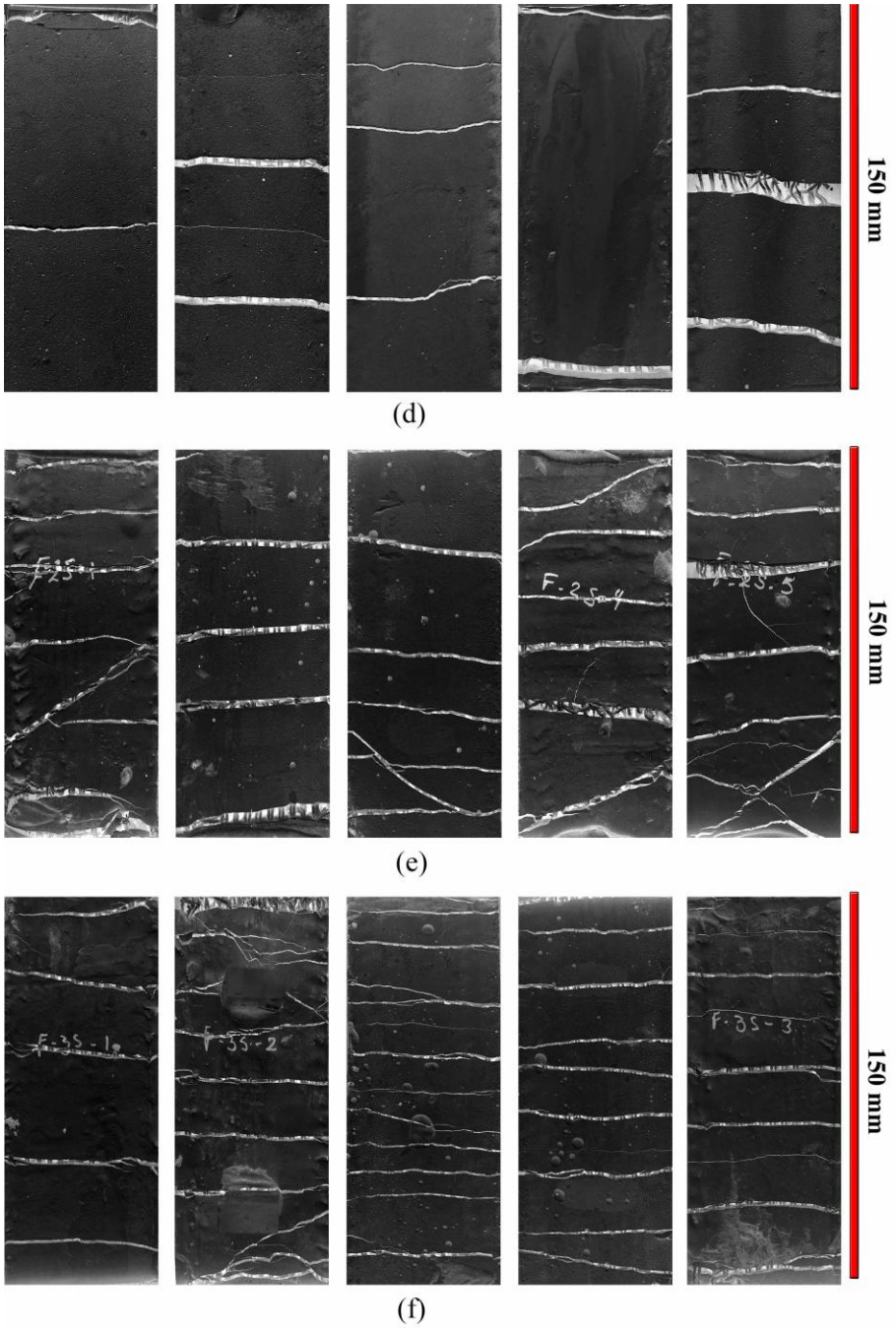

Fig. 4.12 Crack pattern of the fabric-reinforced cementitious composites: (d) flax fabric composites reinforced with one layer; (e) flax fabric composites reinforced with two layers; and (f) flax fabric composites reinforced with three layers. *Continue...*

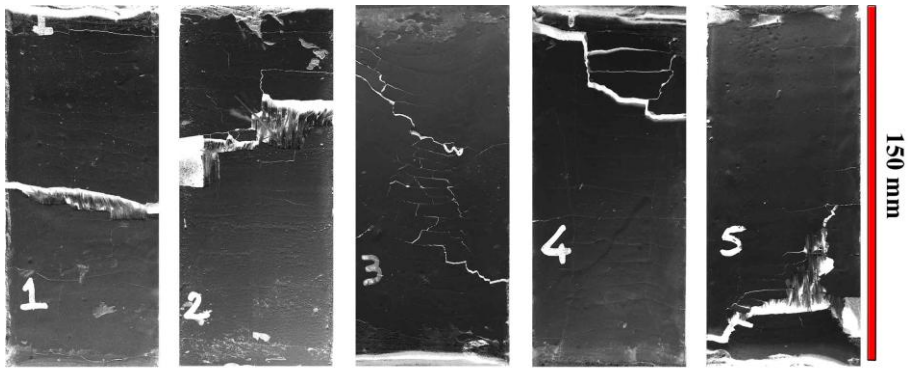

(g)

Fig. 4.12 Crack pattern of the fabric-reinforced cementitious composites: (g) glass fabric composites reinforced with one layer.

4.4 References

[1] Brandt A. Fibre reinforced cement-based (FRC) composites after over 40 years of development in building and civil engineering. Compos Struct 2008;86:3–9.

[2] Dittenber DB, GangaRao HVS. Critical review of recent publications on use of natural composites in infrastructure. Compos Part A: Appl Sci Manuf 2012;43:1419–29.

[3] Murali Mohan Rao K, Mohana Rao K, Ratna Prasad AV. Fabrication and testing of natural fibre composites: vakka, sisal, bamboo and banana. Mater Des 2010;31:508–13.

[4] Pickering KL. Properties and performance of natural-fibre composites. Woodhead Publishing Limited; 2008.

[5] Olivito R, Cevallos O, Carrozzini A. Development of durable cementitious composites using sisal and flax fabrics for reinforcement of masonry structures. Mater Des 2014;57:258–68.

[6] Papanicolaou CG, Triantafillou TC, Karlos K, Papathanasiou M. Textile-reinforced mortar (TRM) versus FRP as strengthening material of URM walls: in-plane cyclic loading. Mater Struct, RILEM 2007;40(10):1081–97.

[7] Ku H et al. A review on the tensile properties of natural fiber reinforced polymer composites. Compos Part B: Eng 2011;42(4):856–73.

[8] Faruk O, Bledzki AK, Fink H, Sain M. Biocomposites reinforced with natural fibers: 2000–2010. Prog Polym Sci 2012;37:1552–96.

[9] Herrera-Franco PJ, Valadez-González A. A study of the mechanical properties of short natural-fiber reinforced composites. Compos Part B: Eng 2005;36(8):597–608.

[10] Yan LB, Chouw N, Jayaraman K. Flax fibre and its composites – a review. Compos Part B 2014;56:296–317.

[11] John K, VenkataNaidu S. Effect of fiber content and fiber treatment on flexural properties of sisal fiber/glass fiber hybrid composites. J Reinf Plast Compos 2004;23(15):1601–5.

[12] Karam GN. Effect of fiber interaction on strength properties of short fiber reinforced with cement. J Compos Sci Technol Res 1994;16:154–9.

[13] Qin C, Soykeabkaew N, Xiuyuan N, Peijs T. The effect of fibre volume fraction and mercerization on the properties of all-cellulose composites. Carbohydrate Polym 2008;71(3):458–67.

[14] Gassan J. A study of fibre and interface parameters affecting the fatigue behaviour of natural fibre composites. Comp Part A-Appl Sci Man 2002;33:369–74.

[15] Mobasher B. Mechanics of Fibre and Textile Reinforced Cement Composites. CRC Press. Taylor & Francis Group, Boca Raton, Fl; 2012.

[16] Codispoti R, Oliveira DV, Fangueiro R, Lourenço P, Olivito R. Experimental Behavior of Natural Fiber-Based Composites Used for Strengthening Masonry Structures. Conference Papers in Materials Science. Article ID 539856, 2013.

[17] Toledo Filho RD, Scrivener K, England GL, Ghavami K. Durability of alkali sensitive sisal and coconut fibres in cement based composites. Cement Concr Compos 2000;6(22):127–43.

[18] Canovas SK. New economical solutions for improvement of durability of portland cement mortars reinforced with sisal fibres. Mater Struct 1992;25:417–22.

[19] BS EN 1015–11. Methods of test for mortar for masonry: determination of flexural and compressive strength of hardened mortar. BSI, 2007.

[20] BS EN 998/2. Specification for mortar for masonry. Masonry mortar. BSI, 2010.
[21] BS EN 1015-1. Methods of test for mortar for masonry - Part 1: Determination of particle size distribution (by sieve analysis). BSI, 1999.
[22] BS EN 13395-2. Products and systems for the protection and repair of concrete structures - Test methods - Determination of workability - Part 2: Test for flow of grout or mortar. BSI, 2002.
[23] BS EN 1015-9. Methods of test for mortar for masonry - Part 9: Determination of workable life and correction time of fresh mortar. BSI, 1999.
[24] BS EN 1015–18. Methods of test for mortar for masonry - Part 18: Determination of water absorption coefficient due to capillary action of hardened mortar. BSI, 2002.
[25] Nicolais L, Meo M, Milella E. Composite materials: a vision for the future. London: Springer; 2011.
[26] CNR-DT 200/2013 R1. Istruzioni per la Progettazione, l'Esecuzione ed il Controllo di Interventi di Consolidamento Statico mediante l'utilizzo di Compositi Fibrorinforzati. Commissione di Studio per la Predisposizione e l'Analisi di Norme Tecniche relative alle costruzioni – CNR; 2013.
[27] Majumddar AJ, Ryder JF. Glass fibre reinforcement for cement products. Glass Technol 1968;9:78–84.
[28] Brameshuber W, editor. State-of-the-art report of RILEM technical committee 201 TRC: textile reinforced concrete (RILEM Report 36). Bagneux: RILEM Publications S.A.R.L., 2006.
[29] Aveston J, Cooper GA, Kelly A. Single and multiple fracture, the properties of fibre composites. In: Proceedings of the conference national physical laboratories, IPC Science and Technology Press Ltf. London, 1971. p. 15–26.
[30] Hegger J, Will N, Bruckermann O, Voss S. Load-bearing behaviour and simulation of textile reinforced concrete. Materials and Structures 2006;39(8):765–76.
[31] Larrinaga P, Chastre C, Biscaia HC, San-Jose JT. Experimental and numerical modeling of basalt textile reinforced mortar behavior under uniaxial tensile stress. Mater Des 2014;55:66–74.

[32] Aveston J, Kelly A. Theory of multiple fracture of fibrous composites. J Mat Sci 1973;8:411–61.

[33] Li VC, Liang E. Fracture processes in concrete and fiber reinforced cementitious composites. J Eng Mech 1986;112(6):566–86.

[34] Bentur A, Mindess S. In: Fibre reinforced cementitious composites. first ed. London & New York: Elsevier applied Science; 1990.

[35] Peled A, Bentur A, Yankelevsky D. Effects of woven fabrics geometry on the bonding performance of cementitious composites: mechanical performance. Adv Cem Based Compos 1998;7:20–27.

[36] Cohen Z, Peled A, Pasder Y, Roye A, Gries T. Effects of warp knitted fabrics made from multifilament in cement- based composites. In: Hegger J, Brameshuber W, Will N (eds) First international RILEM symposium on textile reinforced concrete. RILEM, Bagneux, 2006. p 23–32.

Chapter 5

REPAIR AND STRENGTHENING OF MASONRY ELEMENTS

5.1 Introduction

Although masonry exhibits a high compressive strength, its overall mechanical behaviour is affected by the typically poor bond strength between the mortar and the bricks. Indeed, when unreinforced masonry (URM) elements are studied, their tensile strength is quite often neglected entirely [1]. The bond strength between mortar and bricks has a direct relation to structural problems encountered in masonry because of the poor interface between these two constituent materials [2]. Bond strength is a complex property that depends on several parameters related to building techniques and brick/mortar properties [3]. Groot and Pavía et al. [4,5] concluded that the bond strength of masonry is primarily governed by the water retention of mortar followed by such factors as water content and hydraulic strength. Additionally, Shina and Venumadhava Rao et al. [6,7] observed that bond strength declines 40–50% if the bricks are dry when in

contact with the fresh mortar, reaching its highest strength value when the moisture content of bricks is approximately 80% of the saturation value.

However, one of the most significant load conditions affecting the mechanical response of masonry structures occurs when axial compressive loads are applied outside the centroidal axis of the resistant cross section. This condition, known as eccentric loading, has an undesirable destabilising effect on masonry elements. Masonry walls and piers are particularly vulnerable to eccentric loads because of the nonlinear effects that are produced by the interactions between changes in their geometry and the no-tension response [8]. Consequently, even small eccentricities in the axial load (see Fig. 5.1b) can cause serious problems in masonry structures. As the eccentricity increases, the effects of flexural deformation and crack distribution on the mechanical behaviour of the masonry elements produce an even greater loss of strength. In this study, only large eccentricities of $t/6 < e \leq t/2$ (where t is the width of the section) were considered (see Figs. 5.1a, 5.1c and 5.1d).

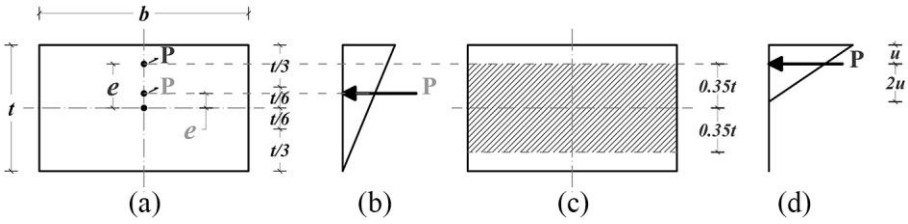

Fig. 5.1: Cases of eccentric loads: (a) rectangular cross-section with the positions of eccentric loads P; (b) stress distribution when the load P is applied with low eccentricities; (c) eccentric load applied outside the 70% width of the section; and (d) stress distribution when the load P is applied with large eccentricities.

To study the mechanical behaviour of masonry structures, simplified unilateral models were developed to idealise the uniaxial masonry-like behaviour [9–11]. According to the number of parameters required for the definition of each model, the models were classified as zero, one and two [1]. For the analysis of the behaviour of old masonry structures, the zero model might be the most appropriate because it is impossible for elastic models to correctly define the initial state of the structure, and the boundary conditions are uncertain; previous experience supports this assertion.

Given the complexity of the structural problems observed in old masonry structures, and the fact that they can cause non-compliance with current rules concerning seismic safety, there is a clear need for strengthened interventions [12]. Techniques such as externally bonded polymer-based composites, steel plates and reinforced concrete (RC) are types of methods that have conventionally been used to strengthen masonry structures. The use of fibre-reinforced polymer (FRP) composites has been found to noticeably improve the load bearing capacity of URM structures [13,14]; however, problems have been encountered with this method under particular temperature or moisture conditions that must be considered. For example, the bond between the composite and substrate material is either very weak or non-existent when the strengthening system is applied to a wet surface, and can be degraded if exposed to conditions of high moisture or extreme temperature (high or low) [15]. Furthermore, these composites do not offer any vapour permeability and are incompatible with masonry substrates [16,17], which has prompted a search for alternative materials and innovative strengthening techniques [18]. Fabric-reinforced cementitious matrix (FRCM) composites have recently emerged as being such a system, offering great potential for strengthening structures [19] as they offers a number of advantages related to their compatibility with the chemical, physical, and mechanical properties of concrete and masonry substrates, their ease of installation, vapour permeability and good performance at elevated temperatures [20,21]. In addition, the efficacy of FRCM composites in strengthening concrete and masonry structures has been demonstrated through both theoretical and experimental studies [22–26], and their bonding behaviour has previously been examined [27,28].

Fabrics used in the reinforcement of cement-based composites have typically been produced from fibres consisting of carbon, alkali-resistant (AR) glass or polymers such as polypropylene (PP), polyethylene (PE), or polyvinyl alcohol (PVA) [21,29]. New research, however, has tended to be directed more toward the use of alternative fibres to produce composites that not only exhibit suitable mechanical performance, but are also based on sustainable resources. In this chapter, the results of using bi-directional flax fabrics to produce FRCM composites that are then applied to masonry elements are presented. Two different mechanical properties of masonry were considered in this study to assess the effectiveness of the strengthened

systems. First, the bond strength of masonry was examined by performing direct tensile tests on URM elements. Three different moisture contents of bricks were considered, and the effectiveness of sustainable FRCM systems to repair masonry elements and improve their tensile bond strength was evaluated in low, medium and high performance cases for the masonry. The resistance of masonry to compression eccentric loads was the second mechanical property used to assess the effectiveness of the composite systems. The mechanical behaviour of the masonry elements strengthened with flax-FRCM composites and subjected to eccentric loads was then compared with specimens strengthened with FRCM composites produced using polyparaphenylene benzobisoxazole (PBO) fabrics. It is worth mentioning here that these two fabrics were intentionally selected on the basis of their inherently different mechanical properties. That is, PBO fibres are comparable or even superior to carbon and aramid fibres in terms of their mechanical properties [30], with their high strength and stiffness being ideally suited to strengthening a variety of structure types [31–33]. In contrast, flax fibres demonstrate the high ductility and strength needed for strengthening brittle materials, such as cement, whilst also exhibiting great anchorage in a matrix and a strong fibre/matrix bond [34,35].

5.2 Materials and Methods

5.2.1 Materials and masonry elements

As mentioned in Section 5.1, two different fabrics were used as the reinforcement in FRCM composites: one produced with natural flax fibres (Figs. 3.1c and 4.1c) and the other with synthetic PBO fibres (Fig. 5.2). Both of the fabrics were produced in Italy and their technical characteristics are summarised in Table 5.1. The physical and mechanical properties of the flax fibres are described in *Chapters 3 and 4* and in [34,35]. To study the tensile behaviour of single yarns of PBO fibres (see Fig 5.3a) according to ISO 2062:2009 (E), specimens measuring 300 mm in length were cut. The tensile strength, Young's modulus and the strain to failure of the fabric strips of the PBO fibre used in this study were evaluated in accordance with BS EN ISO 13934–1, with the testing specimens measuring 300 mm in length x 50 mm

in width (see Fig 5.3b). The tests were performed with a CRE of 20 mm/min and a preload of 5 N.

(a) (b)

Fig. 5.2: PBO fabric: (a) roll of unidirectional fabric; and (b) fabric strip.

Table 5.1: Properties of the reinforcing fabrics.

Fibre properties		**Flax**		**PBO**	
Single yarn	Fibre density (g/cm^3)	1.44	(3.0%)	1.56	-
	Tensile strength (MPa)	397	(6.1%)	4365	(4.0%)
Fabric strip (warp direction)	Design thickness (mm)	0.108	-	0.0455	-
	Mass per unit area (g/m^2)	375	(1.4%)	88	-
	Young's Modulus (GPa)	4	(2.8%)	155	(15%)
	Strain to failure (%)	11	(2.4%)	2	(12%)
	Tensile strength (MPa)	292	(3.2%)	3730	(11%)

Note: The coefficients of variation (CoV %) are reported in brackets.

(a) (b)

Fig. 5.3: Samples subjected to tensile tests: (a) single yarns; and (b) fabric strips

The stress–strain responses of the PBO single yarn and fabric strip samples are shown in Figs. 5.4a and 5.4b, respectively. Physical properties of the PBO fabric, such as its fibre density, design thickness and mass per unit area, were extracted from the manufacturer's product data sheet [30].

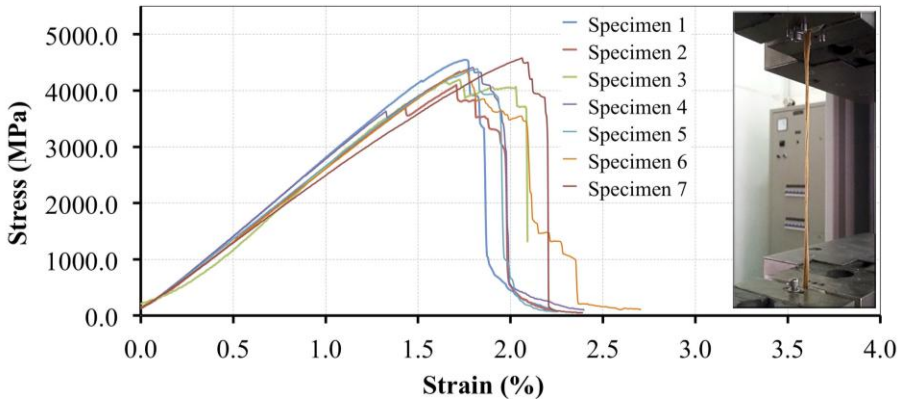

(a)

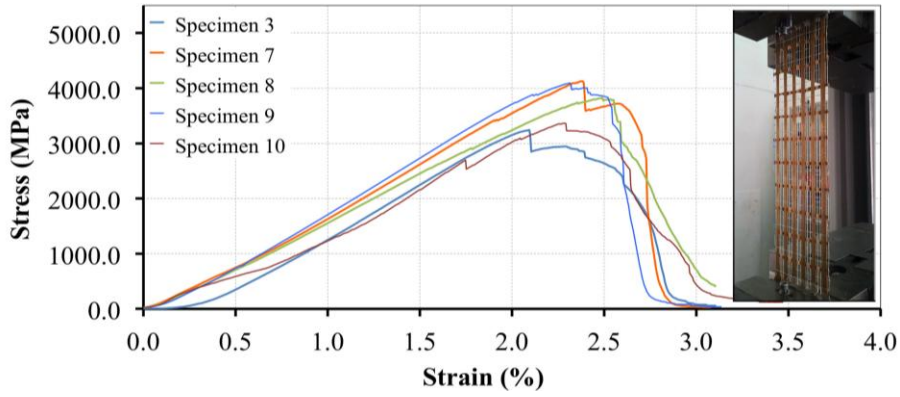

(b)

Fig. 5.4: Stress-strain curves of PBO-fibre samples: (a) single yarns; and (b) fabric strips.

The tensile behaviour of the flax-FRCM composites was analysed (*Chapters 3 and 4*). The results demonstrate that an elastic response was maintained until the formation of the first matrix crack, and then a multiple cracking nature characterised the behaviour of this composite material.

Solid clay bricks (120 x 250 x 55 mm^3) produced in the Southern Italian region of Calabria, with no perforations or frogs, were used to build all of

the masonry samples tested in this study. The properties of these bricks were evaluated by testing 10 individual specimens according to BS EN 772-1 and BS EN 772-13 [36,37], the results of which are provided in Table 5.2. Fig. 5.5b compares the tensile behaviour in terms of stress–strain curves of representative samples of flax and PBO fabric strips. Additionally, Fig. 5.5a shows the stress–strain response of a representative specimen of clay brick.

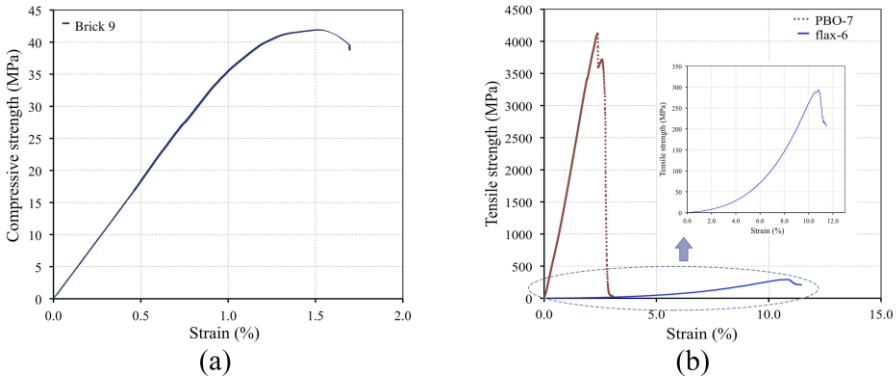

Fig. 5.5: Mechanical behaviour of various samples: (a) compressive stress-strain curve of a representative sample of clay brick; and (b) tensile stress-strain curves of representative samples of fabric strips of flax and PBO fibres.

As this thesis focuses on the use of FRCM composites to improve the mec As this thesis focuses on the use of FRCM composites to improve the mechanical behaviour of old masonry structures, in which lime based materials have typically been used as a binder, a natural hydraulic lime (NHL) mortar mix was used that is hereafter referred to as *Mortar NHL*. The particle size distribution of the *Mortar NHL* was characterised by a maximum particle size of 2 mm and the consistency of the fresh mortar was 150 mm. The matrix used for producing the FRCM composites, denoted as *NLG,* was a lime-based cementitious material containing a carbonate filler and pure natural pozzolans with a high reactive silica (fly-ash) content. Special features of this matrix, such as a particle size distribution of 100% passing 0.09 mm and 90% passing 0.06 mm, a fluidity of 70–80 cm and a workability time of 195 ± 30 min, helped to improve impregnation and simplify the arrangement of the reinforcing fibres. In addition, its capillary-induced water absorption coefficient of 0.40 $kg/m^2 \cdot min^{1/2}$ and low water-

soluble salt content of < 1.5% increased its compatibility with the masonry substrate.

Table 5.2: Mechanical characteristics of the bricks and mortars.

Material	Property	Mean value	
Clay bricks	Compressive strength (MPa)	41.77	(4%)
	Elastic Modulus - compression (MPa)	2778.46	(11.8%)
	Strain to failure - compression (%)	1.52	(9.9%)
	Weight (g)	3022	(1%)
	Specific weight (g/cm^3)	1.76	(1.7%)
	Flexural strength (MPa)	3.16	(14%)
Mortar NHL	Compressive strength (MPa)	18.49	(8.1%)
	Elastic Modulus - compression (MPa)	4704.23	(7.6%)
	Strain to failure - compression (%)	0.39	(5.4%)
	Flexural strength (MPa)	5.74	(12.9%)
	Elastic Modulus - flexion (MPa)	803.26	(15%)
	Strain to failure - flexion (%)	0.72	(6.9%)
NLG matrix	Compressive strength (MPa)	16.49	(10.2%)
	Elastic Modulus - compression (MPa)	3009.69	(27.5%)
	Strain to failure - compression (%)	0.57	(15.8%)
	Flexural strength (MPa)	4.98	(21.1%)
	Elastic Modulus - flexion (MPa)	772.64	(19.2%)
	Strain to failure - flexion (%)	0.68	(13.2%)

As discussed in *Chapter 3*, the *NLG* matrix improves the durability of the flax fibres and provides a suitable interaction with the reinforcing fabrics in composite materials, leading to the conclusion that its specific composition and rheological characteristics make this cementitious material particularly well suited to producing natural-fibre reinforced composites [34,35]. This matrix is a CE-marked material and complies with the European standard BS EN 459 [38]. Following BS EN 196–1 [39], both the *Mortar NHL* and *NLG* matrix were mixed with 25% and 30% water, respectively, but were not modified with the addition of any other component. Mechanical characterisation of these two mortars included compression and three-point bending tests performed on a total of 12 prismatic specimens in accordance with BS EN 1015–11 [40]. On the basis of their technical properties, which are presented in Table 5.2 and were statistically validated by ANOVA one-way analysis, the mortars can be classified according to BS EN 998/2 as M15-type masonry mortars [41].

The mechanical response of the strengthening systems was evaluated in terms of their tensile behaviour. A complete analysis of the tensile behaviour of the flax-FRCM composites is provided in *Chapters 3 and 4*. For the PBO-FRCM composites, tensile tests were conducted on samples (300 mm long x 55 mm wide x 8 mm thick) reinforced with two layers of fabric strips. In addition, the tensile tests were performed using the same test set-up and load conditions that were used for the flax- and sisal-FRCM composites (see *Section 4.2.3*). In Fig. 5.6, the stress–strain curves of the PBO-FRCM composites prepared with two reinforcing layers are shown.

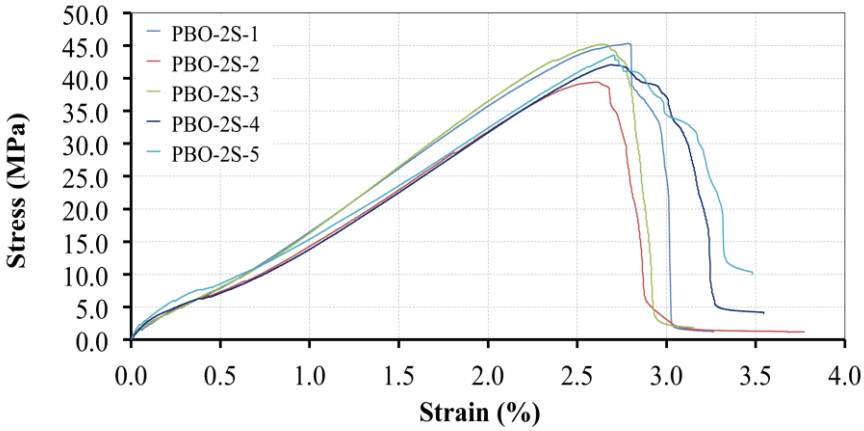

Fig. 5.6: Stress-strain curves of two-reinforcing layer PBO-FRCM composites.

5.2.1.1 Masonry elements for tensile tests

The bond strength between brick and mortar was studied using tensile tests. URM samples (denoted with the letter "PT") were prepared using four clay bricks piled on top of each other with the *Mortar NHL* serving as a binding material.

As previously mentioned, the bond strength of masonry is strongly influenced by the physical and mechanical characteristics that the mortar and brick units possess at the construction of masonry elements. In this study, a variable moisture content of the bricks was used to modify the bonding behaviour of the masonry samples. Thus, six specimens were prepared using three different moisture contents (0%, 80% and 100%). The imposed water contents of the bricks were achieved via oven drying and immersion in water

pre-treatments [5]. Table 5.3 presents the criteria and pre-treatments of the bricks used in the preparation of the masonry elements.

Table 5.3: Preparation of the specimen masonry according to the case study**.**

Masonry specimen	Desired performance	Moisture content of the bricks	Brick pre-treatment
1–2	Low performance	0%	24 hour oven dry
3–4	Medium performance	100%	24 hour water immersion
5–6	High performance	80%	3 minutes water immersion

5.2.1.2 Masonry elements for concentric and eccentric load tests

Three different types of masonry samples were built using the same type of clay brick and *Mortar NHL* as the binding material:

a) Prismatic specimens (denoted by the letter "P") 250 mm long, 120 mm wide and 335 mm high were built by piling five bricks on top of each other.
b) Prismatic specimens (denoted by the letter "M") 510 mm long, 250 mm wide and 660 mm high were built from 40 bricks using a Flemish bond (four bricks per row).
c) Pier specimens (denoted by the letter "C") 250 mm long, 250 mm wide and 1150 mm high, were built from 40 bricks (two bricks per row).

In all samples, the mortar joints were 10 mm thick. The end faces (top and bottom) were also coated with *Mortar NHL* to produce flat and regular surfaces that would allow for the uniform application of a load. The coated surfaces were 10 mm thick, and the height of the specimens was measured considering these surfaces. To help ensure a uniform and appropriate bond between the bricks and mortar, all bricks were soaked in water for 3 minutes prior to the construction of the masonry elements.

The masonry samples were covered with plastic sheets for 56 days to prevent moisture loss and to maintain adequate curing conditions. After an initial curing phase of 28 days and after the application of the flax and PBO fabric composites, four groups of specimens representing samples "P", "M"

and "C" were randomly selected for concentric and eccentric testing as controls.

5.2.2 Strengthening of URM subjected to eccentric loading

The flax-FRCM and PBO-FRCM systems were applied to the 28-day-aged masonry specimens using the hand lay-up technique to only the side affected by the flexural effects of the applied eccentric load. In the case of the flax fabric composites, three reinforcing layers were applied, as shown in Fig. 5.7; whereas with the PBO fabric composites, two reinforcing layers were applied.

Prior to this procedure, the surface of the specimen to which the FRCM composite was applied was first cleaned and then wetted to improve the adhesion between the cementitious matrix and the substrate. A layer of the *NLG* matrix was then applied using a flat metal trowel to a thickness of approximately 3 mm (see Fig. 5.7d), after which the first layer of reinforcing fabric was carefully positioned on top (see Fig. 5.7e). Note that the principal direction (warp) of the yarns was vertically oriented and that the fabrics were embedded into the matrix by applying uniformly light pressure with the trowel. A matrix layer approximately 2 mm thick was applied between each layer of the reinforcing fabric. Finally, after applying the last layer of reinforcing fabric, a final layer of the *NLG* matrix was applied and trowelled to produce a smooth appearance, as shown in Fig. 5.7f. In the case of the flax-FRCM systems, the number of reinforcing layers was selected based on the maximum volume fraction that can optimally be used and, therefore, in consideration of the potential for higher strengthening actions. The effects of the volume fraction of fibres on the tensile behaviour of the flax-FRCM composites were studied in [28], and the results indicated that the strength showed an increasing trend even when three reinforcing layers were used. Two reinforcing layers were used to produce the PBO-FRCM composites because of the lower area of the fabrics, and in this case it was decided to use at least 1% of the fibres' volume fraction.

All of the strengthened samples were cured for an additional 28 days to ensure an appropriate level of maturity in the *NLG* matrix. Thus, all masonry

samples (URM and strengthened) were 56 days old when tested to ensure a consistent level of *Mortar NHL* maturity.

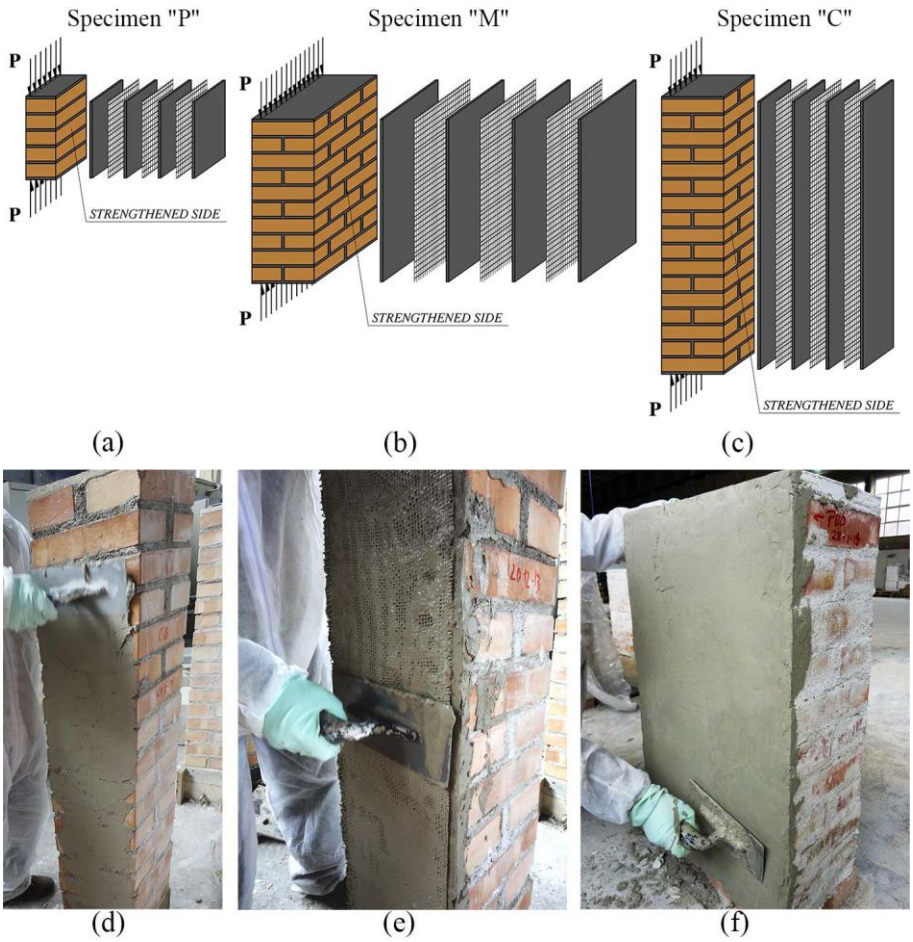

Fig. 5.7: Application of the FRCM systems: (a); (b); and (c) strengthening samples "P", "M" and "C", respectively, using three layers of flax fabrics; (d); application of a first mortar layer; (e) embedment of the fabric into the matrix; and (f) application of a final mortar layer.

5.2.3 Tensile load tests

Six masonry specimens were cured for 28 days and were then subjected to tensile loading using the test set-up shown in Fig. 5.8a. An Instron 5582 100-kN universal testing machine was used to perform the tensile tests, and a rate of extension of 0.5 mm/min was set. The tests were displacement controlled until the failure of the specimens. To prevent the application of

eccentric and torsional loads during testing, the samples were accurately positioned on the testing machine. Additionally, a layer of fine sand was placed at the base of the specimen to facilitate levelling. Two clamping devices especially designed to conduct this type of test were used (see Fig. 5.8b). As shown in this figure, the specimens are attached to the device by means of screws. Therefore, the specimens were prepared to prevent slippage during testing. Four steel plates were bonded to the upper and lower bricks. By means of these plates, the screws maintained the specimen fixed without damaging the surface of the brick. In the strengthened specimens, the deformation induced in the reinforcing fabric during the tensile tests was measured using two strain gauges in the FRCM composite at the mid-heighth of the specimen. The strain gauges had a nominal measuring length of 10 mm.

(a) (b)

Fig. 5.8: Tensile test on masonry specimens: (a) test set-up; and (b) clamping devices.

5.2.4 Concentric and eccentric load tests

A total of 18 URM specimens and 18 strengthened masonry specimens were used to conduct three separate tests:

a) Concentric loading of URM samples (three "P" specimens, three "M" specimens and three "C" specimens were tested).

b) Eccentric loading of URM samples (three "P" specimens, three "M" specimens and three "C" specimens were tested).
c) Eccentric loading of samples strengthened with flax-FRCM and PBO-FRCM systems (three "P" specimens, three "M" specimens and three "C" specimens were strengthened using both flax- and PBO-FRCM systems).

To study the mechanical behaviour of the URM elements, the results of the concentric load tests were compared with those of the eccentric load test. These were then used as a basis for determining the extent to which the FRCM composites strengthened the masonry. As noted in the literature [42,43], eccentric compression tests can be performed by applying an eccentric load using either: i) a hinge above a top plate and another below a bottom plate (Fig. 5.9a), or ii) a hinge above a top plate, with the lower cross section of the specimen being fixed to the base of the loading frame (Fig. 5.9b). In the case of the latter, the eccentric load does not ensure a vertical path of force between the two steel plates, thus cracks are formed diagonally from the upper hinge to the two lower corners of the masonry element. This behaviour suggests that the measured maximum load is related to a non-constant load eccentricity, which means that a complex test set-up is necessary to measure both the variation in eccentricity and the position of the resultant load at different heights of the specimen during testing. In contrast, using the test set-up shown in Fig. 5.9a ensures a constant eccentricity with height and, thus, a path of force generates vertically oriented cracks. For the purpose of this study, therefore, eccentric load tests were conducted according to the test set-up shown in Fig. 5.9a (see Figs. 5.9c, 5.9e and 5.9g). The mechanical behaviour of the masonry elements was examined as a direct function of the load eccentricity by applying the load along the length of its cross section, as this was considered to represent load conditions that could easily occur in masonry walls and piers. For the concentric compression test, the upper and lower hinges were removed from the plates (see Figs. 5.9d, 5.9f and 5.9h), thus ensuring that the loads were applied uniformly in the central region of the cross sections.

All the loading plates were 40 mm thick and can be assumed to be rigid in comparison with the tested specimens. Both a load frame specifically created to perform tests on macro-elements and a WAGE Zelle 100T load

cell were used to test "M" and "C" specimens, whereas "P" specimens were tested in a BPPS 300 MFL compression machine. The tests were displacement controlled until the failure of the specimens, with LVDTs located at each of the four corners of the masonry elements used to measure their deformation and quantify the rotation of the end sections. For specimens "P" and "C", HBM LVDTs with an operating range of ±20 mm were used, whereas HBM LVDTs with an operating range of ±500 mm were used with the "M" specimens. All LVDTs used had a sensitivity of 1%.

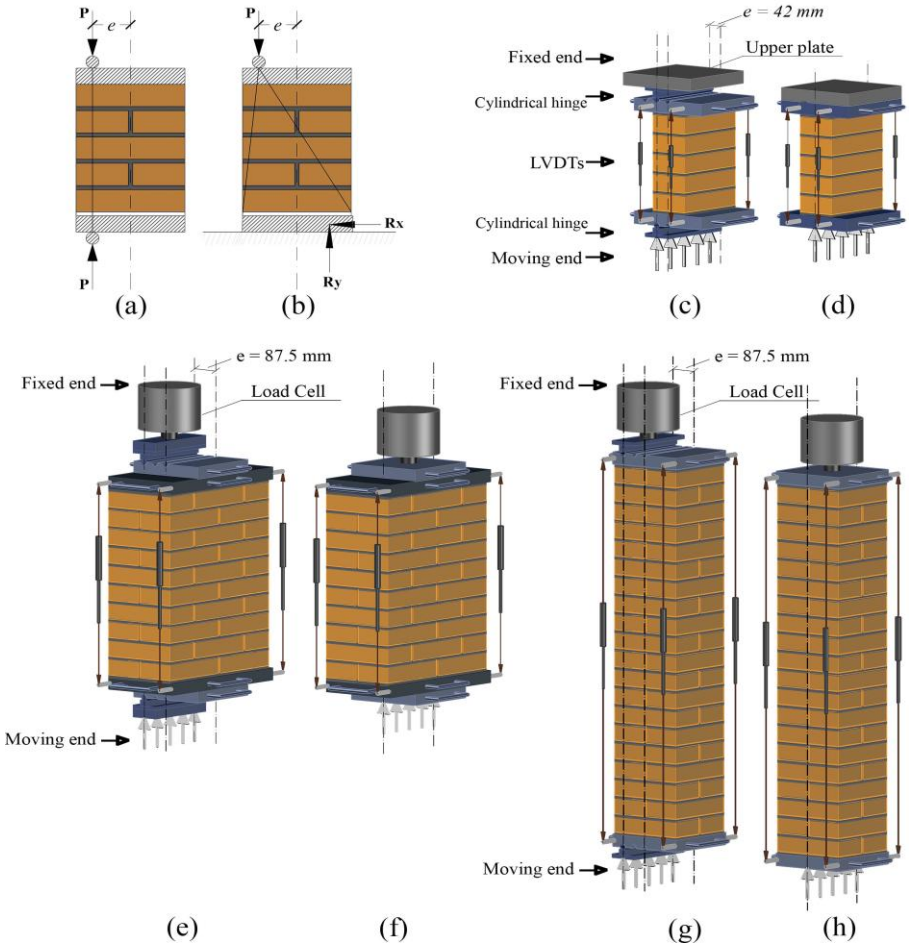

Fig. 5.9: Load-transfer schemes for eccentric load tests and test set-ups: (a) hinge to hinge load-transfer; (b) top hinge to fixed bottom load-transfer; (c) eccentric load test set-up of the "P" samples; (d) concentric load test set-up of the "P" samples; (e) eccentric load test set-up of the "M" samples; (f) concentric load test set-up of the "M" samples; (g) eccentric load test set-up of the "C" samples; (f) concentric load test set-up of the "C" samples.

In the strengthened specimens, the deformation induced in the reinforcing fabric during testing was measured by two strain gauges in the FRCM composite at mid-height of the specimen. The strain gauges applied in specimens "P", "M" and "C" had nominal measuring lengths of 10, 20 and 50 mm, respectively. The applied force and any subsequent deformation was automatically recorded using data acquisition software. As previously discussed, only large eccentricities were considered, which, based on the width of the sections, were 42 mm ("P" specimens) and 87.5 mm ("M" and "C" specimens).

5.2.5 Repair of masonry samples

The tested samples were carefully repaired with the *Mortar NHL* (see Fig 5.10a) and then stored under curing conditions for seven days. The repaired samples tested under tension were strengthened only with the flax-FRCM systems, whereas the repaired samples subjected to eccentric loads were strengthened with both strengthening systems (flax- and PBO-FRCM composites).

(a) (b)

Fig. 5.10: Preparation of masonry specimens for tensile tests: (a) repair of the tested samples; and (b) strengthening of the tested samples.

Three different strengthening systems were applied to the masonry samples subjected to tensile tests (samples "PT"), as shown in Figs. 5.10b and 5.11. The strengthening systems were produced with one and two layers of fabric strips (OLS and TLS, respectively) and two layers of full-face reinforcement (FFS) and were applied by the hand lay-up technique. The

type of strengthening system applied was randomly assigned to each specimen.

The URM samples subjected to eccentric loads (samples "P", "M" and "C") were repaired and then strengthened following the same procedure and technics described in section 5.2.2.

5.3 Results

5.3.1 Tensile behaviour of masonry elements

The tensile behaviour of masonry is governed by its bond strength. Good bond strength between brick and mortar is an important feature in masonry structures, which determines their behaviour in loading conditions caused by external influences such as wind and earthquakes [44]. By conducting tensile tests on masonry samples, it was possible to evaluate the effectiveness of the flax-FRCM composites at improving mechanical performance.

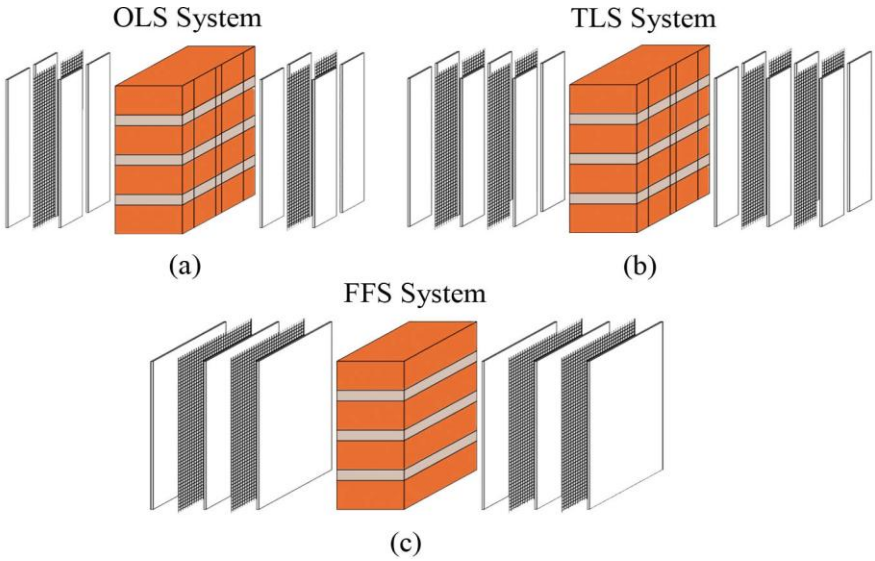

Fig. 5.11: Strengthening systems applied to samples "PT": (a) one-reinforcing-layer system; (b) two-reinforcing-layers system; (c) full-face two-reinforcing-layers system.

Table 5.4 reports the results of the tensile tests conducted on the "PT" samples. The bond strength of the URM samples was compared with that achieved by the repaired samples. In addition, the data are grouped according to the strengthening system used.

Table 5.4: Mechanical behaviour of masonry samples subjected to tensile loads.

Spec.	URM samples		Repaired and reinforced samples					
	P_b (N)	σ_b (MPa)	P_b (N)	P_u (N)	σ_b (MPa)	σ_u (MPa)	Def_u (mm)	Reinforcing system
PT1	1123.73	0.04	6585.57	21836.81	0.22	0.69	29.2	FFS System
PT2	1432.48	0.05	6403.67	10128.53	0.21	0.32	25.7	TLS System
PT3	2892.95	0.1	6730.25	23994.51	0.22	0.73	30.85	FFS System
PT4	4042.58	0.13	8254.1	6585.57	0.28	0.21	0.8	OLS System
PT5	6288.27	0.21	8191.89	6403.67	0.27	0.20	0.8	OLS System
PT6	9201.39	0.31	9641.35	9219.56	0.32	0.29	24.35	TLS System

P_b = Maximum tensile load that produces mortar/brick debonding, σ_b =Tensile bond strength, P_m = Maximum tensile load, σ_m = Maximum tensile strength, Def_m = Maximum extension.

As expected, three ranges of performance of the URM samples were observed. When bricks with moisture contents of 0% and 100% (24 hours of oven dry and 24 hours of water immersion, respectively) were used to build the masonry elements, the tensile bond strength (σ_b) was significantly affected, whereas the samples prepared with bricks with a moisture content of 80% (3 minutes of water immersion) demonstrated the highest strengths. The brittle behaviour of the URM samples produced a sudden failure when the maximum load that causes mortar/brick debonding was reached. Furthermore, because of a poor tensile strain capacity of the URM samples, small deformations of 0.53 to 0.97 mm (average 0.8 mm) were observed (see Fig. 5.12a). The parameters affecting the bond strength of masonry have been extensively studied [4–7]. In this thesis, the reasons that cause adhesion problems on masonry were not studied; the aim was to produce samples with three different ranges of bond strength, and thus study the effectiveness of these systems to improve the bonding behaviour of masonry structures that exhibit different performances (ancient, old and modern masonry). As shown in Table 5.4, the use of flax-FRCM composites increased the tensile bond strength in all masonry samples. In the case of the specimens prepared with bricks with 80% moisture content, the improvement was not as high as the results of the samples prepared with bricks with 0% and 100% moisture

content; the strength in the later cases was increased four and two times, respectively.

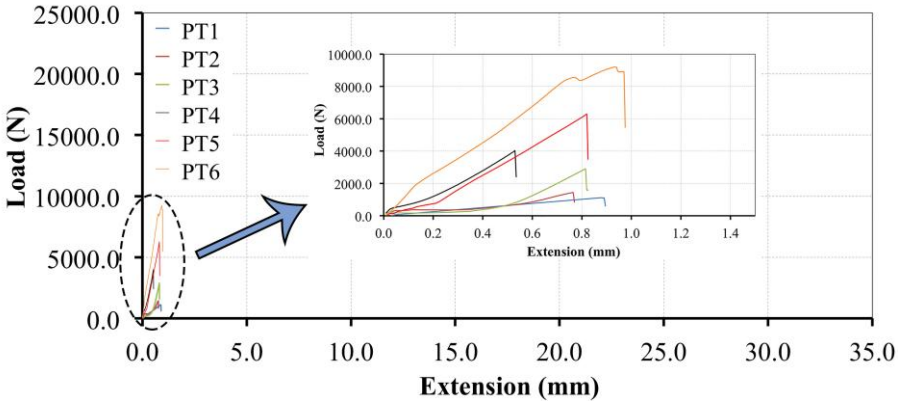

(a)

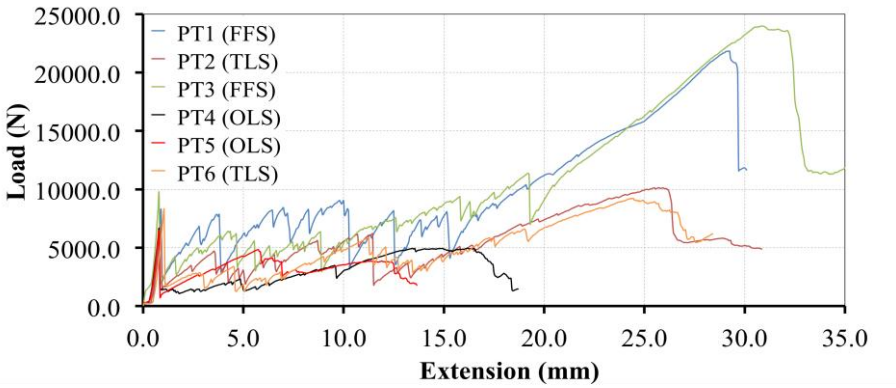

(b)

Fig. 5.12: Tensile behaviour of masonry elements: (a) URM masonry elements; and (b) strengthened masonry elements.

Because of the increased ductility of flax fibres, the deformability of the strengthened specimens increased substantially (see Fig. 5.12b). In all tests, the sample integrity was preserved despite the damage caused by the debonding of the bricks (see Fig. 5.13). As discussed in *Chapters 2 and 3*, the flax-FRCM composites exhibited a multiple cracking behaviour during the tests. Because of this feature, the masonry samples exhibited enhanced ductility, and the distribution of tensile stress occurred along all the mortar joints of the specimens. Once the multiple-cracking stage was completed,

the reinforcing fabrics developed their maximum tensile strength until sample failure; this is the maximum tensile strength reported in Table 5.4.

Fig. 5.13: Strengthened samples subjected to tensile load: (a) sample PT5 strengthened with the OLS system; and (b) sample PT1 strengthened with FFS system.

5.3.2 Concentric and eccentric load tests on masonry elements

5.3.2.1 URM specimens under concentric loads

Owing to the small and erratic tensile response in masonry elements, it can be assumed that only compressive stresses are transmitted (no-tension response). As such, the mechanical behaviour of the three different masonry samples was initially examined in terms of compressive strength, and the compressive strength-strain curves obtained are plotted in Fig. 5.14a. Analysis of these curves reveals that specimens "P", "M" and "C" all behave elastically up to 90%, 87% and 82% of their respective compressive strengths, values that agree well with those reported in the literature [1]. Beyond this linear or quasi-linear stage, the behaviour of the masonry specimens changes quite significantly, with damage and cracking of the samples resulting in a non-linear stress–strain response up to the point of failure.

The "P" and "M" samples exhibited compressive strengths of 19 MPa (CoV 2.5%) and 17 MPa (CoV 16%), respectively, values that are notably higher than that obtained for sample "C" (8 MPa (CoV 10%). As the constituent materials were the same in all samples, the low compressive

strength of sample "C" can be explained by the slenderness of the individual elements. The results for sample "M", however, showed a high degree of scattering that is attributed at least in part to the dimensional differences between the bricks and surface irregularities, which makes it impossible to maintain a uniform thickness amongst the vertical mortar joints between the bricks in any given row. Nevertheless, it should be noted that this level of dimensional irregularity is considered acceptable by current manufacturing standards.

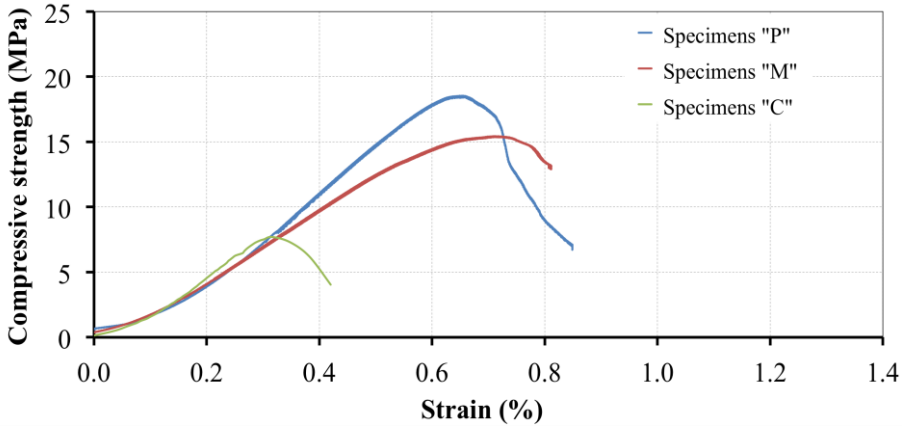

(a)

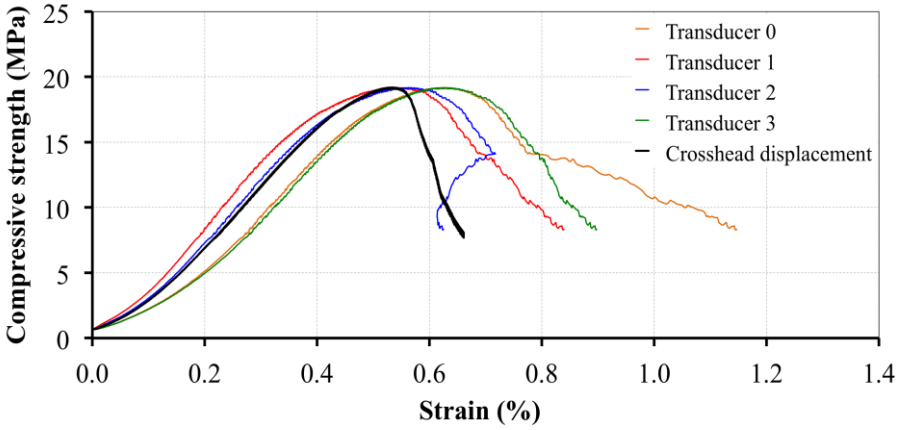

(b)

Fig. 5.14: Stress-strain curves of representative specimens subjected to concentric load: (a) compressive behaviour of specimens "P", "M" and "C"; and (b) non-uniform strain distribution in a specimen "P".

The longitudinal deformation during axial loading was recorded by four LVDTs (T0, T1, T2 and T3) distributed at each corner of the specimen (see Fig. 5.9). As shown in Fig. 5.14b, these measurements reveal that although the loads were applied without eccentricity, a non-uniform strain distribution was generated. These strain values were averaged for the purposes of analysis, and in the case of sample "P", the crosshead displacements that were automatically registered by the compression machine were not considered. The compressive strength of each sample was calculated by simply dividing the maximum load by the cross-sectional area of the specimens; however, only with a concentric load can it be assumed that the stress distribution is uniform. Since eccentric load tests induce an unknown stress distribution in the specimen, this creates a statically indeterminate problem. Photographs of each of the masonry specimens subjected to concentric loads are provided in Fig. 5.15, in which the vertical cracks produced by loading are clearly observed. It should also be noted that specimen failure was, in this case, a result of the material being crushed.

(a) (b) (c)

Fig. 5.15: Cracking of specimens subjected to concentric loads (masonry being crushed): (a) specimen "P"; (b) specimen "C"; and specimen "M".

5.3.2.2 URM specimens under eccentric loads

The testing method used was designed to ensure that the eccentricities at the upper and lower ends of the sample were equal, which as mentioned in Section 5.2, was achieved by using two cylindrical hinges to apply the eccentric load. The eccentricity used with each sample type was selected

using the relation: $2e = 0.70t$ (see Fig. 5.1c). This meant that the eccentricities were proportional to the width of the sections, and in all cases were located in the outer edge of the 70% width. Table 5.5 provides a summary of the test conditions, and Table 5.6 reports the results of the eccentric load tests conducted on the URM sample series. Note that the slenderness ratio, calculated as the ratio of the effective height (H_{ef}) to width (t), has been provided for each sample. A dimensionless ratio of the cross section (t/b), which describes the inertial capacity of the samples in the direction of the destabilising effect, the eccentricity and the eccentricity ratio (e/t) are also listed. Other variables listed include the load-bearing capacity of each sample when subjected to an eccentric load (P_{max}) and the ratio of the maximum load to the maximum uniformly distributed load (P_{max}/P_u). By knowing the longitudinal deformation (Def_1 and Def_2) caused by the rotation of the end sections (steel plates), as well as the values of t and H_{ef}, it was possible to calculate the curvatures given in Fig. 5.16.

Table 5.5: Test conditions for the eccentric load tests.

Sample	Slenderness H_{ef} / t	t / b	e (mm)	e / t
"P"	3.1	0.5	42.0	0.4
"M"	2.8	0.5	87.5	0.4
"C"	4.6	1.0	87.5	0.4

Table 5.6: Results of the eccentric load tests conducted on the URM samples.

Sample	P_{max} (kN)	P_{max} / P_u (%)	Def_1 (mm)	Def_2 (mm)	M_{max} (kN x mm)	ϕ_{max} (mm^{-1} x 10^{-5})
"P"	129.7 (5%)	23.2	2.1	2.3	5447.5 (5%)	8.9 (35%)
"M"	215.3 (21%)	10.2	1.6	2.3	18839.6 (21%)	1.9 (19%)
"C"	226.5 (10%)	43.8	3.5	7.5	19815.6 (10%)	2.4 (8%)

Note: The coefficients of variation (CoV %) are reported in brackets.

To compare the rotational behaviour of the URM to that of the strengthened masonry samples, the moments were also calculated using *Eq. 5.1*, and the moments (M_{max}) and curvatures (ϕ_{max}) listed in Table 5.6 are discussed in *Section 5.4*.

$$M = e \times P_{max} \quad (5.1)$$

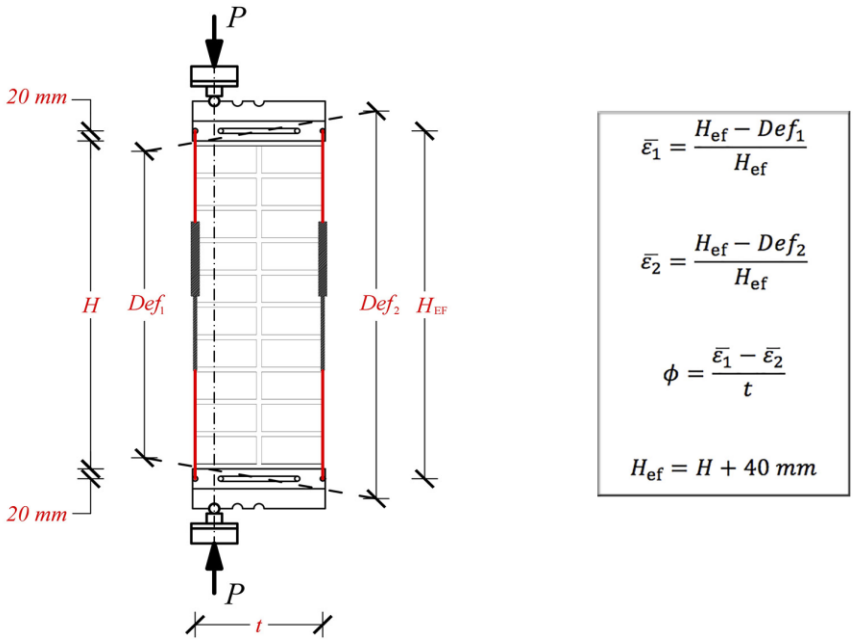

Fig. 5.16: Curvature in specimens subjected to eccentric loads.

The load-displacement curves for the representative specimens of samples "P", "M" and "C" subjected to concentric and eccentric loads are shown in Fig. 5.17. As expected, the maximum eccentric loads (see Figs. 5.17b, 5.17c and 5.17d) were much lower than those observed in the concentric load tests (see Fig. 5.17a). For instance, samples "P", "M" and "C" supported concentric loads (P_u) of 560 kN (CoV 3%), 2114 kN (CoV 16%) and 517 kN (CoV 10%), respectively, whereas the average eccentric loads (P_{max}) were 130 kN (CoV 5%), 215 kN (CoV 21%) and 226 kN (CoV 10%).

This is typical of an eccentric load test, as the rotation of the plates produces a positive strain in the side subjected to compression, whilst a negative strain is induced in the opposite side. Naturally, as shown in Fig. 5.17c, this only occurs once the eccentric load is sufficient to overcome the initial compressive stage and produce second-order bending effects.

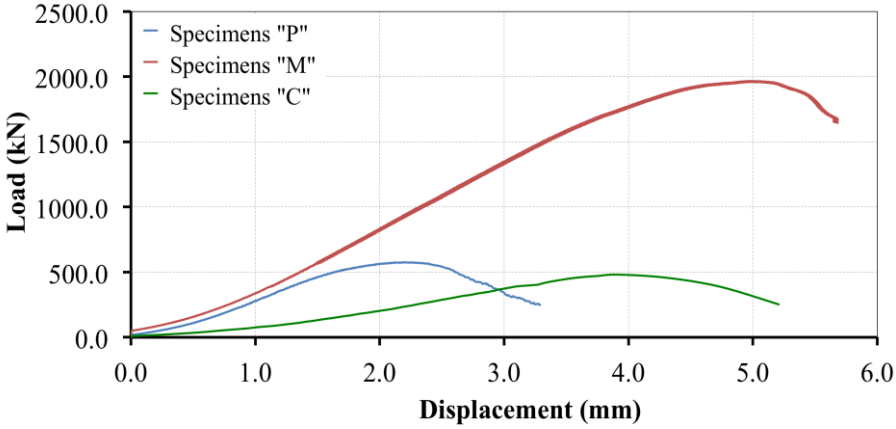
Specimens "P"
Specimens "M"
Specimens "C"
Load (kN)
2500.0
2000.0
1500.0
1000.0
500.0
0.0
0.0
1.0
2.0
3.0
4.0
5.0
6.0
Displacement (mm)

(a)

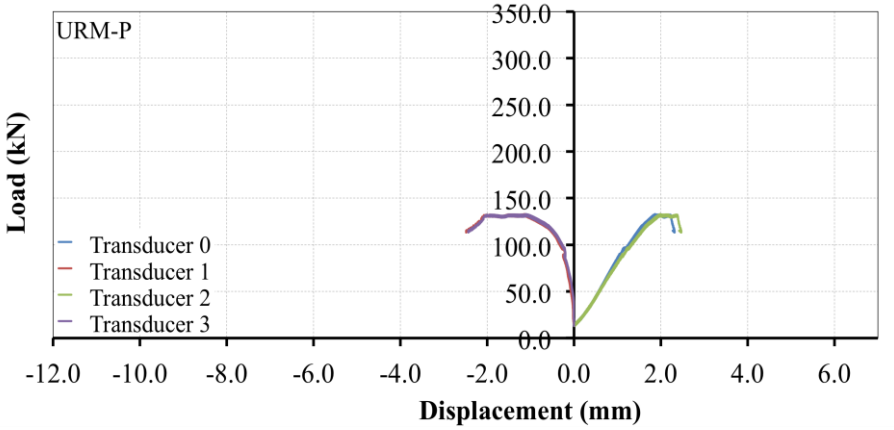
URM-P
Transducer 0
Transducer 1
Transducer 2
Transducer 3
Load (kN)
350.0
300.0
250.0
200.0
150.0
100.0
50.0
0.0
-12.0
-10.0
-8.0
-6.0
-4.0
-2.0
0.0
2.0
4.0
6.0
Displacement (mm)

(b)

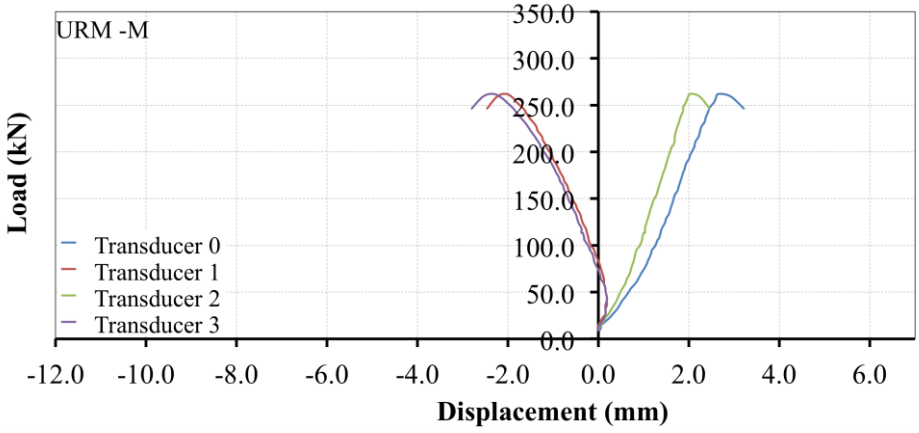
URM -M
Transducer 0
Transducer 1
Transducer 2
Transducer 3
Load (kN)
350.0
300.0
250.0
200.0
150.0
100.0
50.0
0.0
-12.0
-10.0
-8.0
-6.0
-4.0
-2.0
0.0
2.0
4.0
6.0
Displacement (mm)

(c)

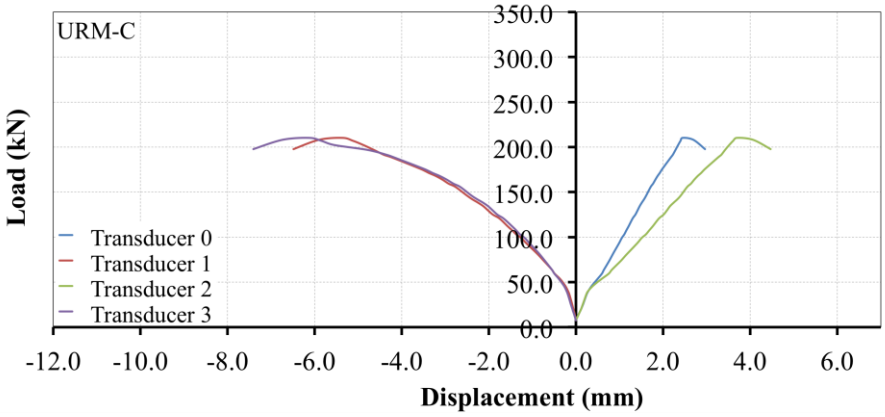

(d)

Fig. 5.17: Load-displacement curves of representative URM specimens: (a) compressive response of specimens "P", "M" and "C"; (b) "P" specimen subjected to eccentric loads; (c) "M" specimen subjected to eccentric loads; and (d) "C" specimen subjected to eccentric loads.

In *Section 5.3.2.1*, it was mentioned that the slenderness of sample "C" influenced its strength when subjected to concentric loads; however, under eccentric loading, other geometrical parameters can also affect the strength. Thus, the inertial capacity of the sections in the direction of the destabilising effect explains why sample "C" lost only 56% of its initial strength, whereas the losses in samples "P" and "M" were 77% and 90%, respectively. Furthermore, the effect of the cross-sectional ratio (t/b) on the inertial capacity and geometric stability means that samples "P" and "M" experience more rapid growth of out-of-plane deformations.

The failure of the URM specimens was caused by a combination of second-order bending and buckling. Moreover, given that the restraint conditions used in the end sections produced rotations associated with a single-curvature mode of deflection, the specimens exhibited sudden failure upon reaching their maximum load. This failure was characterised by the formation of much finer detachment fractures on the compressed surface of the bricks, with a sudden increment in displacements and collapse of the entire element. Thus, an eccentric load resulted in a single mortar joint opening in the tensile side (see Figs. 5.18a and 5.18b). The strength of sample "M" subject to eccentric loading was affected by this failure mode. For the samples analysed in this study, this can be attributed to a connection between the area of the mortar/brick contact and the gross imperfections or

larger irregular surfaces (typically present in this type of clay bricks), which caused adhesion problems.

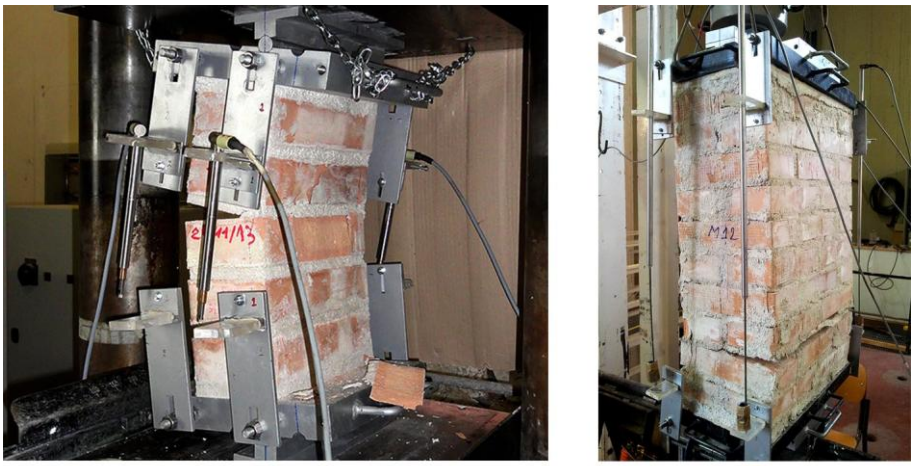

(a) (b)

Fig. 5.18: Failure of URM specimens subjected to eccentric loads: (a) "P" specimen; and (b) "M" specimen.

5.3.2.3 Strengthened specimens under eccentric loads

The reinforced samples were subjected to eccentric loads using the same considerations and experimental set-up as was used with the URM samples. The load-displacement response obtained from each of the FRCM-strengthened samples (Fig. 5.19) shows that the deformation produced in some specimens was affected by the presence of the FRCM composites, resulting in a less uniform deformability than in the URM elements (see Fig. 5.17). For example, both compressive and tensile deformation followed an uneven path in the Re-C-4-Flax specimen (Fig. 5.19e), despite the fact that its T0-T2 and T1-T3 transducers were aligned on the same loading axis. This is indicative of small rotations being generated in the end sections perpendicular to those produced by the effects of the eccentric load. In other specimens, the presence of the FRCM composites caused an irregular development of stiffness during the tests, as shown in Fig. 5.19d. These irregularities can be attributed not only to the inconsistent properties of the constituent materials of the masonry elements but also to the uneven distribution of stresses along the FRCM composites and between each reinforcing layer.

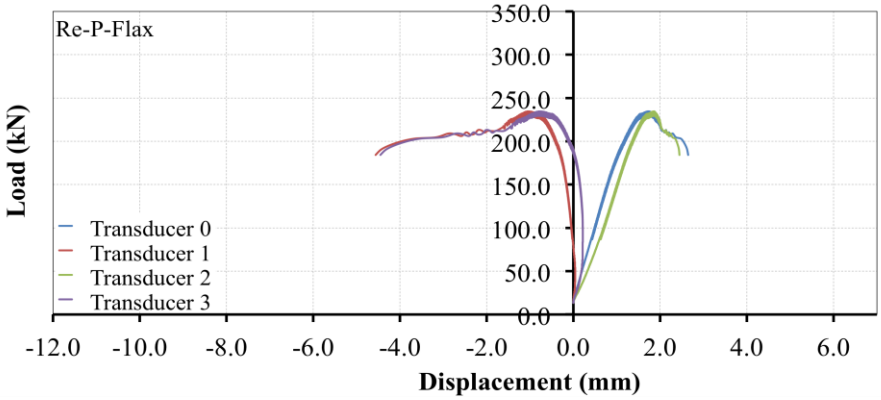

(a)

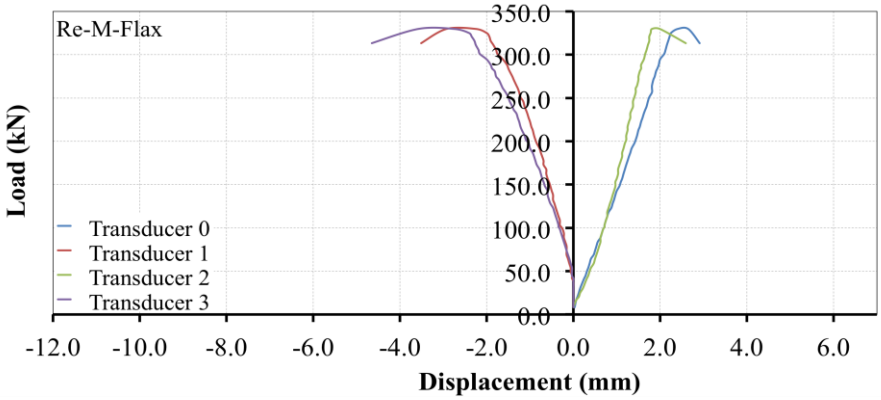

(b)

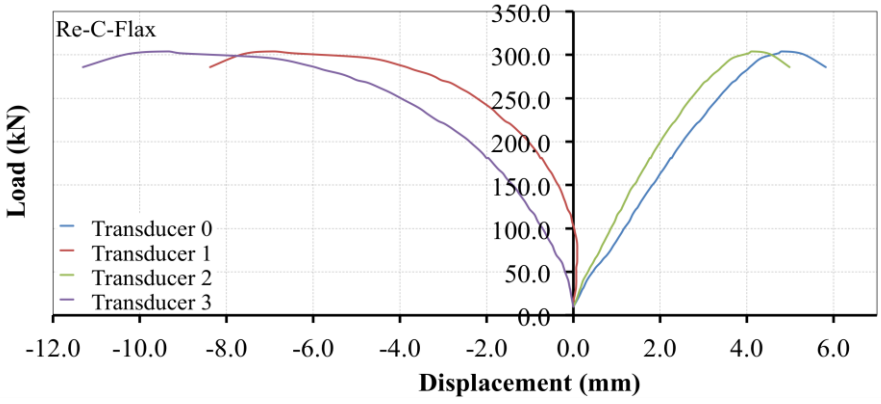

(c)

Fig. 5.19: Load-displacement curves of representative strengthened specimens: (a), (b) & (c) responses of specimens "P", "M" and "C" strengthened with flax-FRCM composites.

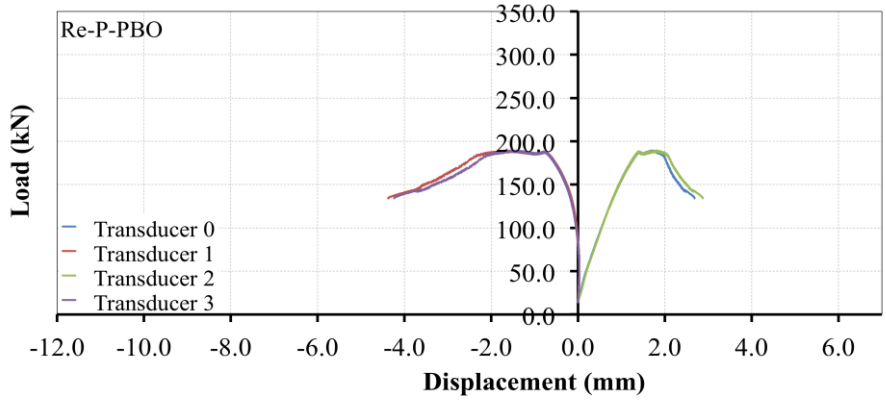

(d)

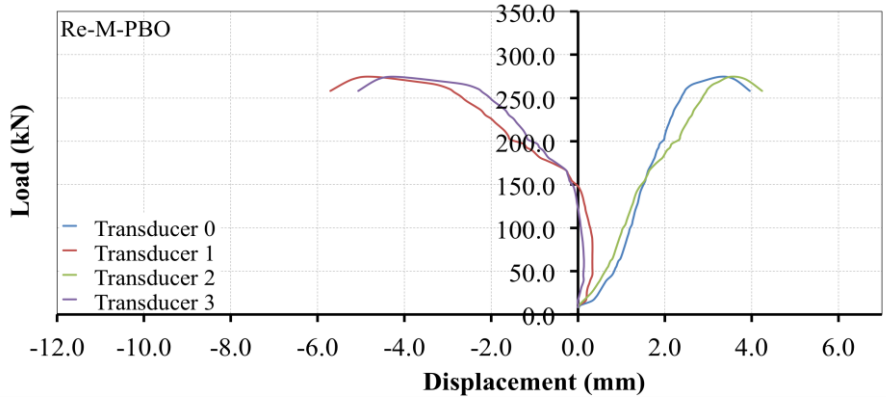

(e)

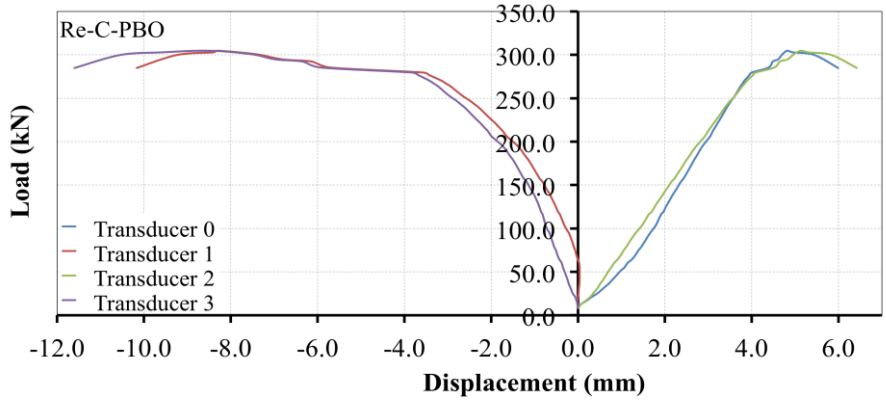

(f)

Continued Fig. 5.19: (d), (e) & (f) responses of specimens "P", "M" and "C" strengthened with PBO-FRCM composites.

The rotations per unit length along the axis of each end section were related to the bending moment along the entire range of loading up to failure, resulting in the moment-curvature diagrams shown in Fig. 5.20.

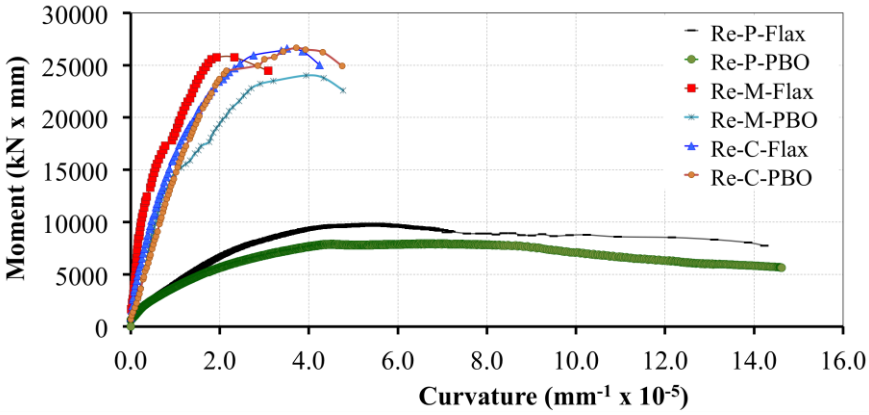

Fig. 5.20: Moment-curvature diagrams of representative strengthened specimens.

For these curves, the deformations recorded by each of the LVDTs were considered separately, and the measurements of the transducers aligned along the same loading axis were averaged. Note also that the higher rotation capacity of the cross-section of specimen "P" is not attributable to the presence of the FRCM composites, and thus the geometry of these specimens resulted in a major deformation relative to the height of the specimens and the width of the sections. The bending moments of specimen "P" were also much lower than the values calculated for specimens "M" and "C", but these are related to the eccentricity used, which in the case of specimen "P" was less than half of what was used with the other sample types.

Much unlike the URM samples, the mechanical response of the strengthened specimens was characterised by a gradual loss of strength once a peak load was reached. Furthermore, the strengthened material was able to withstand much higher deformation through an increase in the extent of softening prior to collapse. As shown in Fig. 5.17 and 5.19, the greater deformation of the strengthened specimens is concordant with an increase in ductility, and thus is very different to the behaviour that is observed when the FRP composites are used to strengthen masonry structures [45].

The mechanism of collapse in the strengthened samples was markedly different to that observed in the URM specimens, with the FRCM composites preventing the failure when openings in the mortar joints were manifested by the tensile stresses. This suggests that the composites are able to better distribute the load and increase the load-bearing capacity, resulting in multiple mortar joint openings before their eventual collapse. In all tests, neither the flax nor the PBO fibres exceeded their maximum load capacity, and thus failure occurred as a result of the masonry in the compressed side being crushed.

The fact that the specimens were loaded by means of upper and lower hinges should have resulted in a load path characterised by the formation of longitudinal cracks from one hinge to the other [8]. However, as a result of the high eccentricities used in this study and the poor bond strength of the masonry, only the strengthened samples exhibited such a crack pattern (Fig. 5.21a, 5.21b and 5.21c).

The behaviour of the FRCM composites was also monitored with two strain gauges in direct contact with the reinforcing fibres, which recorded the composite strain up until the point of failure. Fig. 5.22 shows the load-strain curves for the flax-FRCM system. The composite strain results are discussed in more detail in the next section.

(a) (b) (c)

Fig. 5.21: Hinge to hinge vertically oriented cracks: (a) specimen "M" strengthened with PBO-FRCM composite; (b) specimen "P" strengthened with flax-FRCM composite; and (c) specimen "P" strengthened with PBO-FRCM composite.

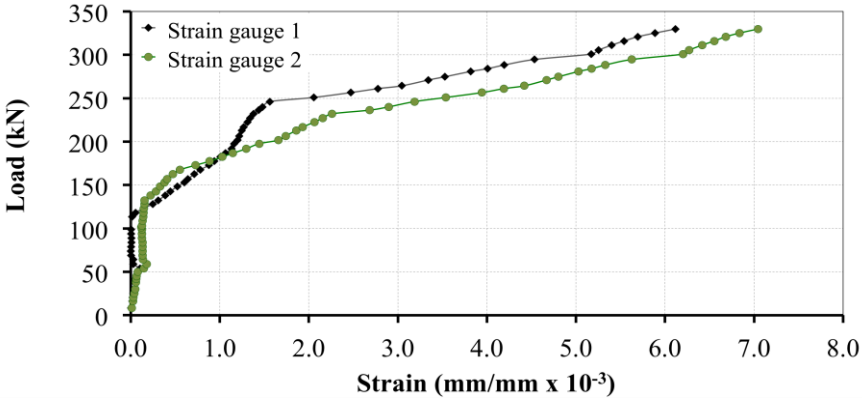

Fig. 5.22: Representative load-strain curves of a flax-FRCM composite (strain gauges applied on the Re-M-Flax-8 specimen).

5.4 Discussion

The results of a comparative analysis of the eccentric load test results for the strengthened samples, which took into account both the collapse mechanism and the mechanical response, are summarised in Table 5.7. In this, the load-bearing capacities of the URM samples subjected to eccentric loads *(*P_{max}) are compared with those of the strengthened samples (P_d). The ratios P_d/P_u and P_d/P_{max} are also included, along with the maximum moment (M_{max}), the curvature (ϕ_{max}) and the ultimate composite strain (ε_u). On the basis of the load-displacement curves and the data presented in Table 5.6 and Table 5.7, it is concluded that both of the strengthening systems studied provide a substantial gain in strength and deformability. However, if the results of the two FRCM systems are compared, it becomes apparent that the difference in the ductility and the stiffness of the fibres has a pronounced effect. For instance, the higher ductility of the flax fibres allows for a higher strain in the FRCM composite forming openings in the mortar joints. These openings are normally the place in which matrix cracks are formed; however, in the composites reinforced with flax fabrics, cracks propagated in these openings during the tests, as shown in Fig. 5.23a and 5.23b. This provides an explanation as to why the specimens strengthened with flax-FRCM composites exhibited a higher strain, as this propagation of matrix cracks was perpendicular to second-order bending effects and therefore allowed energy produced in the bended specimen to be released.

Table 5.7: Results of the eccentric load tests conducted on the strengthened samples.

Sample	URM	Strengthened samples											
	P_{max} (kN)	P_d (kN)		P_d/P_u (%)		P_d/P_{max} (%)		M_{max} (kN x mm)		ϕ_{max} (mm^{-1} x 10^{-5})		ε_u (mm/mm x10^{-3})	
		Flax	PBO	Flax	PBO	Flax	PBO	Flax	PBO	Flax	PBO	Flax	PBO
"P"	129.7 (CoV %)	214.6 (9%)	185.9 (4%)	38.3	33.2	165.5	143.3	9015.1 (9%)	7807.33 (4%)	5.9 (34%)	6.8 (6%)	1.4 (47%)	0.3 (22%)
"M"	215.3 (CoV %)	334.8 (13%)	275.0 (7%)	15.8	13.0	155.5	127.7	29296.3 (13%)	24058.53 (7%)	1.7 (44%)	3.4 (13%)	6.6 (10%)	0.68 (13%)
"C"	226.5 (CoV %)	271.8 (17%)	346.16 (17%)	52.6	67.0	120	152.8	23781.28 (17%)	30288.62 (17%)	3.21 (13%)	2.93 (38%)	7.65 (45%)	1.8 (9%)

Cracking in the cementitious matrix of those samples strengthened with the PBO-FRCM composites, on the other hand, was clearly affected by the properties of the fibres. Indeed, most of the "P" and "M" specimens did not manifest visible cracks in their matrix (see Fig. 5.21a and 5.21c), which subsequently reduced their deformability. Meanwhile, in the "C" specimens, only a few minor cracks in the matrix were formed (see Fig. 5.23c).

Fig. 5.23: Collapse mechanisms observed in the strengthened specimens: (a) & (b) propagation of matrix cracks in the flax-FRCM composite; and (c) matrix cracks in the PBO-FRCM composite applied to a specimen "C".

On the basis of the ultimate composite strains (ε_u) reported in Table 5.7, it can be said that PBO-FRCM composites achieve lower strains than flax-FRCM composites. More importantly, not only does the lower strain capacity and higher stiffness of PBO fibres affect the ductility of masonry samples and limit the composites ability to release stored energy, but it also causes an accumulation of stress in the deformed surface of the elements and between the composite and substrate that leads to debonding of the strengthening systems. When debonding does occur, it is immediately followed by the sudden failure and collapse of individual elements due to a combination of the masonry in the compressed side being crushed and mortar-brick debonding (see Fig. 5.24). Indeed, composite debonding was only observed in those specimens strengthened with PBO-FRCM.

Fig. 5.24: Failure due to a combination of masonry in the compressed side being crushed and mortar-brick debonding: (a) & (b) specimens "P" strengthened with PBO-FRCM; and (c) specimen "C" strengthened with PBO-FRCM.

Based on the mechanical response of the URM samples subjected to eccentric loads, the increase in strength in the flax-strengthened "P" and "M" samples was 66% and 56%, respectively, whereas the "P" and "M" samples strengthened with PBO fabric showed an increase in strength of 43% and 28%, respectively. Furthermore, using the flax-FRCM and PBO-FRCM systems increased deformability up to 45% and 37%, respectively. Given these results, it is clear that the flax-FRCM composite is the more effective at strengthening masonry elements. In the case of sample “C”, however, the efficacy of the PBO-FRCM system was not affected, and so the aforementioned problems of debonding and low ductility were much less pronounced. The PBO-FRCM composite therefore produced a much greater increase in strength of 53% that can be attributed to: i) a lower destabilising effect under eccentric load that allowed the PBO-FRCM composite to release the energy stored in the sides of the specimen by forming minor matrix cracks, and ii) a reduction in deformation due to the higher stiffness and strength of the PBO fabric, which caused a reduced rotation of the end sections. Note that this latter point is consistent with the maximum curvature values in Table 5.7, which show a clear relationship to the bearing capacity of the sample if the moment-curvature envelops shown in Fig. 5.25a, 5.25b and 5.25c are considered. Finally, based on the analysis of destabilising effects on masonry piers subjected to eccentric loads provided in [46], it is

apparent that greater lateral deformation can increase the eccentricity in sections and reduce the resistance area of samples. This would therefore provide an explanation as to why the reduction of the resistant sections in sample "C" was lower when strengthened with PBO fabric composites.

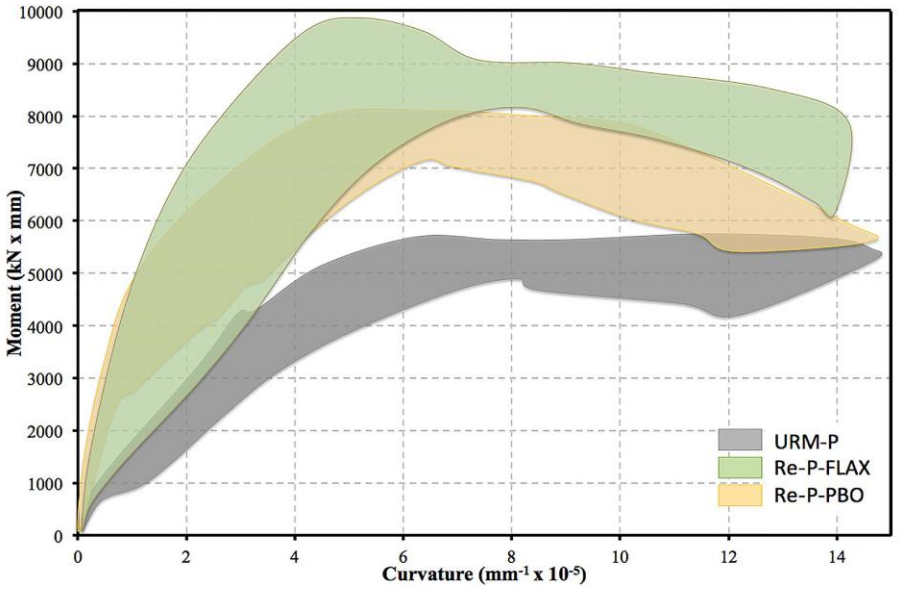

(a)

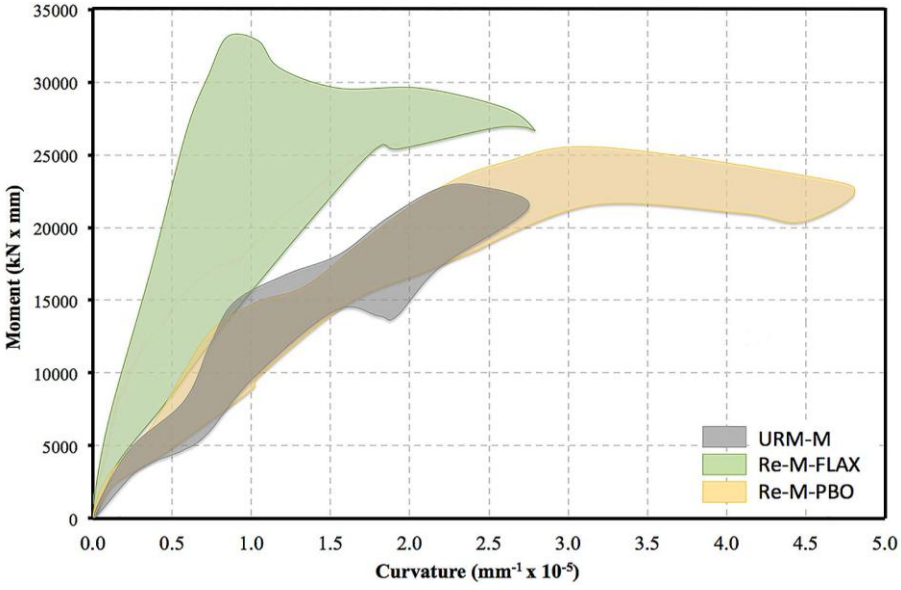

(b)

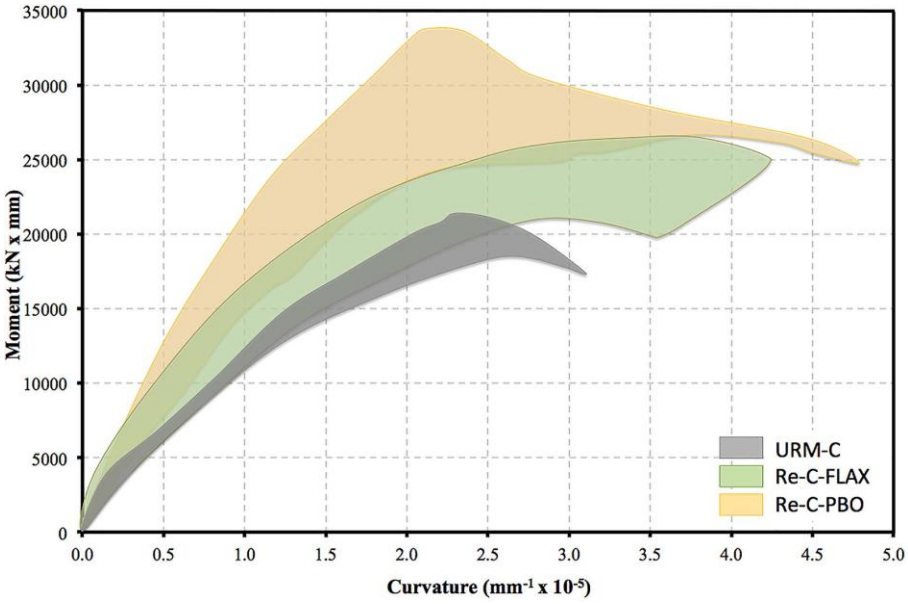

(c)

Fig. 5.25: Moment-curvature envelopes: (a) "P" samples; (b) "M" samples; and (c) "C" samples.

5.5 References

[1] M. Angelillo, editor. Mechanics of Masonry Structures. CISM International Centre for Mechanical Sciences. CISM, Udine; 2014.

[2] Colville J, Made AM, Miltenberger M (1999) Tensile bond strength of polymer modified mortar. J Mat Civil Eng 11:1–5.

[3] Hendry AW, Khalaf FM (2001) Masonry wall construc- tion. E & FN Spon, London

[4] Groot C (1993) Effects of water on mortar brick bond. University of Delft, The Netherlands.

[5] Pavia S, Hanley R. Flexural bond strength of natural hydraulic lime mortar and clay brick. Mater Struct 2009;40:230–45.

[6] Sinha BP (1967) Model studies relating to load bearing brickwork. PhD thesis, University of Edinburgh, UK, Venumadhava Rao K.

[7] Venkatarama Reddy BV, Jagadish KS (1996) Flexural bond strength of masonry using various blocks and mortars. Mater Struct 29:119–124.

[8] Como M. Statics of historic masonry constructions. Berlin: Springer; 2013.
[9] Fortunato A. Elastic solutions for masonry-like panels. J Elast 2010;98:87–110.
[10] Angelillo M, Cardamone L, Fortunato A. A numerical model for masonry-like structures. J Mech Mater Struct 2010;5:583–615.
[11] Angelillo M, Babilio E, Fortunato A. Singular stress fields for masonry-like vaults. Continuum Mecha Thermodynam 2013;25:423–41.
[12] Park J, Towashirapornb P, Craigc JI, Goodnod BJ. Seismic fragility analysis of low-rise unreinforced masonry structures. Eng Struct 2009;31(1):125–37.
[13] Marcari G, Manfredi G, Prota A, Pecce M. In-plane shear performance of masonry panels strengthened with FRP. Composites: Part B 2007;38:887–901.
[14] Buchan PA, Chen JF. Blast resistance of FRP composite and polymer strengthened concrete and masonry structures: a state-of-the-art review. Compos Part B: Eng 2007;38(5/6):509–22.
[15] Ghiassi B, Marcari G, Oliveira D, Lourenco P. Water degrading effects on the bond behavior in FRP-strengthened masonry. Compos Part B: En 2013;54:11–9.
[16] Shrive N. The use of fibre reinforced polymers to improve seismic resistance of masonry. Constr Build Mater 2006;20:269–77.
[17] Papanicolaou C, Triantafillou T, Lekka M. Externally bonded grids as strengthening and seismic retrofitting materials of masonry panels. Constr Build Mater 2011;25:504–14.
[18] Corradi M, Borri A, Castori G, Sisti R. Shear strengthening of wall panels through jacketing with cement mortar reinforced by GFRP grids. Compos Part B: En 2014;64:33–42.
[19] Papanicolaou CG, Triantafillou TC, Papathanasiou M, Karlos K. Textile-reinforced mortar (TRM) versus FRP as strengthening material of URM walls: out-of-plane cyclic loading. Mater Struct, RILEM 2008;41(1):143–57.
[20] ACI 549.4R-13. Guide to Design and Construction of Externally Bonded Fabric-Reinforced Cementitious Matrix (FRCM) Systems for

Repair and Strengthening Concrete and Masonry Structures. ACI, 2013.

[21] Brameshuber W, editor. State-of-the-art report of RILEM technical committee 201 TRC: textile reinforced concrete (RILEM Report 36). Bagneux: RILEM Publications S.A.R.L., 2006.

[22] Triantafillou TC, Papanicolaou CG. Shear strengthening of reinforced concrete members with textile reinforced mortar (TRM) jackets. Mater Struct, RILEM 2006;39(1):93–103.

[23] Ombres L. Flexural analysis of reinforced concrete beams strengthened with a cement based high strength composite material. Compos Struct 2011;94(1): 143–55.

[24] Ombres L. Concrete confinement with a cement based high strength composite material. Compos Struct 2014;109: 294–304.

[25] Codispoti R, Oliveira DV, Fangueiro R, Lourenço P, Olivito R. Experimental Behavior of Natural Fiber-Based Composites Used for Strengthening Masonry Structures. Conference Papers in Materials Science. Article ID 539856, 2013. doi:10.1155/2013/539856

[26] Prota A, Marcari G, Fabbrocino G, Manfredi G, Aldea C. Experimental in-plane behavior of tuff masonry strengthened with cementitious matrix–grid composites. J Compos Construct, ASCE 2006;10(3):223–33.

[27] D'Ambrisi A, Feo L, Focacci F. Experimental and analytical investigation on bond between carbon-FRCM materials and masonry. Compos Part B: En 2013;46:15–20.

[28] D'Ambrisi A, Feo L, Focacci F. Bond-slip relations for PBO-FRCM materials externally bonded to concrete. Compos Part B: En 2012;43(8):2938–49.

[29] Mobasher B. Mechanics of Fibre and Textile Reinforced Cement Composites. CRC Press. Taylor & Francis Group, Boca Raton, Fl; 2012.

[30] Ruredil. X mesh gold data sheet. Ruredil S.p.A. 2009, Milan, Italy. <http://english.ruredil.it/SchedeProdottoENG/RuredilXMeshGOLD_ing_1.pdf>.

[31] D'Ambrisi A, Focacci F, Caporale A. Strengthening of masonry-unreinforced concrete railway bridges with PBP-FRCM materials. Compos Struct 2013;107:193–204.

[32] Trapko T. Behaviour of fibre reinforced cementitious matrix strengthened concrete columns under eccentric compression loading. Mater Des 2014;54:947–57.
[33] Wu ZS, Iwashita K, Hayashi K, Higuchi T, Murakami S, Koseki Y. Strengthening PC structures with externally prestressed PBO fiber sheets. In: Teng J, editor. Proc of int conf on FRP composites in civil engineering, CICE2001, Elsevier Science, Honk Hong; 2001. p. 1085–92.
[34] Olivito R, Cevallos O, Carrozzini A. Development of durable cementitious composites using sisal and flax fabrics for reinforcement of masonry structures. Mater Des 2014;57:258–68.
[35] Cevallos O, Olivito R. Effects of fabric parameters on the tensile behaviour of sustainable cementitious composites. Compos Part B: En 2015;69:256–66.
[36] BS EN 772-1. Methods of test for masonry units. Determination of compressive strength. BSI, 2011.
[37] BS EN 772-13, Methods of test for masonry units – Part 13: Determination of net and gross dry density of masonry units (except for natural stone). BSI, 2000.
[38] BS EN 459. Building lime. Definitions, specifications and conformity criteria. BSI, 2010.
[39] BS EN 196–1. Methods of testing cement: determination of strength. BSI, 2005.
[40] BS EN 1015–11. Methods of test for mortar for masonry: determination of flexural and compressive strength of hardened mortar. BSI, 1999.
[41] BS EN 998/2. Specification for mortar for masonry. Masonry mortar. BSI, 2010.
[42] Sandoval C, Roca P. Study of the influence of different parameters on the buckling behaviour of masonry walls. Constr Built Mater 2012;35:888–99.
[43] Martinez JLM. Theoretical and experimental determination of the limit domains of masonry structures, and application to historical structures. PhD thesis, T. U. of Madrid, Madrid, Spain, 2003 [in Spanish].

[44] Lawrence SJ, Sugo HO, Page AW. Masonry bond strength and the effects of supplementary cementitious materials. Engineers Australia; 2005. p. 876.

[45] Papanicolaou CG, Triantafillou TC, Karlos K, Papathanasiou M. Textile-reinforced mortar (TRM) versus FRP as strengthening material of URM walls: in-plane cyclic loading. Mater Struct, RILEM 2007;40(10):1081–97.

[46] La Mendola L, Papia M. Stability of masonry piers under their own weight and eccentric load. Journal of Structural Engineering (ASCE) 1993;119(6):1678–93.

Chapter 6

PREDICTING THE STRESS-STRAIN RESPONSE OF SUSTAINABLE FRCM SYSTEMS

6.1 Introduction

Throughout this study, several investigations were conducted to determine the possibility of using sustainable-FRCM composites to strengthen masonry elements. As discussed in Chapter 5, these composite systems can significantly improve the mechanical response of masonry elements subjected to eccentric loads, a finding that has been the culmination of extensive experimental research. As a complementary part of this research, a numerical analysis of the tensile behaviour of the developed composites is included in this chapter. The numerical analysis provided herein may be used in future research to expand the knowledge on this issue as the implementation of this system as a regular strengthening technique is still distant.

Modelling the mechanical behaviour of composite materials used to

strengthen structures is essential to developing future applications in real situations, and thus, since composites generally are designed to bear tensile loads, it is highly relevant to model the tensile response (e.g., tensile stress–strain response). For the flax- and sisal-FRCM composites developed in this research, the tensile behaviour (experimentally examined) was characterised by multiple cracking. The distributed transverse cracks formed gradually as the composite was loaded, and three main stages were clearly defined (see *Chapters 3 and 4*). The occurrence of these transverse matrix cracks (perpendicular to the loading direction) marked the deviation of the composite from linear elastic behaviour [1–5]. With the monotonic load increment, the matrix cracks continued to develop, accompanied by other damage events such as the debonding of the fibre/matrix interface and fibre fracture.

The mechanics of crack development and tensile behaviour of brittle matrix composites have been described by the familiar ACK model [6,7], which relates the spacing between the parallel transverse cracks to the frictional shear stress transfer rate [8]. This model, however, has a limited applicability because of the simplifying assumptions, such as the perfect bond and no-tension stiffening effect, which are defined as the ability of the non-cracked segments in between the two parallel cracks to carry tensile force [9]. According to several authors [10–17], another important limitation in the ACK model is the non-consideration of the stochastic nature of the strength of cementitious matrices. On the basis of these drawbacks, the tensile behaviour of cementitious composites has been modelled using several approaches. One of the most frequently used methods that considers the stochastic nature of such matrices has been developed by Curtin et al. [14,17]. In these studies, it was shown that it is possible to determine statistical Weibull parameters from pure matrix specimens and transfer them to the matrix behaviour in the composite, while also considering stochastic fibre damage and ultimate failure. However, it has been determined that this is not the case when textile reinforcement is used in a cementitious matrix. Based on the model developed by Cutin et al. [14,17], Cuypers and Wastiels [18] extended the ACK model by incorporating a two-parameter Weibull distribution [14,17] in the simulation of the stochastic cracking strength of the matrix in cementitious composites reinforced with fabrics or textiles.

In this chapter, the tensile behaviour of flax- and sisal-FRCM composites is numerically analysed considering both the ACK theory and the stochastic model developed by Cuypers and Wastiels [18]. The numerical responses obtained with both models consider the mechanical properties of the fibres and matrix. These values were obtained performing an extensive mechanical characterisation, as described in *Chapters 3 and 4*. The fact that the properties of natural fibres are very different from those commonly used in FRCM composites (e.g., glass, carbon, etc.) results in a limited estimation of the mechanical behaviour. However, for the composites developed in this research, this estimation may allow for a suitable approximation of some important mechanical parameters such as the tensile strength, ultimate strain and elastic modulus. The experimental results of tensile tests conducted on composite samples produced with one, two and three layers of reinforcing fabrics are compared with the theoretical results in terms of tensile stress–strain curves.

6.2 Theoretical background

From the tensile test conducted on composite samples, conclusions can be formulated concerning changes in the stress–strain behaviour and the development of matrix cracks. Figs. 4.4 and 4.5 show the tensile responses of flax- and sisal-FRCM composites, which are divided into four stages. The initial linear stage (pre-cracking stage) ends when the first crack in the matrix appears. The pre-cracking stiffness (E_I) is determined from the experimental curves. Usually it is assumed that the bond between the matrix and reinforcing fabrics is not affected in this stage. After the first crack appears, the force grows more slowly (decreased stiffness) and fine transversal cracks form. This is the multiple cracking stage (second stage). In the vicinity of a matrix crack, the stress transfer between the matrix and fibres becomes frictional. At this point, the distance between cracks or actual crack spacing (x) is a function of the applied stress and can still decrease when the load increases. The saturation crack spacing (X) is achieved when a certain stress level is reached and no extra matrix cracking occurs even though the applied load is increased, and the load is carried only by the fibres. The stress transfer between the matrix and fibres is frictional along

the whole composite and only the fibres provide post-cracking stiffness (E_{III}).

This mechanical behaviour is typically observed in cementitious composites reinforced with fabrics and may be modelled using different theories. Basic assumptions used in the development of the ACK theory as well as in the stochastic model are:

- The fibres are only capable of carrying a load along their longitudinal axis; they provide no bending stiffness.
- The fibre–matrix bond is weak. The adhesion shear bond strength is low. Propagation of matrix cracks leads to fibre–matrix debonding along a certain length in the vicinity of a matrix crack.
- Once the matrix and the fibre are debonded, a pure frictional shear stress replaces the previously existing adhesion shear stress.
- At the debonded fibre–matrix interface, this sliding shear stress is constant with the slip.
- The frictional interface shear stress is constant along the debonded interface.
- Poisson effects of the fibre and matrix are neglected.
- Global load sharing is used for the fibres.
- Normal matrix stresses, transversal to the loading direction, are uniform in a cross section.

6.2.1 ACK theory

The Aveston–Cooper–Kelly theory was developed to model the stress–strain behaviour of composites produced with a brittle matrix, considering that the fibre–matrix bond remains intact after the matrix has cracked [6,7]. This model also considers the increased strain capacity of the matrix and the multiple cracking mechanisms in the presence of fibres in unidirectional composites, without considering the tension stiffening effect. The extent of fibre debonding and crack spacing in a partially debonded composite are closely linked to the maximum shear stress at the fibre–matrix interface. Several authors have already modelled the tensile behaviour and multiple cracking in brittle matrix composites basing their theories on the ACK model [19,20]. This model typically describes the first three stages of the

tensile behaviour (see *Chapters 3 and 4*). The ACK theory assumes that in the first stage both the fibres and the matrix equally resist the applied load, and the behaviour of the composite is characterised by a linear elastic response. The composite stiffness in the first stage is described by the law of mixtures:

$$E_{c1} = E_m V_m + E_f V_f \tag{6.1}$$

where E_f and E_m are the elastic modulus of the fibre and matrix, respectively. V_f and V_m are the relative volume fractions of the fibres and matrix, respectively.

In the second stage, cracks initiate and propagate in the brittle matrix. To bridge these micro-cracks, both the length of the fibres and the fibre volume fraction should be sufficiently high. At the vicinity of each crack face, it is assumed that there is a linear, frictional stress transfer between the fibres and matrix. The length, which is needed to transfer stresses from the fibre at the crack face of the matrix, denoted as the debonding length (δ), can be determined by expressing the equilibrium of stresses along δ:

$$\delta = \frac{\sigma_c E_m r V_m}{2 V_f \tau E_{c1}} \tag{6.2}$$

where σ_c is the composite stress, τ is the constant frictional interface shear stress between the fibres and matrix (which is supposed to be constant in this theory) and r is the fibre diameter. According to the ACK model, the matrix has a determinate tensile failure stress (σ_{mu}) and a corresponding failure strain (ε_{mu}). Once σ_{mu} is reached, the matrix shows multiple cracking. This means that matrix cracks are initiated and propagated along the entire volume, and the stress at which this takes place (σ_{mc}) is:

$$\sigma_{mc} = \frac{E_{c1} \sigma_{mu}}{E_m} \tag{6.3}$$

When a first matrix crack appears and reaches a fibre, debonding of the fibre-matrix interface occurs, in accordance with the model assumptions.

Along the debonded interface, the interface shear stress (τ) provides normal stress transfer from the fibres to the matrix as shown in Fig. 6.1. The far field matrix stress (σ_m^{ff}), indicated in Fig. 6.1 is the stress in the matrix at an infinite distance from one crack. Actually, σ_m^{ff} is the stress in the matrix, calculated as if the composite would still behave elastically linear.

Since for the ACK model it is assumed that all matrix cracking occurs at the same fixed stress level, the value of σ_m^{ff} is the same as σ_{mu}. Since the matrix stress is lower than σ_{mu} along the debonding length, no extra crack will be introduced within a distance 2δ from the crack face (see Fig. 2). As long as the distance between two adjacent cracks is larger than 2δ, a new crack can be formed at a distance at least δ from both neighbouring existing cracks [18].

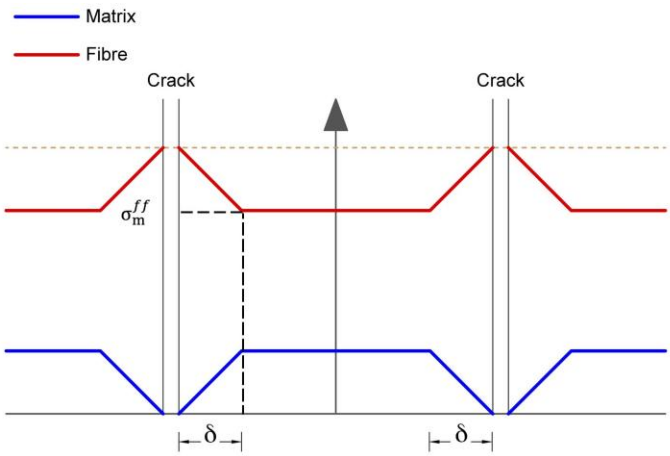

Fig. 6.1: Evolution of the normal stresses produced in the fibres and matrix.

At the multiple cracking stage, distances between cracks are no smaller than δ and no larger than 2δ. The spatial introduction of cracks occurs randomly until no space remains for new cracks. Widom [21] determined that the average distance between cracks (X) is:

$$X = 1.337\ \delta \tag{6.4}$$

For this value, the composite strain ε_{cII} (end of stage II) can be defined as:

$$\varepsilon_{cII} = [1 + 0.666(\alpha)]\ \frac{\sigma_{mu}}{E_m} \tag{6.5}$$

When it is assumed that the spatial distribution of the cracking phenomenon can be considered to occur stochastically, the final average crack spacing will be situated between δ and 2δ and the strain at the end of multiple cracking is situated between two limit values:

$$\left(1 + \frac{\alpha}{2}\right)\varepsilon_{mu} \leq \varepsilon_{cII} \leq \left(1 + \frac{3\alpha}{4}\right)\varepsilon_{mu} \tag{6.6}$$

where ε_{mu} is the failure strain of the matrix, and:

$$\alpha = \frac{E_m\, V_m}{E_f\, V_f} \tag{6.7}$$

After ε_{cII} is reached and the multiple cracking stage ends, the matrix stresses remain constant with an increasing applied external load. In the third stage, prior to failure, the composite behaves with modulus E_fV_f because only the fibres are stressed as they slide through the matrix [22].

6.2.2 Stochastic model

The stochastic cracking theory is based on several assumptions of the ACK theory, but it is now assumed that the multiple cracking stage does not occur at one stress level, but along a wide stress range. The distinction between the three stages, as assumed in the ACK theory, disappears. The composite strain ε_c will be formulated as a function of the stress by means of

a function of the percentage of matrix cracks that already appeared at this stress [14,17,18]

As will be discussed in the following section, the ACK model shows some discrepancies with the experimental curves of FRCM composites. Generally, in a FRCM composite, the multiple cracking stage does not occur at a constant stress level, as assumed in the ACK theory. These differences have led to the development of the so-called stochastic model [18]. In this model, both the first and third stages of the stress–strain curve are modelled as in the ACK theory. However, to model the multiple cracking stage, a statistical approach is used to predict the percentage of matrix cracks that have already been formed depending on the composite stress. In the multiple cracking stage, the mean crack distance (x) will decrease with increasing stress level until the distance equals X. Because the assumption of a deterministic matrix cracking value σ_{mu} is not valid in the stochastic model, the far field matrix stress $\left(\sigma_m^{ff}\right)$, in this case, becomes a function of the composite stress (σ_c):

$$\sigma_m^{ff} = \sigma_c \left(\frac{E_m}{E_{cI}}\right) \tag{6.8}$$

On the basis of the latter, the final average crack spacing will not be equal to that defined in the ACK theory. Furthermore, the parameter δ also varies with the stress. The statistical function used to represent the matrix cracking strength is the 2-parameter Weibull distribution function as it properly fits the experimental data [23]. This cumulative distribution function is determined empirically and can be written as in *Eq. 6.9*. The formula provides the necessary information on the percentage of inherent imperfections that can grow and form a crack at a certain stress level (*Eq. 6.10*).

$$P = 1 - exp\left[-\left(\frac{\sigma_c}{\sigma_{Rc}}\right)^m\right] \tag{6.9}$$

$$x(\sigma_c) = \frac{X}{P(\sigma_c)} \tag{6.10}$$

where P is the probability of fracture (cracking) at the applied stress level, m is the Weibull modulus that defines the width of the distribution on the matrix cracking strength and σ_{Rc} is the reference cracking composite stress, which is a measure of the multiple cracking composite stress.

In the stochastic model, δ is expressed in a similar way as for the ACK theory (see *Eq. 6.2*) where it is obtained by expressing the force equilibrium along the distance δ. Depending on the value of the composite stress (σ_c), the value of the crack distance (x) may be less than, equal to or greater than 2δ. Fig. 6.1 shows the matrix and fibre stresses between 2 cracks when the actual crack spacing x is larger than 2δ, whereas Fig. 6.2 shows this stress distribution when the distance is equal to or less than 2δ.

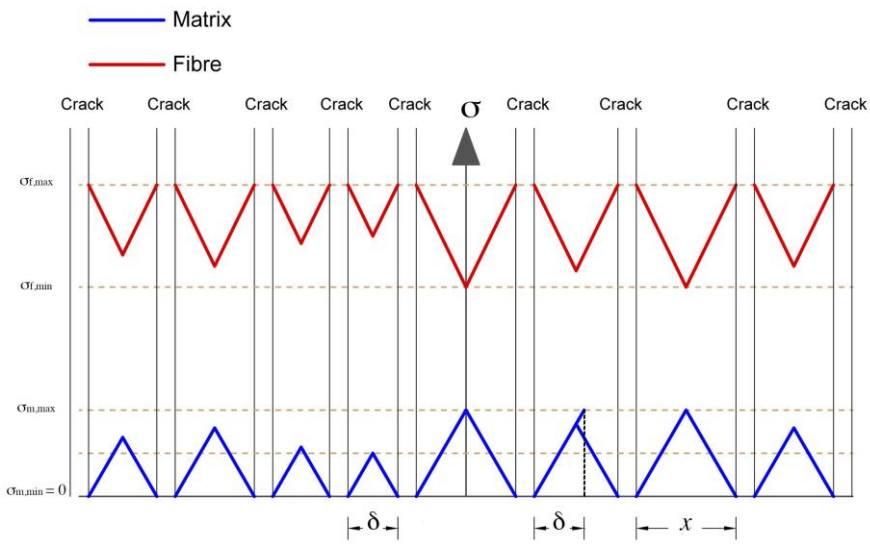

Fig. 6.2: Normal stresses in fibre and matrix (case $x = X \leq 2\delta$).

The stress–strain relationship could be derived for $x > 2\delta$ (Fig. 6.1), whereas the expression for the average strain of the composite could be found by deriving along the debonded parts and also along the non-

debonded parts, with a total length of x-2δ. The fibre stresses along the non-debonded parts are still in pre-cracking state. Therefore, the average fibre stress along x-2δ is:

$$\sigma_f = \frac{E_f \sigma_c}{E_{c1}} \tag{6.11}$$

The maximum and minimum fibre stresses can be expressed at the crack surface and at distance δ from the crack surface, respectively:

$$\sigma_{f,max} = \frac{\sigma_c}{V_f} \tag{6.12}$$

$$\sigma_{f,min} = \frac{E_f \sigma_c}{E_{c1}} \tag{6.13}$$

The average fibre stress along the debonded parts with length δ is:

$$\sigma_f = \frac{\left(\frac{\sigma_c}{V_f} + \frac{E_f \sigma_c}{E_{c1}}\right)}{2} \tag{6.14}$$

Because the average fibre stresses along δ and *x*-2δ are known, the average fibre stress along *x* can be determined:

$$\langle \sigma_f \rangle_{\text{along } x} = \frac{E_f \sigma_c}{E_{c1}} + \frac{\delta E_m V_m \sigma_c}{x V_f E_{c1}} \tag{6.15}$$

The average fibre strain can simply be obtained by dividing the average fibre stress by the stiffness of the fibres (E_f). Because the composite strain ε_c equals the average fibre strain along *x*, it is possible to rearrange the equations to find:

$$\varepsilon_c = \frac{\sigma_c}{E_{c1}} \left(1 + \frac{\alpha\,\delta}{x}\right) \tag{6.16}$$

From Fig. 6.2, the composite stress–strain formulation can be extracted in similar way as for $x < 2\delta$:

$$\varepsilon_c = \sigma_c \left(\frac{1}{E_f V_f} - \frac{\alpha\,x}{4\,\delta\,E_{c1}}\right) \tag{6.17}$$

6.2.3 Modification of the stochastic model

Cuypers et al. developed the stochastic model based on the assumptions of the ACK theory but also proposed some modifications to consider the effects of textile materials in the numerical analysis of the stress–strain responses [22]. The assumptions made in the ACK model are generally not valid for FRCM composites. Moreover, it is assumed that all the parameters included in the model are deterministic. Among the important discrepancies regarding the model for FRCM, the following are highlighted:

a) In the FRCM composites, fibre bundles are used instead of individual fibres (monofilaments).
b) Unlike FRCM composites, the fibres are generally not oriented in the same direction of the load application.
c) The length of the fibres may be limited in the composites generally modelled using this theory.

Analysing the latter considerations, when fibre bundles are used instead of monofilaments, not all fibres are in contact with the surrounding matrix. This happens because usually only partial penetration of the matrix occurs within the outer filaments of the bundle. However, because of the fibre-fibre interactions, major or full activation of the fibres may still occur, and the bundle effect would not produce significant discrepancies when this method is used to model fabric-reinforced composites. Considering fibre length and orientation, there is also limited efficiency of the fibres along the axis of loading.

Based on this modified stochastic model, the numerical analysis of the tensile behaviour of the sustainable composites studied in this investigation is performed using factors (η_1 and η_3) that represent the efficiency of the fibres. Therefore, the composite stiffness in stage 1 (E_{c1}) can be rewritten as:

$$E_{c1} = E_m V_m + E_f (\eta_1 V_f) \tag{6.18}$$

were η_1 is the efficacy of the fibres at the first stage. In the third stage, the stiffness E_{c3} can be rewritten as:

$$E_{c3} = E_f (\eta_3 V_f) \tag{6.18}$$

were η_3 is the efficacy of the fibres at the third stage. Because the end of the second stage is the beginning of the third stage, *Eq. 6.2* and *Eq. 6.7* can be rewritten as:

$$\delta = \frac{\sigma_c E_m r V_m}{2 \eta_s V_f \tau E_{c1}} \tag{6.19}$$

$$\alpha = \frac{E_m V_m}{E_f \eta_s V_f} \tag{6.20}$$

6.3 Experimental programme

The results of the tensile tests conducted on the composite specimens produced with the NLG matrix and fabric strips of flax and sisal fibres were analysed. The composite samples reinforced with one, two and three layers of fabric strips were tested. The test set-up and testing considerations, as well as the specimen characteristics, are described in *Chapters 3 and 4*. The experimental results, in terms of the tensile stress–strain curves, are used to provide a comparison between the ACK model and stochastic model.

The data required to run both the ACK and the stochastic models are summarised in Tables 6.1, 6.2 and 6.3.

Table 6.1: Properties of the fibres and matrix used in the numerical analysis.

	flax-FRCM composites	sisal-FRCM composites
E_f (MPa)	3750	4360
E_m (MPa)	5420.739	5420.739
σ_{mu} (MPa)	1.026	1.026
ε_f (%)	11	7.9

Table 6.2: Volume fraction of fibres and matrix of the FRCM composites.

	flax-FRCM composites			sisal-FRCM composites		
	one-layer	two-layers	three-layers	one-layer	two-layers	three-layers
V_f	0.0135	0.027	0.0405	0.01575	0.0315	0.04725
V_m	0.9865	0.973	0.9595	0.98425	0.9685	0.95275

Table 6.3: Factors and Weibull parameters used in the stochastic model.

	flax-FRCM composites			sisal-FRCM composites		
	one-layer	two-layers	three-layers	one-layer	two-layers	three-layers
$\eta 1$	0.5	0.8	0.8	0.5	1.0	1.0
$\eta 3$	1.0	1.0	1.0	1.0	1.0	1.0
σ_{Rc} (MPa)	1.3	3.5	5	1.3	3.5	5
m	9	5	4	9	5	4
X (mm)	76.8	31.2	23.6	49.2	28.8	14.6

In the first stage, the efficiency factors of the fibres were determined considering the mechanical response of the experimentally tested samples, and, thus, observing the stress–strain curves of the fabric strips of flax and sisal fabrics and those of the FRCM composites, it is possible to note the low contribution of the fibres when the strains are in the first stage. This is the reason why the η_1 factors were 0.5, 0.8 and 1.0 (see Table 6.3). Moreover, the contribution of the reinforcing fibres in the third stage is complete, and, therefore, the η_3 factors were equal to 1.0 in all cases. Modifying the Weibull parameters m and σ_{Rc}, a curve fitting of the described stochastic model on all the experimentally obtained curves was performed. The curves were fitted by using a least square method that minimises the differences between the experimental and the theoretical curves.

6.4 FRCM modelling

Response curves of the specimens considered for statistical validation are used to compare the tensile stress–strain diagrams obtained using both the ACK theory and the stochastic model. The modelled responses using the ACK theory are analysed first, then the results of the stochastic model are provided. To facilitate a clear understanding of the figures shown in this section, the area covered by the experimental curves is highlighted in grey.

6.4.1 ACK theory

By using the theoretical expressions presented in *section 6.2.1* and the data reported in Tables 6.1 and 6.2, the numerical responses were plotted. As assumed in the ACK theory, the tensile behaviour, in terms of the stress–strain curve of the cementitious composites studied, is clearly described by three straight lines (theoretical tri-linear tensile behaviour), which represent the linear elastic stage (first stage), the multiple cracking stage (second stage) and the post cracking stage (third stage). The ACK model does not takes into account the fourth stage observed in the behaviour of the sisal and flax-reinforced composites (see *Chapter 4*) [24]. In Figs. 6.3 and 6.4, the stress–strain relationship obtained by employing the ACK model is directly compared with the experimental results of the flax- and sisal-FRCM composites prepared with one, two and three reinforcing layers.

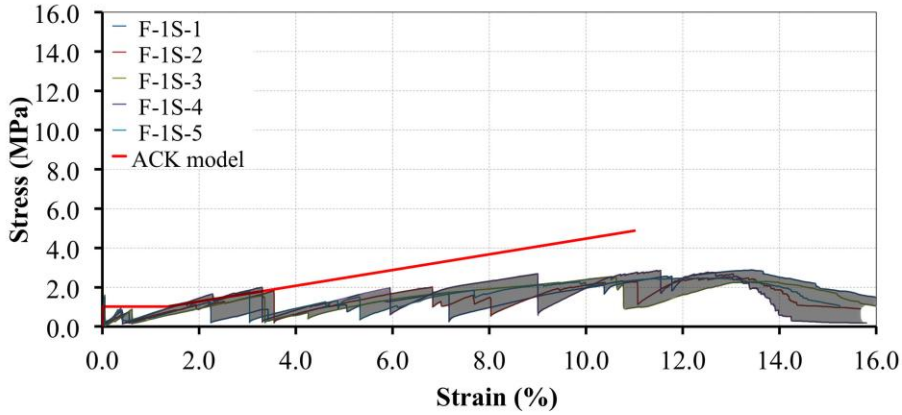

(a)

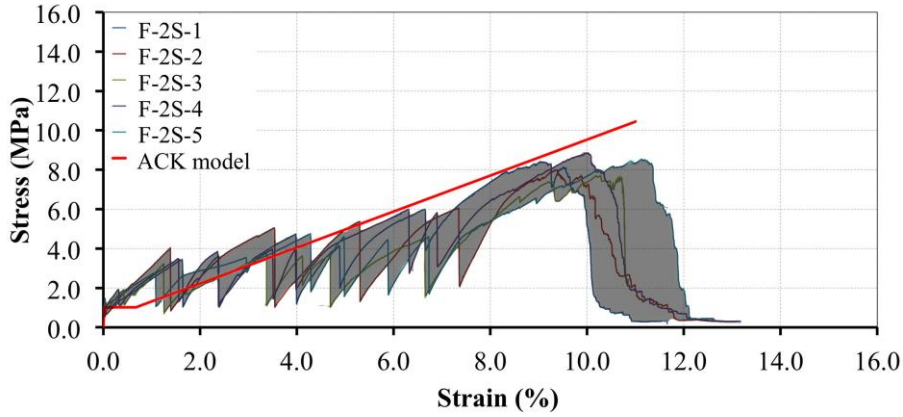

(b)

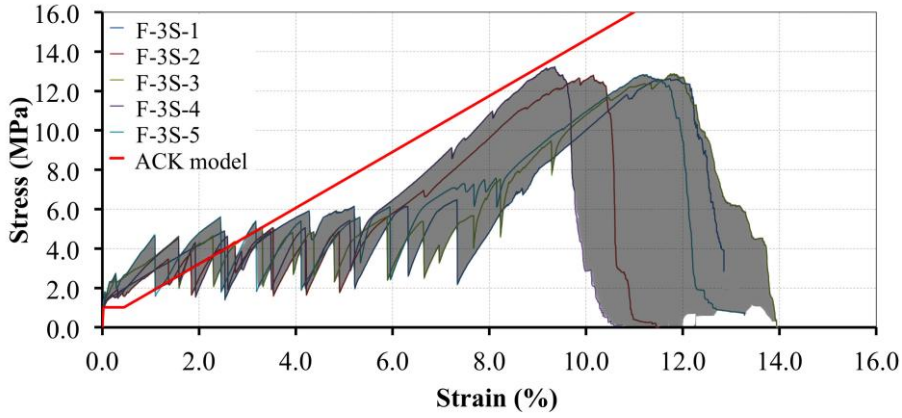

(c)

Fig. 6.3: Predicted stress-strain responses of flax-FRCM composites using the ACK theory: (a) one-layer reinforced composites; (b) two-layer reinforced composites; and (c) three-layer reinforced composites.

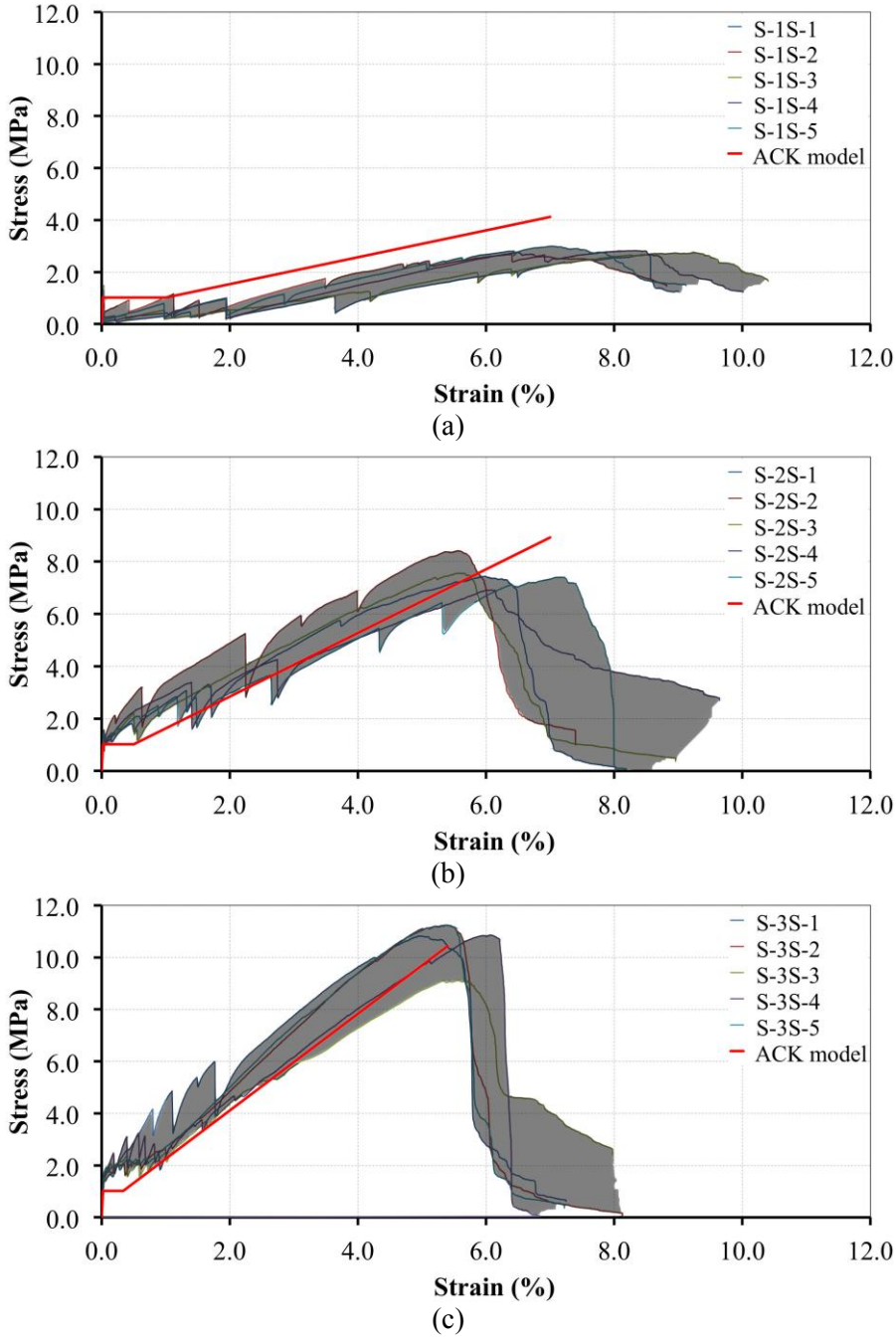

Fig. 6.4: Predicted stress-strain responses of sisal-FRCM composites using the ACK theory: (a) one-layer reinforced composites; (b) two-layer reinforced composites; and (c) three-layer reinforced composites.

The specimens are identified with the letters "F" and "S", denoting the type of reinforcing fibres (flax or sisal, respectively), and the number of reinforcing layers is identified by "1S", "2S" and "3S" characters (one layer, two layers and three layers, respectively). Considering the results, the ACK model proved to be less than fully effective for predicting the third stage of the behaviour of these types of FRCM systems. One of the main discrepancies is the strain at the end of the multi-cracking stage (ε_{cII}). This suggests that the results of this model are greatly affected by the high ductility of the flax and sisal fabrics. Moreover, the stiffness at the third stage appears to be affected in the model when the behaviour of the flax-FRCM composites is predicted. This discrepancy is caused by the changes in stiffness when the volume fraction is increased. For the sisal-FRCM composites, the model shows a better correlation. This can be attributed to the difference in the ductility between the flax and sisal fibres and, particularly, to the lower strains produced during the multiple cracking stage in the sisal-FRCM composites. However, by analysing the response curves shown in Figs. 6.3 and 6.4, the ACK model is not effective at predicting the tensile behaviour of both sustainable composite systems.

6.4.2 Stochastic model

The experimental curves show that the multiple cracking stage does not take place at a constant stress level. In this model, the nature of the matrix failure strength is introduced through a probability distribution, and the Weibull cumulative distribution is used to describe the failure of the specimens under tensile loads. Using photographs of the specimens during testing, it was possible to quantify the average distance between cracks (X), which is one of the primary Weibull parameters, and, thus, the final average crack distance was experimentally determined (see Table 6.3). Applying a best-fit procedure between the experimental and theoretical curve, the other Weibull parameters such as the Weibull modulus (m) and reference cracking stress (σ_{Rc}) were designated. The final values used to better fit the stress–strain curves of the FRCM composites are also shown in Table 6.3.

As for the ACK model, the stress–strain relationship obtained by employing the stochastic model is directly compared with the experimental results of the FRCM composites (see Figs. 6.5 and 6.6).

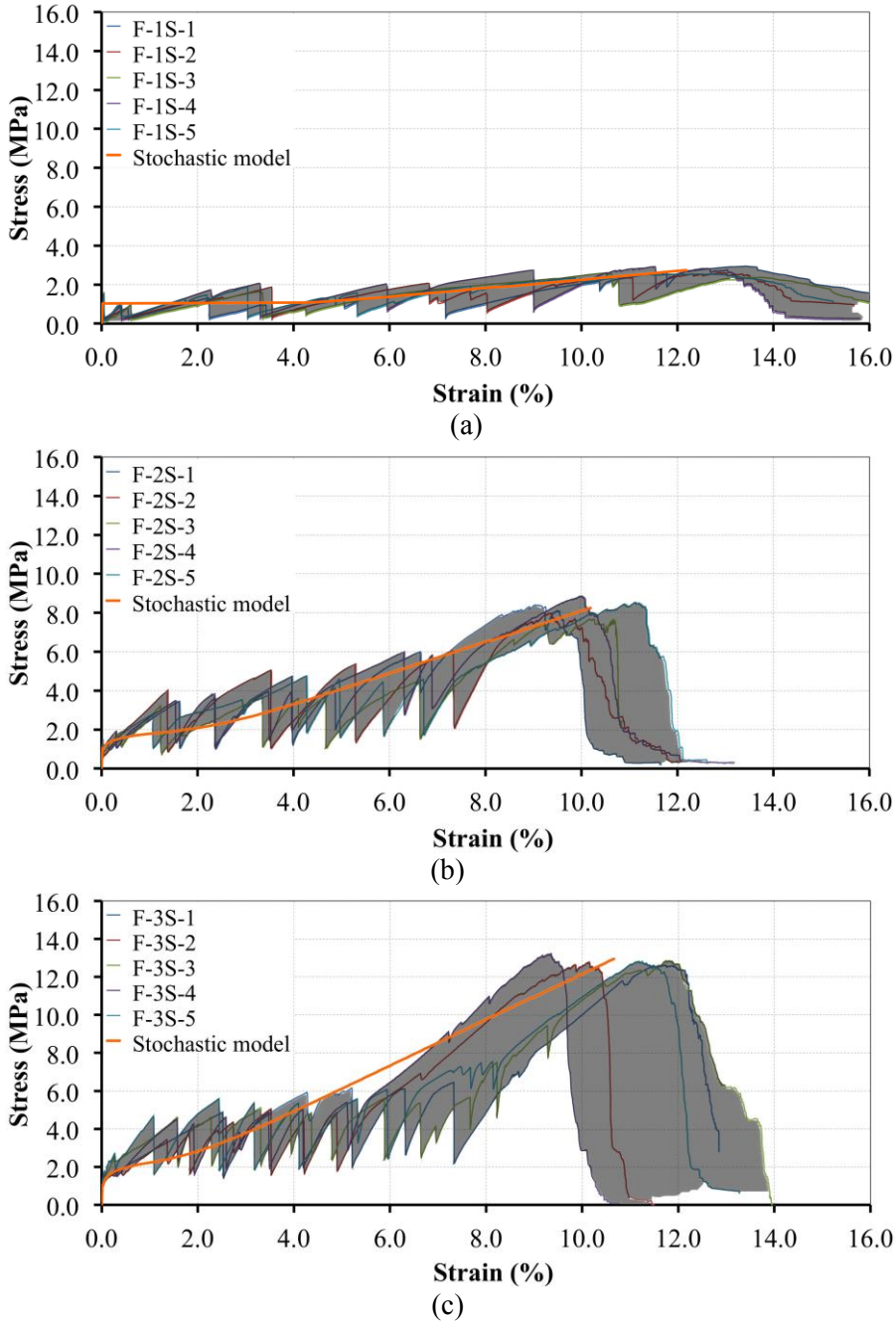

Fig. 6.5: Predicted stress-strain responses of flax-FRCM composites using the stochastic model: (a) one-layer reinforced composites; (b) two-layer reinforced composites; and (c) three-layer reinforced composites.

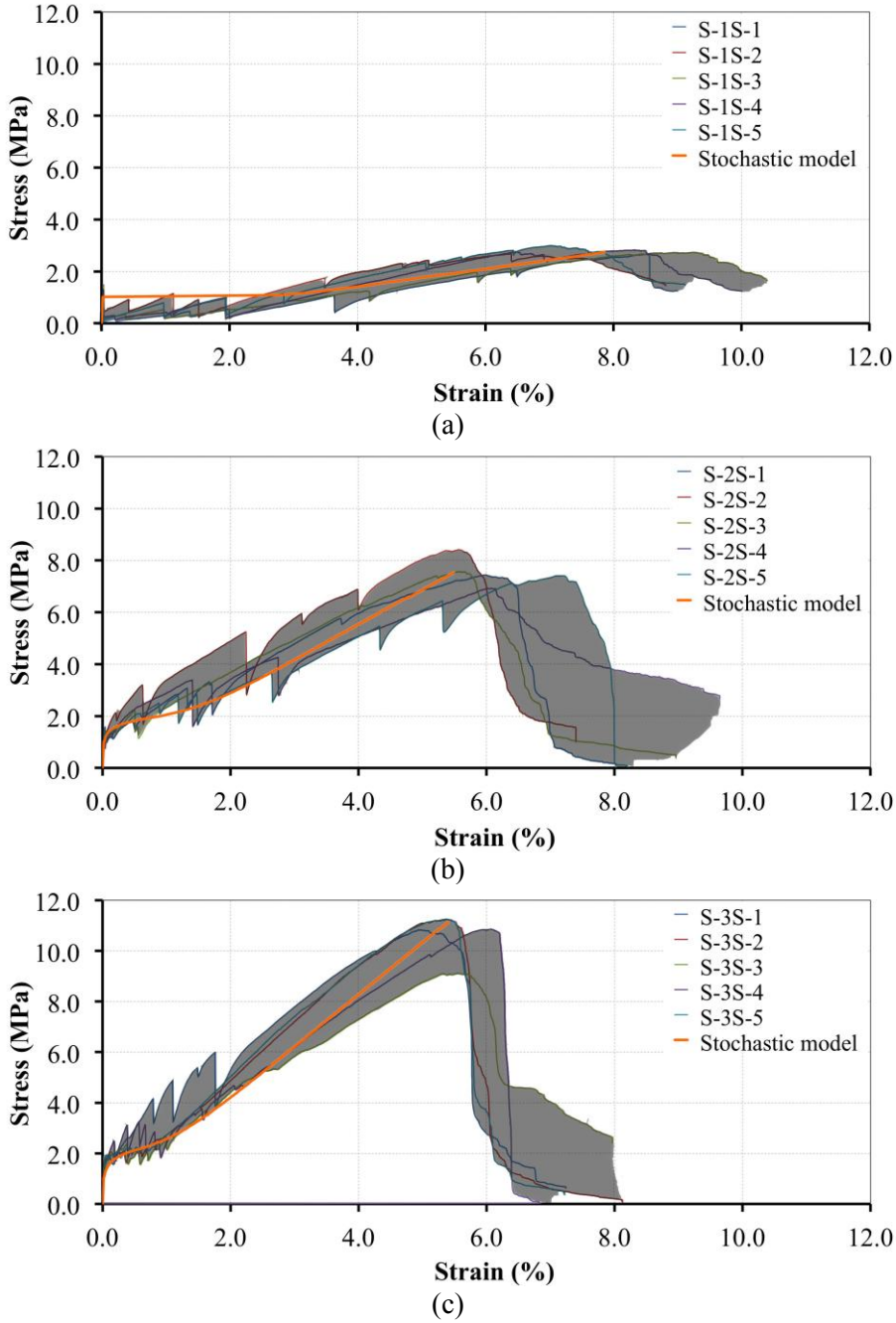

Fig. 6.6: Predicted stress-strain responses of sisal-FRCM composites using the stochastic model: (a) one-layer reinforced composites; (b) two-layer reinforced composites; and (c) three-layer reinforced composites.

As observed in Figs. 6.6 and 6.7, the correlation between the experimental and theoretical results is better than that of the ACK theory. The model produces responses that best fit the envelope curves of the experimental responses. Predicted curves describe a multiple cracking stage developed in different stress ranges. However, on the one hand, because of the high ductility of the fibres, the model has a limited correlation with the transition between the second and third stages, primarily for the flax-FRCM composites (see Figs. 6.5b and 6.5c). On the other hand, the multiple cracking stage of the flax- and sisal-FRCM composites that were experimentally investigated were characterised by the formation of large matrix cracks, resulting in major reductions in strength. Currently, there is no model that can describe this behaviour due to the irregular response of these materials and the many factors that may be involved in the formation of new matrix cracks. Whereas, for FRCM composites produced with synthetic or mineral fibres, which exhibit higher stiffness and much lower strain capacities than those observed in the sustainable composites examined in this research, the multiple cracking stage may be modelled with good correlation [25].

By using the stochastic model, the predicted stress–strain responses of the flax- and sisal-FRCM composites allow for the estimate of the tensile strength and ultimate strain capacity, as well as the elastic modulus of the composites in the first and third stages. Both the Weibull modulus (m) and reference cracking stress (σ_{Rc}) (see Table 6.3) determined for each composite system may be used to simulate the tensile behaviour of FRCM composites produced with lime-based cementitious matrices and reinforced with vegetable fabrics exhibiting similar strain capacities as those of the fabrics investigated in this research.

6.5 References

[1] Marshall D, Evans A. Failure mechanisms in ceramic-fiber/ceramic-matrix composites. Journal of the American Ceramic Society 1985;68:225–31.

[2] Kim R, Pagano N. Crack initiation in unidirectional brittle-matrix composites. Journal of the American Ceramics Society 1991;74:1082–90.

[3] Barsoum M, Kangutkar P, Wang A.S.D. Matrix crack initiation in ceramic matrix composites. Part I: Experiments and test results. Composite Science and Technology 1992; 257–69.

[4] Wang A.S.D, Huang X. and Barsoum M. Matrix crack initiation in ceramic matrix composites. Part II: Models and simulation results. Composite Science and Technology 1992;44:271–82.

[5] Lee S, Stinchcomb W. Damage mechanisms and fracture modes in nicalon/CAS-II Lami- nates. Fracture of Composites. Key Engineering Materials (edited by Armanios, E.) vols. 121–122 Transtec Publications; 1996.

[6] Aveston J, Cooper GA, Kelly A. Single and multiple fracture, the properties of fibre composites. In: Proceedings of the conference national physical laboratories, IPC Science and Technology Press Ltf. London, 1971. p. 15–24.

[7] Aveston J, Kelly A. Theory of multiple fracture of fibrous composites. J Mat Sci 1973;8:411–61.

[8] Purnell P, Short NR, Page CL, Majumdar AJ, Walton PL. Acceleratedageing characteristics of glass-fibre reinforced cement made with new cementitious matrices. Compos Part A 1999;30:1073–80.

[9] Mobasher B. Development of Design Procedures for Flexural Applications of Textile Composite Systems Based on Tension Stiffening Models. In 6th Colloquium on Textile Reinforced Structures (CTRS6). Berlin; 2011. p. 297–314.

[10] Zok FW, Spearings SM. Matrix crack spacing in brittle matrix composites. Acta metall. mater 1992;40:2033.

[11] Pryce AW, Smith PA. Matrix cracking in unidirectional ceramic composites under quasi-static and cyclic loading. Acta metall Mater 1993;41:1269– 81.

[12] Rouby D, Reynaud P. Fatigue behaviour related to interface modification during load cycling in ceramic-matrix fibre composites. Composite Science and Technology 1993;48:109– 18.

[13] Ahn BK, Curtin WA. Strain and hysteresis by stochastic matrix cracking in ceramic matrix composites. J Mech Phys Solids 1997;45(2):177–209.

[14] Curtin WA. Stochastic Damage Evolution and Failure in Fibre-Reinforced Composites. Advances in Applied Mechanics 1999;36:163–253.
[15] Bentur A, Mindess S Fibre reinforced Cementitious Composites. Elsevier Applied Science 1990.
[16] Allen HG The purpose and methods of fibre reinforcement. In: Prospects of fibre reinforced construction materials. Proc Int Building Exhibition Conference. Building Research Station, UK 1971, 3–14.
[17] Curtin WA, Ahn BK, Takeda N. Modeling Brittle and Tough Stress-Strain Behaviour in Unidirectional Ceramic Composites. Acta mater 1998;10:3409– 20.
[18] Cuypers H, Wastiels J. Stochastic matrix–cracking model for textile reinforced cementitious composites under textile loading. Mater Struct 2006;39:777–86.
[19] Da Silva ARC. Probabilistic approach to predict cracking in lightly reinforced microconcrete panels. J Eng Mech 2004;8(130):931–41.
[20] Mobasher B, Pahilajani J, Peled A. Analytical simulation of tensile response of fabric reinforced cement based composites. Cem Concr Compos 2006;28:77–89.
[21] Widom B. Random sequential addition of hard spheres to a volume. J Chem Phys 1966;44:3888–94.
[22] Cuypers H, Wastiels J. Thin and Strong Concrete Composites with Glass Textile Reinforcement: Modeling the Tensile Response. ACI Special Publication Textile- Reinforced Concrete, SP-250, American Concrete Institute, p. 131-148, 2008.
[23] W. Weibull. A statistical distribution function of wide applicability. ASME journal 1952;293–97.
[24] Cevallos O, Olivito R. Effects of fabric parameters on the tensile behaviour of sustainable cementitious composites. Compos Part B: En 2015;69:256–66.
[25] Van Hemelrijck D, Cuypers H, Wastiels J, Kalogiannakis G, De Wilde W.P. Experimental and Numerical Analysis of Matrix Cracking in Brittle Composites. In Conf Proc. Recent Advances in Composite Materials. Kluwer Academic Publishers; 2003. pp. 95-108.

CONCLUSIONS

In this PhD thesis, cementitious composites reinforced with sustainable fibres were developed. The tensile behaviour, crack growth and propagation of cementitious composites produced with layers of flax and sisal fabric strips were comprehensively studied. The effects of the fibre type, fabric geometry, physical and mechanical properties of the fabrics and volume fraction of the fibres on the tensile behaviour of the natural fabric-reinforced cementitious composites were investigated. To study the effects of fibre type, the stress–strain response and crack propagation of glass fabric-reinforced cementitious composites was compared with that of the natural fabric-reinforced composites. The mechanical response and effectiveness to strengthen masonry elements of these composite systems was compared to that of FRCM composites produced with mineral and synthetic fabrics. The tensile stress–strain response was numerically analysed to determine the feasibility of using models, such as the ACK theory and the stochastic model, to predict the tensile behaviour and estimate the mechanical properties.

Both flax and sisal fabric strips exhibit similar tensile properties, but flax fabrics show a slightly higher tensile strength. The strong tensile properties of sisal and flax fibres are a good indication of the high performance potential of these fabrics in fibre-reinforced composite applications. However, the flax fabrics were stronger and more ductile than the sisal fabrics and thus produced composites exhibiting better tensile performance.

The lower alkalinity of the NLG matrix, and the presence of carbonate filler and pure pozzolan with a high content of reactive silica makes this matrix potentially well suited for incorporation into vegetable fibre reinforcement composites to strengthen masonry structures. The NLG matrix is an interesting alternative to OPC matrices in natural fibre composite production.

The flax- and sisal-FRCM composite systems investigated in this study demonstrate ductile behaviour and moderate tensile strengths. The tensile performance of these sustainable composites can be improved with higher fibre volume fractions.

Unlike the flax- and sisal-FRCM composites, the stiffness of the glass-FRCM composites allowed high levels of strength to be attained at relatively low strains; this feature suggests the feasibility of using these composites for low-strain applications.

In the natural fabric composites, the formation of matrix cracks was observed during all the loading stages, resulting in significant reductions in strength. The NLG matrix was able to store energy even when the stiffness of the composite was largely affected by the stiffness of the natural fabrics. The contribution of the matrix to the mechanical behaviour in the third stage should not be neglected in the flax- and sisal-FRCM composites.

Considering fabric geometry and physical properties, such as the mass per unit area and the linear density, the flax fabric provided better anchorage development than the sisal and glass fabrics in the cement-based composites. Both the dimensional irregularity and the higher linear density of the sisal yarns produced lower penetrability in the sisal fabric-reinforced composites.

The parameter that had the greatest effect on the crack development of the cementitious composites reinforced with flax and sisal fabrics was the

volume fraction of fibres. The flax fabric-reinforced composites developed fewer cracks than did the sisal fabric composites because of the lower volume fraction of fibres. The volume fraction of fibres began to be effective at a value of approximately 3% for both flax and sisal fabric-reinforced composites.

The analyses of the effects of the fabric parameters as set forth in this study have provided new knowledge on the behaviour of fabric-reinforced cementitious composites produced with natural fabrics.

The tensile behaviour of unreinforced masonry elements, in terms of the tensile mortar/brick bond strength and ductility, were significantly improved by the use of flax-FRCM composites for strengthening, and the specimens did not collapse despite the extensive damage generated during the test.

The mechanical behaviour of unreinforced masonry elements subjected to eccentric loads was compared against results obtained with masonry samples strengthened using flax-FRCM systems and PBO-FRCM systems. Through this, it was found that both strengthening systems can improve strength and deformability, but the strength of the composite was not a decisive factor. Indeed, debonding problems related to the higher stiffness and lower strain capacity of the PBO fibres greatly affected the efficacy of the PBO-FRCM system with prismatic and Flemish-bonded specimens. However, by using a *NLG* matrix, the flax-FRCM composite was able to release stored stress by forming cracks in the matrix and was prevented from debonding in all tests. On the basis of these results, the flax-FRCM composite system is considered to have great potential for strengthening masonry structures subjected to compression loads with large eccentricities, but still requires further improvement and optimisation.

By numerically analysing the tensile behaviour of the FRCM composites, it was possible to predict the stress–strain response with limited correlation. For the flax- and sisal-FRCM composites, the ACK model was not effective at predicting the multiple cracking and third stages of the behaviour. The stochastic model provided a better fit of the tensile response of the composites. However, because of the high ductility of the flax and sisal fibres, the model was not effective at describing the transition between the second and third stages.

Cementitious composites reinforced with natural fibres represent sustainable alternative materials for the construction industry, and the ability to recycle these materials can provide new opportunities for developing countries to generate energy and economic resources. The future of FRCM composites reinforced with natural fibres appears to be bright because they have good behaviour and, generally, are environmentally superior to glass fibre-reinforced composites. However, the implementation of this system as a regular strengthening technique is still distant. Further research is needed to improve the technical performance and component service life, as well as to better understand the performance of flax- and sisal-FRCM systems and their interaction with masonry structures by performing numerical analyses and developing theoretical models.

ACKNOWLEDGMENTS

Through this short but exciting journey I have been very fortunate to meet those wonderful people who have guided, supported and accompanied me. These few words are not enough to thank everyone who walked with me directly or indirectly as this thesis project came to fruition.

First, I would like to thank my advisor, Prof. Renato Olivito, who guided me and gave me the necessary knowledge and priceless advice for completing each step of this research. Additionally, I am appreciative for the help he provided when the obstacles, inevitable in research, made the finish line seem more distant.

I also extend my thanks to all the technical staff at the Laboratory of Testing Materials and Structures of the Department of Civil Engineering at the University of Calabria, for their patience, advice and assistance in conducting the laboratory tests. I especially want to thank Tonino because, despite the many problems and delays encountered, he was always supporting me to push through with the experiments.

I would also like to thank Prof. Luciano Ombres, whose door was always open for discussion and advice, for supporting me in the various stages of the experimental research.

I cannot forget to thank all my colleagues and friends at the Laboratory of Research, Elisa, Stefania, Francesca, Valentina, Rosamaria, Fabio, Lorenzo, Arturo, Antonio, Salvatore, Antonio, Carmelo, Antonio and Alessadro, who also helped me when I needed their professional talent and knowledge. They exhibited human qualities and always gave me a hand, advice or anything I needed.

Agradezco a la Universidad Nacional de Chimborazo por su apoyo y colaboración para que pueda realizar mis estudios de doctorado de la mejor manera. Durante el tiempo que he necesitado ausentarme, son tantas las autoridades, compañeros y amigos que me han brindado su ayuda en la Universidad Nacional de Chimborazo; estoy muy agradecido con todos ellos.

No terminaré de agradecer nunca a mi familia, en especial a mi Madre y Esposa, quienes con amor me han dado la fuerza para seguir adelante en todo momento. El camino que he recorrido durante estos tres años ha sido muy hermoso; sin embargo, los senderos y pasajes en ocasiones presentaron grandes obstáculos difíciles de superar, y gracias al apoyo de mi familia, gracias a las oraciones y palabras de aliento de mi Madre y al apoyo incondicional de mi Esposa me encuentro, finalmente, aquí.

DIOS te agradezco porque siempre has estado junto a mi. Gracias por TUS infinitas bendiciones.